Title
The role of PSD-95 in AMPA receptor clustering and synaptic plasticity

Author
Schnell, Eric,

Publication Date
2002

Peer reviewed|Thesis/dissertation

The Role of PSD-95 in AMPA Receptor Clustering and Synaptic Plasticity

by

Eric Schnell

DISSERTATION

Submitted in partial satisfaction of the requirements for the degree of

DOCTOR OF PHILOSOPHY

in

Neuroscience

in the

GRADUATE DIVISION

of the

UNIVERSITY OF CALIFORNIA, SAN FRANCISCO

Acknowledgements

I would like to thank several people whose work and support greatly contributed to the production of this thesis. First of all, this work was all made possible through the inspiration and guidance of my graduate advisor, Roger Nicoll. Roger's curiosity and commitment to elucidating the core elements of synaptic transmission have been instrumental in the design and execution of the experiments presented here. He was an extremely attentive and available mentor to me during graduate school. His insistence on the highest quality experimental design and data acquisition has been crucial to the quality of this work. The clarity of mind and purpose he taught me will influence all my future work, irrespective of my future career path. And perhaps most of all, Roger's sense of humor and the joy he obtained from seeing virtually any kind of data made it a pleasure to work with him.

I thank David Bredt, who also supervised me during much of my graduate career. All of the work presented here was produced in collaboration with his lab. My rotation with him was instrumental in developing my knowledge of molecular biology techniques, and ultimately allowed me to combine these techniques with physiology in Roger's lab. We had many hours of enlightening discussion and I enjoyed having his input into my work, as it provided a completely novel perspective.

I also thank Rob Malenka, both for initially taking me into his lab and for encouraging and supporting my development of the slice culture system. I learned many of the neurophysiology techniques I performed throughout my graduate career in his lab, and very much enjoyed being part of his collaboration with Roger.

I was able to work with many great people who contributed both directly and indirectly to my work as well as my growth and development as a scientist. First of all, I would like to thank the many members of the Nicoll lab with whom I was able to work during my time there. These include Max Sizemore, Siavash Karimzadegan, Lu Chen, Kaspar Vogt, Steve Gomperts, Qiang Zhou, Rachel Wilson, Dietmar Schmitz, Jack Mellor, Matt Frerking, Chris Lüscher, Carl Petersen, Min-Yi Xiao, Sue Giller, Kaiwen Kam, Kim Moore, Joel Greenwood, Valentin Stein, and Joerg Breustedt. I would particularly like to acknowledge Lu Chen not only for making her seminal discovery about the role of stargazin in AMPA receptor trafficking, but also for being a great friend and collaborator during the past 3 years. Also, Max Sizemore and Siavash Karimzadegan directly contributed to the slice culture experiments and I wish them the best with their undoubtedly successful careers in graduate school.

Additionally, the "original" members of the Malenka lab were very helpful in teaching me physiology as well as providing my first lab home at UCSF. These include Reed Carroll, Thanos Tzounopoulos, Greg Hjelmstad, David Selig, Saleem Nicola, Dan Feldman, Hugh Xia, Mark Thomas, Antonello Bonci, Chad Christine, and Eric Beattie. I thank them for their time and energy. Also, members of the Bredt lab both taught me molecular biology and how to use these tools to perform meaningful experiments. These include David Bredt, Alaa El-Din El-Husseini, Sri Dakoji, Dane Chetkovich, Rick Topinka, Sarah Craven, and Aaron McGee. I would like to particularly acknowledge Alaa El-Husseini, as we collaborated very closely on the PSD-95 work in dissociated cultures. He was a never-ending fountain of exciting observations, including the initial discovery that PSD-95 overexpression enhanced GluR1 staining.

I thank the members of my thesis committee, Lily Jan, David Copenhagen, David Bredt, Roger Nicoll, and Rob Malenka, as well as the members of my qualifying exam committee, Rob Edwards, Dan Lowenstein, David Bredt, David Copenhage, and Lily Jan. They all generously donated their time to supervising and evaluating my work and made themselves available to me at any time. I am very grateful for their input as it improved my focus and the quality of my work. I would also like to thank the Medical Scientist Training Program, and specifically Tris Parslow, Jana Toutolmin, and Catherine Norton, for support throughout graduate school, and the Neuroscience Program, particularly Pat Veitch and Lisa Magargal, for making everything run so smoothly.

Finally, I would like to thank my family for their unconditional support throughout my graduate years. My wife, Jenny, has been the greatest joy in my life and infuses me with a continuous positive mood that undoubtedly improved my science. My parents, Rudy and Liz, have been my strongest advocates and have always encouraged my education and my interest in science. Their guidance and support brought me to this place.

Contributions

The work in Chapters 2-6 was conducted in collaboration with other authors.

The data presented in Chapter 3 was collected by Eric as well as Alaa El- Husseini, Sarah Craven, Dane Chetkovich and Bonnie Firestein, members of the laboratory of David Bredt. Specifically, Eric created the PSD-95 and PSD-95 C3,5S GFP fusion constructs, analyzed their palmitoylation in COS-7 cells, performed some of immunohistochemistry shown in Figure 1, and worked on the neuronal transfections. The rest of the data shown was collected by the Bredt lab. Chiye Aoki performed the electron microscopy. Reproduced from **The Journal of Cell Biology, 2000, 148, 159-172** by copyright permission of the Rockefeller University Press.

The data presented in Chapter 4 was collected by Eric and Alaa El-Husseini. Eric performed all of the electrophysiological experiments, and filled transfected cells with Lucifer yellow for the spine morphology studies. Alaa performed the immunohistochemical analyses. Reprinted with permission from El-Husseini et al., PSD-95 Involvement in Maturation of Excitatory Synapses, Science 290, 1364 (2000). Copyright 2000, American Association for the Advancement of Science.

The data presented in Chapter 5 was collected by Eric along with Max Sizemore and Siavash Karimzadegan of the Nicoll Lab. Eric established the slice culture transfection and recording system, performed all of the electrophysiological experiments, constructed the PSD-95 and stargazin point-mutants, and conceived of all of the experiments. Max prepared all of the slice cultures and performed the confocal imaging; Siavash prepared DNA constructs and performed the GST binding studies. This work has been submitted for publication.

The data in Chapter 6 was collected by Eric in collaboration with Alaa El-Husseini, Sri Dakoji, Neal Sweeney, and Andrea Aguilera-Moreno in the Bredt Lab, as well as Qiang Zhou of the Nicoll Lab. Eric contributed intellectually to the project and performed all electrophysiology experiments, including work with 2-bromopalmitate in slice cultures and acute slices. Alaa and Sri performed all of the immunohistochemistry and radiolabelling studies. Qiang performed some of the clustering analyses. This work has been published (El-Husseini et al., 2002) and permission has been granted for its reproduction in this thesis

The Role of PSD-95 in AMPA Receptor Clustering and Synaptic Plasticity

Eric Schnell

Abstract

Glutamatergic synaptic transmission mediates the majority of excitatory communication between neurons in the brain. The strength of individual glutamatergic synapses is largely due to differences in the number of post-synaptic AMPA receptors (AMPARs). In this series of studies we investigated the molecular mechanisms controlling the localization of AMPARs to synapses. We have found that the synaptic protein PSD-95 is largely responsible for the synaptic localization of AMPARs.

We analyzed the trafficking of PSD-95 using a GFP fusion construct. Proper trafficking, ion channel clustering, and synaptic targeting of PSD-95 requires its N-terminal palmitoylation. Prolonged overexpression of PSD-95 in dissociated hippocampal neurons accelerates maturation of glutamatergic synapses. PSD-95 expression enhances postsynaptic clustering and activity of glutamate receptors. Postsynaptic expression of PSD-95 also enhances maturation of the presynaptic terminal, and increases the number and size of dendritic spines.

In transfected hippocampal slice cultures, PSD-95 overexpression selectively increases synaptic AMPAR number. This effect requires palmitoylation and the PDZ domains of PSD-95. As PSD-95 does not interact directly with AMPARs, we performed studies with the putative adaptor protein, stargazin. Stargazin binds both PSD-95 and AMPARs, and synaptic AMPAR targeting requires the PDZ-binding domain of stargazin. By making compensatory mutations to both PSD-95 and stargazin, we ablate and

reconsititute PSD-95 binding to stargazin. These constructs show that PSD-95 is directly responsible for the synaptic targeting of stargazin and thus controls the number of synaptic AMPARs. Furthermore, overexpressing stargazin dramatically increases the number of extrasynaptic AMPARs, and the amount of synaptic PSD-95 controls the number of receptors at the synapse.

Dynamic regulation of AMPARs represents a primary mechanism for controlling synaptic strength. We identify palmitate cycling on PSD-95 at the synapse and find that glutamate receptor activity regulates palmitate turnover on PSD-95. Blocking palmitoylation disperses synaptic clusters of PSD-95, and causes a selective loss of synaptic AMPARs. Rapid glutamate-mediated AMPAR internalization requires depalmitoylation of PSD-95. These studies suggest that palmitate cycling on PSD-95 can regulate synaptic strength and regulates aspects of activity-dependent plasticity.

We present a model in which the number of synaptic AMPARs, and thus synaptic strength, is directly dependent on the amount of PSD-95 at the synapse. We propose that changes in the amount of synaptic PSD-95 mediate synaptic plasticity.

Table of Contents

List of Figures

CHAPTER 2

CHAPTER 3

CHAPTER 4

CHAPTER 5

CHAPTER 6

CHAPTER 7

CHAPTER 1:

General Introduction

Information is processed in the brain as the selective activation of sets of neurons. As a particular thought is being processed, activity passes from one group of neurons to the next; one pattern of activity excites another. This process of information transfer between neurons occurs at synapses, the sites of physical contact between neurons, using a chemical process known as synaptic transmission. During synaptic transmission, activity in one neuron influences the activity of another. An electrical impulse arrives at a pre-synaptic terminal, and evokes the release of a chemical from that cell. This chemical then binds to specific receptors on the post-synaptic cell and induces an electrical response.

Most neuronal impulses are passed from one neuron to another very quickly, allowing for the rapid processing of information crucial to behavior. The synapse is an extremely specialized structure, having evolved to allow for this rapid, point-to-point communication, and thus rapid information processing. One of its key features involves a concentration of appropriate receptors at the post-synaptic side of the synapse, allowing for extremely rapid detection of neurotransmitter release from the pre-synaptic cell. Mechanisms that localize these receptors to the appropriate connections are central to the fast interneuronal communication that we perceive as thought.

Features of Synaptic Transmission

Fast synaptic transmission in the nervous system involves two main categories of neurotransmitter: excitatory and inhibitory. Inhibitory neurotransmitters, such as

GABA and glycine, make the post-synaptic cell less likely to fire. These transmitters have a critical role in dampening neuronal activity and are essential to the proper patterning of information flow around the brain.

Excitatory neurotransmission allows for the presynaptic cell to excite the postsynaptic cell. The principal excitatory transmitter in the CNS is glutamate, and glutamatergic transmission is almost exclusively the engine driving information flow throughout the brain. The speed of excitatory neurotransmission is extremely rapid: the interval between impulse arrival in the presynaptic terminal and the glutamate-evoked post-synaptic response is less than 1 millisecond. The specialized nature of the synapse allows for this extremely rapid transfer of excitation between cells by aligning pre-and post-synaptic elements at the same sites.

One additional feature of many glutamatergic synapses in the CNS is their ability to change their synaptic strength. Individual synaptic connections are able to undergo a long-term increase in efficacy, known as long-term potentiation (LTP), or a long-term decrease in efficacy, known as long-term depression (LTD). Such synaptic plasticity changes the flow of excitation within the brain, and thus is likely to mediate the changes in information processing that underlie learning and memory.

Issues Regarding Synapse Development and Function

Much work has been devoted to obtaining an understanding of how new synapses are established and how existing synapses are modified. The first stage in synaptic development involves an initial contact between the axon of one cell and the dendritic arbor of a second cell. Soon thereafter, elements of both the presynaptic and postsynaptic

apparati are brought to the opposing sites of this contact, and this nascent synapse becomes more firmly established (Bresler et al., 2001; Friedman et al., 2000). Within hours, these nascent synapses acquire several of the functional characteristics of more mature synapses, such as pre-synaptic vesicle cycling (Ahmari et al., 2000). As development progresses, different glutamate receptors arrive at the post-synaptic side of excitatory synapses in a distinct temporal and spatial progression (Rao et al., 1998). A central issue in studies of synaptic development is concerned with understanding how the machinery required for synaptic transmission reaches and is retained at synaptic sites.

While synapses undergo radical changes during development, it is also believed that mature synapses are quite dynamic structures (see (Lüscher et al., 2000)). Mature post-synaptic structures are constantly changing in ways that can be detected anatomically, and might be dependent on synaptic activity (Fischer et al., 2000; Maletic-Savatic et al., 1999; Matus et al., 2000; McKinney et al., 1999; Rao et al., 1998). At the same time, it is also believed that receptors are moving into and out of synapses continuously (Lüscher et al., 1999; Shi et al., 1999b; Tovar and Westbrook, 2002). These observations suggest that synapses are able to change in complex ways, even after "maturation". Many different kinases, phosphatases, and second messenger systems are active in neurons, and are believed to modulate synapses both functionally and structurally. Thus, changes in synaptic structure and function are likely to be regulated by many distinct signals. Thorough knowledge of these signaling pathways will lead to an understanding of how their activity ultimately changes synaptic function.

In recent years, many investigators have begun to use molecular biology in an attempt to identify proteins involved in determining post-synaptic structure and function. Yeast-based two hybrid screens and other methods have identified scores of synaptic proteins (Kennedy, 2000; Lüscher et al., 1999; Ziff, 1997). In one extreme example (Husi et al., 2000), proteomics identifies a 77 protein synaptic mega-complex containing many post-synaptic density proteins. Together, these methods have identified many putative scaffolding proteins, signaling enzymes, and cell adhesion molecules that might potentially regulate post-synaptic receptor trafficking and the clustering of glutamate receptors at synapses. However, while many synaptic proteins have been cloned, very few of them have clearly defined functions. Further research will shed light on how these many proteins interact to create a functional, dynamic, synapse.

The Post-Synaptic Density

Early investigations into synaptic ultrastructure were performed with electron microscopy. These studies were able to clearly identify synaptic contacts between neurons, and were quite revealing in their detail. Two important features were identified from these early images. First of all, the presynaptic terminal was found to contain many small vesicular membrane structures, anatomical correlates for the quantal nature of synaptic transmission. Each vesicle contains a packet of neurotransmitter, waiting for an electrical impulse to arrive in the terminal. The impulse triggers the membrane fusion of these small vesicles, introducing thousands of neurotransmitter molecules into the synaptic cleft.

The second ultrastructural detail of interest consisted of a thick band of electron-dense material concentrated at the post-synaptic side of the synapse, and was called the post-synaptic density (Gray, 1959; Palay, 1958). The post-synaptic density (PSD) is presumed to contain the receptors and signaling machinery required to transduce the post-synaptic signal. The synaptic cleft, the extracellular space between the two cells, is extremely narrow: approximately 20 nm. As the study of synaptic physiology progressed, it became apparent that there must be many different post-synaptic proteins at synapses, thus accounting for the electron dense nature of the PSD. The machinery that mediates synaptic plasticity at most glutamatergic synapses is located at the post-synaptic density (Malenka and Nicoll, 1999), and thus an understanding of its molecular components becomes extremely desirable.

Ionotropic Glutamate Receptors

Synaptically released glutamate acts on two main categories of post-synaptic receptors. Ionotropic glutamate receptors mediate fast electrogenic responses to glutamate, and are largely responsible for initiating cell firing. Metabotropic glutamate receptors initiate slow second messenger cascades within the post-synaptic cell that modulate neuronal excitability. Ionotropic receptors have been studied much more extensively, as their responses are much easier to measure and the pharmacology for these receptors has been extensive for a long period of time.

There are two main classes of ionotropic glutamate receptors, AMPA and NMDA receptors. These classes have many gross molecular similarities. Both receptors are

tetramers of individual subunits, and each subunit consists of 3 transmembrane domains, along with a separate intramembrane pore-forming domain. Both have a large extracellular N-terminus, and an intracellular C-terminus. Currently, four separate AMPA receptor subunits (Glur1-4) and 3 separate classes of NMDA receptor subunits (NR1-3) have been identified.

AMPA and NMDA receptors are distinct in several important physiologic respects. AMPA receptors have extremely fast activation and deactivation kinetics, while NMDA receptors activate and deactivate much more slowly. Only AMPA receptors are able to depolarize neurons from rest, due to the voltage-dependent magnesium-block of NMDA receptors at resting membrane potentials. As a neuron is depolarized, however, the magnesium block of the NMDA receptor is relieved. While both are sodium and potassium permeable cation channels, the NMDA receptor is also calcium-permeable. Thus, calcium enters through the NMDA receptor when it binds glutamate while at a depolarized potential. It is widely believed that calcium influx through the NMDA receptor initiates the change in synaptic strength associated with synaptic plasticity.

Post-Synaptic Receptor Composition at Individual Synapses and Implications for Synaptic Plasticity

Individual glutamatergic synapses vary with respect to post-synaptic ionotropic glutamate receptor composition. Immunogold electron microscopy has demonstrated differential modes of AMPA and NMDA receptor expression. While most, if not all, excitatory synapses contain NMDA receptors, the number of AMPA receptors varies

immensely at synapses (Nusser et al., 1998; Petralia et al., 1999; Takumi et al., 1999). Some synapses appear to be completely devoid of AMPA receptors, containing only NMDA receptors. Dissociated neuronal cultures also provide physiological and immunohistochemical evidence for NMDAR-only synapses (Gomperts et al., 1998).

This discrepancy was first observed physiologically in the form of post-synaptically silent synapses (Isaac et al., 1995; Liao et al., 1995). These synapses did not show an evoked response when the membrane potential of the cell was at rest (-70mV), suggesting an absence of AMPA receptors, but did show a response at +40 mV, suggesting functional glutamate release and the presence of NMDA receptors. These "silent synapses" could be functionally unsilenced through an LTP-inducing "pairing" protocol. The appearance of an AMPAR-mediated response suggested the de novo delivery of AMPARs or the activation of AMPARs that had been previously present, but silent. It is presumed that AMPA receptors would be trafficked by membranous organelles, and that receptor insertion would involve fusion of these organelles with the plasma membrane. Consistent with the hypothesis that LTP involves deliver of AMPARs, postsynaptic injection of membrane fusion inhibitors blocks LTP (Lledo et al., 1998). Additionally, patterns of tetanic stimuli known to induce LTP elicit dendritic exocytosis of trans-Golgi derived organelles (Maletic-Savatic et al., 1998; Maletic-Savatic and Malinow, 1998). These studies suggest a strong association between dendritic exocytosis and the expression of LTP.

Analogous processes may be involved in the expression of LTD. LTD is accompanied by a rapid loss of synaptic AMPA receptors in cultured neurons (Carroll et al., 1999a; Carroll et al., 1999b), and blocking endocytosis with a dominant negative

dynamin fragment or GDPβS prevents LTD (Lüscher et al., 1999). Perhaps even more provocatively, inhibition of endocytosis causes the steady-state EPSC to increase, while blockade of exocytosis causes the EPSC to run down (Lüscher et al., 1999) implying that AMPA receptor trafficking occurs in steady-state conditions. Plasticity might involve a redistribution of this cycling pool to either the plasma membrane (LTP) or an intracellular compartment (LTD).

In a recent set of studies, work by Malinow and colleagues has shown that LTP involves the insertion of GluR1-containing AMPA receptors at synaptic sites (Hayashi et al., 2000; Shi et al., 1999a). Furthermore, LTP is severely impaired in GluR1 knockout mice (Zamanillo et al., 1999). Thus, the postsynaptic density appears to contain not only the machinery required for the induction of synaptic plasticity, but is also the locus of its expression (Malenka and Nicoll, 1999; Malinow et al., 2000).

Currently, one very active field of scientific inquiry has focused on understanding the molecular mechanism underlying synaptic glutamate receptor clustering. It was hoped that this would lead not only to a molecular understanding of PSD structure, but also would give us new insights into the mechanisms of post-synaptic receptor regulation. In the case of AMPA and NMDA receptor trafficking and clustering proteins, both forward and reverse approaches were employed, and several very interesting proteins were identified.

PDZ-Domain Containing Proteins

One hallmark of most proteins believed to cluster glutamate receptors at the synapse is the presence of one or more PDZ domains. The name for this domain derives from three of the first proteins in which this domain was identified, namely postsynaptic density-95 (Cho et al., 1992), *discs-large* (Woods and Bryant, 1991), and zona-occludens-1 (Itoh et al., 1993). This domain is of considerable interest as it binds proteins with an appropriate consensus binding sequence. Most significantly, some PDZ domains interact strongly with the C-terminus of several integral membrane proteins, including both AMPA and NMDA receptors. Through these interactions, it is thought that these PDZ-domain containing proteins are able to cluster and localize receptors at the synapse.

The structures of several PDZ domains have been solved and provide insights into their interactions. Overall, these domains are very similar in terms of their 3-dimensional structure, and bind to similar protein ligands. One general feature is that these domains form several important interactions with the carboxylate at the extreme C-terminus of proteins and the peptide backbone of the last few amino-acid residues. Additionally, PDZ domains bind to proteins such that the side chains of the last amino acid ("0 position") and the residue two before it ("-2 position") point into the ligand-binding pocket of the PDZ domain. PDZ domains can differ substantially in terms of binding preferences, and it appears that residues in the ligand-binding pocket of the domain determine these preferences (Daniels et al., 1998; Doyle et al., 1996; Songyang et al., 1997).

The C-termini of several ionotropic glutamate receptors bind to PDZ-domains of several identified proteins. These interactions have been the starting points for investigations into the molecular mechanisms underlying glutamate receptor clustering. As some of these PDZ proteins are synaptic, understanding the functional role of these interactions might lead to a more thorough understanding of the mechanisms controlling synaptic glutamate receptor localization, and perhaps synaptic plasticity.

Membrane-Associated Guanylate Kinase (MAGUK) Proteins

One of the most abundant PDZ proteins concentrated at glutamatergic synapses is PSD-95 (Cho et al., 1992; Kistner et al., 1993). PSD-95 is a member of a family of membrane-associated guanylate kinase (MAGUK) proteins. PSD-95 contains three PDZ domains, as well as an SH3 and guanylate kinase (GK) domain. The 3 PDZ domains of PSD-95 bind to the C-terminus of proteins which end with the sequence -S/T-X-V (Harris and Lim, 2001). The three other mammalian MAGUK proteins are also expressed in neurons, namely PSD-93/Chapsyn-110 (Brenman et al., 1996b; Kim et al., 1996), SAP97 (Muller et al., 1995), and SAP102 (Muller et al., 1996). Several important insights into the possible functions of these proteins in mammalian neurons come from studies of the *Drosophila* homolog, *discs-large* (Dlg-A).

Dlg-A was originally cloned through analyses of *dlg* mutant flies, and was identified as an important tumor suppressor gene (Woods and Bryant, 1991). *dlg* mutants showed aberrant imaginal disk growth and hyperplasia which suggested a failure of cell adhesion (Stewart et al., 1972; Woods and Bryant, 1989). Further analyses showed that

dlg was required for normal synaptic bouton structure, and was expressed both pre- and post- synaptically (Lahey et al., 1994). Further analyses showed that the *dlg* protein was required for the synaptic clustering of Shaker K^+ channels (Tejedor et al., 1997) and FasII, a cell adhesion molecule (Thomas et al., 1997; Zito et al., 1997). By analogy with the putative roles of *dlg* in Drosophila, it has been suggested that PSD-95 and other mammalian MAGUK proteins might be involved in synaptic protein clustering in mammalian neurons (Sheng and Sala, 2001).

PDZ Proteins Interacting with NMDA Receptors

The first protein found to interact with an ionotropic glutamate receptor was PSD-95 (Kornau et al., 1995). Through yeast two-hybrid screens, PSD-95 was identified to interact with the extreme C-terminus of the NMDAR NR2 subunits, NR2A and NR2B. These proteins terminate with an appropriate -SDV consensus, and bind PSD-95 in GST pull down assays (Kornau et al., 1995; Niethammer et al., 1996). As PSD-95 is able to cluster NMDA receptors containing the 2A or 2B subunit in heterologous cells, it has been suggested that PSD-95 might be involved in clustering endogenous NMDA receptors at synapses (Kennedy, 2000; Kim et al., 1996; Niethammer et al., 1996).

Several observations, however, have provided evidence inconsistent with this theory. NMDA receptors form clusters in developing neurons that do not stain for PSD-95 (Rao et al., 1998), and experimental manipulations which disperse synaptic PSD-95 clusters in neurons do not result in the de-clustering of NMDA receptors (El-Husseini et al., 2002; Passafaro et al., 1999). Conversely, a manipulation that massively increased

the number of NMDA receptor clusters in hippocampal pyramidal cells was not accompanied by any change in the number of PSD-95 clusters (Rao and Craig, 1997), and overexpression of PSD-95 in hippocampal cultures did not lead to any change in synaptic NMDA receptor staining (El-Husseini et al., 2000b). Thus, the putative assignment of PSD-95 as an NMDAR clustering protein remains to be convincingly demonstrated.

PDZ Proteins interacting with AMPA receptors

Work to identify proteins that might cluster AMPARs at synapses has also focused on PDZ-domain containing proteins. These include GRIP (Dong et al., 1997), ABP (Srivastava et al., 1998), and PICK1 (Daw et al., 2000; Xia et al., 1999), which each contain PDZ domains that interact with the C-termini of GluR2 and GluR3. GluR2 and GluR3 each terminate with a –VKI consensus, which has been found to bind a separate set of PDZ domains than the –S/TXV consensus for those in PSD-95.

GRIP was the first protein identified to interact with GluR2/3 (Dong et al., 1997), and this was followed closely by the identification of a separate homologous protein, ABP (Srivastava et al., 1998). Each of these proteins contains seven PDZ domains, and interact quite strongly with GluR2/3. However, while initial attempts to identify the subcellular localization of GRIP in neurons suggested it was clustered at synapses (Dong et al., 1997), not all neuronal AMPA receptor clusters contained GRIP immunoreactivity. Additionally, GRIP/ABP are not able to cluster GluR2 in heterologous cells (Srivastava et al., 1998).

More recently, PICK1 was identified as a single PDZ-domain containing protein which also interacted with the C-terminus of GluR2/3 (Dev et al., 1999; Xia et al., 1999). Unlike GRIP/ABP, PICK1 not only colocalized with AMPARs at excitatory synapses, but it also induced the clustering of GluR2 in heterologous cells. Overexpression of PICK1 in neurons led to greatly diminished surface GluR2 expression, and it has been suggested that PICK1 is involved in regulating GluR2 endocytosis (Perez et al., 2001).

Intriguingly, a protein closely related to PSD-95, SAP97, was found to bind directly to the AMPA receptor subunit GluR1 (Leonard et al., 1998). GluR1 ends with a motif (-TGL) quite similar to the consensus for binding to the domains of PSD-95. However, SAP97 is localized throughout the cell, and is associated with immature forms of GluR1 (Sans et al., 2001). Additionally, GluR1-associated SAP 97 is localized primary to intracellular membranes, and SAP97 rarely colocalizes with synaptic GluR1 (Sans et al., 2001). Due to this, it is believed that SAP97 might function as a trafficking protein rather than be involved in the post-synaptic clustering of GluR1.

Other Proteins Interacting with AMPA Receptors

Two non-PDZ domain containing proteins have also been implicated in synaptic AMPA receptor clustering. The first protein, Narp, is the secreted product of a neuronal immediate early gene, and has been shown to induce GluR1 clustering on the surface of neighboring cells (O'Brien et al., 1999). While quite distinct from the PDZ-binding proteins, it is not present at mature glutamatergic synapses (O'Brien et al., 1999), and thus has been suggested to play a role in synapse development.

More recent work led to the identification of stargazin, an integral membrane protein that interacts with AMPA receptors (Chen et al., 2000). Studies of the stargazer mouse, a spontaneously generated epileptic mutant, found an almost complete absence of synaptic AMPA-mediated currents in cerebellar granule cells (Chen et al., 1999; Hashimoto et al., 1999). The mutant gene encodes a 4 transmembrane domain protein, stargazin, that bears some homology to the voltage-dependent Ca^{++} channel γ subunit and claudin, a tight junction protein. Studies of this protein show that it is required for both the surface trafficking and the synaptic targeting of AMPARs in cerebellar granule cells (Chen et al., 2000). Stargazin terminates with a PDZ-binding motif (–TPV), and this domain is required for the synaptic localization of AMPARs in both granule cells and hippocampal neurons (Chen et al., 2000). This observation expands the number of putative AMPA receptor clustering proteins, as they might be able to interact with AMPARs via stargazin.

CHAPTER 2:

Methods

cDNA Cloning and Mutagenesis

Wild-type and N-terminal mutant full-length PSD-95 constructs (PSD-95–GFP, C35S, C3S, and C5S) were generated by PCR and subcloned into the HindIII and EcoRI of GW1 (British Biotechnology) (Topinka and Bredt, 1998). GFP was subcloned in-frame at the C terminus of PSD-95 at the EcoRI site. Deletion mutants of PSD-95 (1-PDZ2 to amino acid 309, which includes the 67 amino acid linker region between PDZ2 and PDZ3; 1-PDZ3 to amino acid 433, which includes the 40 amino acid linker region between PDZ3 and the SH3 domain; 1-SH3 to amino acid 502) were generated by PCR and subcloned into GW1 at the HindIII and KpnI sites in-frame with GFP that was subcloned into GW1 at the KpnI and EcoRI sites (Craven et al., 1999). Deletion mutants containing the last 25 C-terminal amino acids of PSD-95 (1-PDZ2+25, 1-PDZ3+25, and 1-SH3+25) were generated by PCR and subcloned into PSD-95–GFP GW1 with the HindIII of GW1 and the internal BglII site of PSD-95 (Craven et al., 1999). The PSD-95-GFP-prenyl chimera was generated by appending oligos encoding the prenylation motif of paralemmin (amino acids: DMKKHRSKSCSIM (Kutzleb et al., 1998)) to the C-terminus of the PSD-95 (C3,5S) GFP construct.

Point mutant constructs in the three PDZ domains of PSD-95 were generated using nested PCR of the fragment between the HindIII site on PSD-95 GFP-GW1 and the BglII site in PSD-95, with bi-directional primers coding for the mutation as well as silent mutations to create marker restriction sites. For PDZ1, the H130V mutation was created coincident with the introduction of a SacII site and the destruction of a PvuII site. For

PDZ2, the H225V mutation was created coincident with the introduction of a XhoI site and the destruction of an AatII site. For PDZ3, the H372V mutation was created coincident with the introduction of NsiI and FspI sites. For double and triple point mutant constructs, a corresponding point mutant was used as a template for the introduction of additional mutations (ie, PSD-95 H130V GFP was used as a template to introduce the point mutation in PDZ2, thus creating the H130,225V double mutant).

Wild-type SAP-97 construct was generated by PCR and subcloned into GW1 at the SalI and KpnI sites in-frame to GFP that was subcloned into GW1 at the KpnI and EcoRI sites. SAP-97 constructs containing the first 13 amino acids of PSD-95 (95/97) were generated by PCR with an N-terminal primer encoding these amino acids and subcloned as done for wild-type SAP-97 into GW1 (Craven et al., 1999). SAP-102 GFP was generated as described previously (El-Husseini et al., 2000b).

Stargazin constructs had GFP inserted in frame at the Bgl II site in the C-terminus as described previously (Chen et al., 2000). The stargazin-C-terminus construct was created by amplifying the DNA encoding the C-terminal 120 residues of stargazin and subcloning it into pEGFP-C1 (D.C.). The stargazin T321F mutant was created using PCR of the fragment between the engineered KpnI site on Stargazin-GFP and the EcoR1 site on GW1.

Proper introduction of all mutations and absence of undesirable mutations was verified by DNA sequencing.

Cell Transfection and Metabolic Labeling

COS-7, HEK-293 and MDCK cells were grown in Dulbecco's modified Eagle's medium (DMEM) containing 10% fetal bovine serum, penicillin, and streptomycin. PC12 cells used the same media containing 5% fetal bovine serum and 10% horse serum and were differentiated for 3 d after transfection in media containing 50 ng/ml NGF. Cells were transfected using Lipofectamine reagent according to the manufacturer's protocol (Gibco). For studies of palmitoylation, metabolic labeling of transfected COS-7 cells was done as previously described (Topinka and Bredt, 1998).

GST-Fusion Analysis

GST-stargazin fusion proteins were expressed and purified as described previously (Brenman et al., 1995). COS-7 cells were transfected with wildtype or mutant PSD-95 constructs and extracts were prepared as described previously (McGee and Bredt, 1999). Three μg of GST protein coupled to Sepharose beads was added to the soluble fraction of the COS-7 cell extracts, and the samples were incubated at 4 ^{o}C for 60 minutes. The protein-coupled GST beads were pelleted by centrifugation and then washed 5 times with resuspension buffer: 25mM Tris-HCl (pH 7.5), 150 mM NaCl, 5 mM EDTA, 5 mM EGTA. The beads were resuspended in 5x protein loading buffer, and samples were separated by SDS-polyacrylamide gel electrophoresis and analyzed by Western blotting using monoclonal mouse PSD-95 antibodies.

Cell Labeling and Immunoprecipitation

Synthesis of [^{125}I]palmitic acid was done as described (Berthiaume et al., 1995). For labeling with [^{125}I]palmitate, cortical neurons (4 x 10^6 cells / well) were labeled for 3 hr in neurobasal media containing 25 μCi/ml [^{125}I]palmitic acid. For metabolic labeling with [^{35}S]methionine, cells were incubated for 15 min with methionine-free neurobasal media and then for 1 hr in this media containing 300 μCi/ml EXPRE^{35}S^{35}S methionine (1175 Ci/mmol; NEN life Science Products, Inc.). For cycloheximide treatment 10 μg/ml was added to neurobasal media. For pulse-chase experiments using [^{125}I]palmitate and [^{35}S]methionine, cells were washed once with neurobasal media and then were incubated for variable times in conditioned neurobasal media containing 100 μM palmitate or 2 mM methionine respectively. Labeled cells were washed with ice-cold PBS and resuspended in 0.1 ml lysis buffer containing TEE (50 mM Tris-HCl pH 7.4, 1 mM EDTA, 1 mM EGTA), 150 mM NaCl and 1% SDS. After extracting for 5 min at 4°C, Triton X-100 was added to 1% to neutralize the SDS in a final volume of 0.5 ml. Insoluble material was removed by centrifugation at 10,000xg for 10 min. For immunoprecipitation, the samples were then incubated with PSD-95 antibodies (anti-rabbit, 1:100 dilution) for 1 hr at 4°C. After addition of 20 μl of Protein G-Sepharose beads (Pharmacia), samples were incubated for 1 hr at 4°C. Immunoprecipitates were washed three times with buffer containing TEE, 150 mM NaCl and 1% Triton X-100, boiled in SDS-PAGE sample buffer with 1 mM DTT for 2 min. and analyzed by SDS-PAGE. For fluorography, protein samples were separated by SDS-PAGE, and dried under vacuum. For [^{35}S]labeled samples, gels were exposed to Kodak Biomax MS at -80°C for 3 to 5 days.

For [^{125}I]labeled samples, gels were exposed to Kodak X-Omat MR with intensifying screens at -80°C for 15 to 20 days.

Subcellular Cell Fractionation

Cultured cortical neurons (DIV 14-17; 12 x 10^6 cells) were treated for 8 hr in neurobasal media with or without 100μM palmitate or 2-Br palmitate. Cells were washed 1x with PBS, harvested, and then suspended in 200 μl sonication buffer (50 mM Tris pH 7.4, 0.1 mM EGTA) supplemented with a protease inhibitor cocktail (2.5 μg/ml leupeptin, 2.5 μg/ml aprotinin and 1μM PMSF). Cells were sonicated briefly and nuclei were pelleted at 14,000xg at 4°C for 10 min. Lysates were centrifuged at 49,000xg for 1 hr at 4°C. The supernatants were collected and pellets were resuspended in 150 μl resuspension buffer (RB; 50 mM Tris pH 7.4, 0.1 mM EGTA, 1M KCl, 10% glycerol, 1.5 μl/10ml BME and protease inhibitors. Fractions (10 μl each) were analyzed by SDS-PAGE and immunoblotting for PSD-95.

Primary Neuronal Culture, Transfection and Immunofluorescence

Low-density neuronal cultures (5 X 10^4 cells / cm^{-2}) were prepared from hippocampi of E18/E19 rats. Hippocampi were dissociated by enzyme digestion with papain followed by brief mechanical trituration. Cells were plated on poly-D-lysine (Sigma) treated glass coverslips (12 mm in diameter) and maintained in Neurobasal media (Gibco) supplemented with B27, penicillin, streptomycin, and L-glutamine as

described in Brewer et al. (1993). For transfection of PSD-95 GFP and mutant forms, hippocampal cultures were transfected by lipid-mediated gene transfer kit (DOTAP) as described (Craven et al., 1999).

Where indicated, protein synthesis blockers and glutamate receptor agonists and antagonists were used at the following concentrations: cycloheximide (10 g/ml), APV (100 μM), AMPA (100 μM), CNQX (100 μM), kynurenate (10 mM). For calcium depletion, 4.75 mM EGTA was added to the neurobasal media, and $MgCl_2$ was adjusted to a final concentration of 5 mM.

Coverslips were removed from culture wells and fixed in methanol for 10 min. The cells were washed with Tris-buffered saline containing 0.1% Triton-X-100 (TBST) and blocked in TBST with 3% normal goat serum for 1 hr. Mouse monoclonal antibodies to PSD-95 (#46; Affinity Bioreagents), NR1 (PharMingen), and synaptophysin (Sigma), and rabbit polyclonal antibodies to GluR1 (Upstate), synaptophysin (Sigma), GKAP (17), GAD-65 (gift from S. Baekkeskov), CaMKII, and PSD-93 were used. Dr. Frances Brodsky (University of California San Francisco) kindly provided rabbit polyclonal antibodies to Golgi 58K (TGN-38), and to the cation-independent mannose-6-phosphate-receptor (CI-M6PR). Primary antibodies were added to blocking solution for 1 hr at room temperature followed by donkey anti-mouse conjugated to Cy3 fluorophores (diluted 1:200 in blocking solution) for 1 hr. Coverslips were then mounted on slides (Frost Plus; Fisher) with Fluoromount-G (Southern Biotechnology Associates), and

images were taken under fluorescence microscopy with a 60x objective affixed to a Zeiss inverted microscope.

Quantitative Measurement of Protein Clustering and Receptor Internalization

Images of neurons were acquired with a CCD camera with a 60x oil-immersion objective (NA=1.4) affixed to a Zeiss inverted microscope and quantitated using Metamorph imaging software (Universal Imaging). Protein clustering was quantified on 10 fields chosen randomly from at least 3 independent neuronal cultures as previously described (El-Husseini et al., 2000a). For each neuron studied, the three largest caliber proximal dendrites (~20 μm length) were analyzed. To quantitate changes in clustering, the average pixel intensities of all synaptic clusters along these dendritic segments were measured in transfected and neighboring non-transfected cells, and data were analyzed by paired t-test. All clusters that co-localized with synaptophysin and were at least twice the background intensity were analyzed. Data were analyzed by t-test using two-tailed distribution and two-sample equal variance.

Internalization assays were done as described (Lin et al., 2000). Briefly, live hippocampal neurons were labeled with an antibody (5 μg / ml) to an extracellular epitope of GluR1 (Oncogene Research). After washing with PBS, neurons were incubated with 100 μM glutamate for 15 min, washed and fixed with 4% paraformaldehyde + 4% sucrose in PBS for 20 min, and then incubated with unlabeled anti-rabbit secondary antibodies for 1 hr to block staining of surface receptors. Cells

were then permeabilized with 0.25% Triton for 5 min, followed by incubation with anti-rabbit Cy3 to visualize internalized AMPA receptors. To avoid observer bias, slides were then coded and image analysis done without knowledge of the cDNA transfected. For image analysis, a cell was centered in the visual field and its body and dendrites within one visual field were analyzed. Automated analysis was performed using custom software routines in Northern Eclipse (EMPIX Imaging). For each cell analyzed, AMPA receptor internalization was quantitated as the fluorescence density of internalized AMPA receptor puncta. This value was normalized to the average density of non-transfected, non-treated cells. Statistical analysis was performed using the non-parametric Mann-Whitney test.

Primary Culture Electrophysiology

Whole-cell recordings were made at room temperature from 11-22 day old cultured neurons, with 3-6 MΩ patch pipettes. For PSD-95 GFP experiments, pipette solutions contained (in mM): 94 Cs-Gluconate, 2 CsCl, 8 TEA-Cl, 4 QX-314Cl, 7 NaCl, 8 HEPES, 0.2 EGTA, 3 MgATP, 0.3 Na_3GTP; 0.02-0.1% Lucifer yellow CH. For 2-bromopalmitate experiments, the pipette solution contained (in mM): 115 Cs-$MeSO_3$, 20 CsCl, 2.5 Mg_2Cl, 10 HEPES, 0.6 EGTA, 4 Na_2ATP, 10 Na-phosphocreatinine, 0.4 Na_3GTP. Cultures were continuously superfused with buffer containing (in mM) 112 NaCl, 3 KCl, 16 glucose, 8 HEPES, 2 $CaCl_2$, 2 $MgCl_2$, 0.1 picrotoxin, 0.001 TTX (saturated with 95%O_2 / 5%CO_2) at 1 ml/min. Cells were patched under visual guidance using a water immersion microscope. Transfected cells were identified prior to recording

using fluorescence. Current records were low-pass filtered at 2kHz, stored on tape and digitized off-line at 5kHz.

Cells were held at –70mV, and recording stability was monitored in real time using –4mV steps every 10 seconds. Series resistances ranged between 10 and 25 MΩ, and did not differ between treatment groups. Recordings were made for 2-10 minutes from each cell, depending on mEPSC frequency (cells with higher frequencies were recorded for less time). mEPSCs were analyzed with customized software (E. Schnell), using an amplitude threshold of 5 pA. In the case of recordings from transfected cells, neighboring transfected and untransfected cells were selected for recording to control for variability. In order to identify each cell as either a pyramidal cell or an interneuron, neurons were fixed with 4% PFA in PBS after recording. Lucifer Yellow was present in the internal solution during these experiments, and an image was obtained from the cell before fixation in order to facilitate subsequent identification. Fixed cells were identified after permeabilization and staining for GAD-65 (Fig. 1). Transfected and untransfected cells were compared using the unpaired t-test.

Prior to recording, some cultures were treated for 8 hours with 20μM 2-Br palmitate (or vehicle control) by a separate experimenter. An experimenter blinded with regard to 2-palmitate treatment performed all recordings and mEPSC analyses. For dual component mEPSC recordings, the external buffer contained 20 μM glycine, and magnesium was omitted.

To assess spine morphology, 21 - 22 DIV neurons were filled with 0.1% Lucifer yellow for 3 minutes, fixed in PFA, and stained for GAD-65 to exclude interneurons. Images were taken using a 100x oil immersion objective, and an observer blinded concerning neuronal transfection quantitated spine size and density.

Slice Culture Preparation and Transfection

Hippocampal slice cultures were prepared from 7-11 day old rats as described previously (Shi et al., 1999; Stoppini et al., 1991), and maintained on Millipore membrane filters at 37 ^{O}C in humidified 5% CO_2 for 3-7 days before transfection. Culture medium consisted of 25 % Hank's Balanced Salt Solution, 25% heat-inactivated fetal horse serum, and 50% MEM w/ Hank's salts, 25 mM HEPES, supplemented with 2 mM glutamine. Transfections were carried out with the Helios Gene Gun (Biorad), using 1.0 μm gold particles coated with DNA per the manufacturer's protocol. Each batch of approximately 30 bullets was made using 20 mg gold and 50 μg plasmid DNA. In the case of co-transfections, 50 μg of each construct was used (total 100 μg, mixed prior to DNA precipitation), except for the GFP-StarCterm experiments, in which the amount of PSD-95 was reduced to 20 μg. Bullets coated with two cDNAs reliably yielded co-expression in >90% of transfected cells when dsRed and PSD-95 GFP were co-transfected in preliminary experiments.

Slice Culture Electrophysiology

Recordings were made from transfected cells 1-4 days after transfection, using 2-3 MΩ glass electrodes filled with an internal solution consisting of 115 mM $CsMeSO_3$, 20 mM CsCl, 10 mM HEPES, 2.5 mM $MgCl_2$, 4 mM Na_2-ATP, 0.4 mM Na-GTP, 10 mM Na-phosphocreatine, 0.6 mM EGTA, and 0.1 mM spermine, pH 7.2. External perfusion medium consisted of 119 mM NaCl, 2.5 mM KCl, 2.5 mM $CaCl_2$, 1.3 mM $MgSO_4$, 2.7 mM $MgCl_2$, 1 mM NaH_2PO_4, 26.2 mM $NaHCO_3$, and 11 mM glucose, saturated with 95% O_2 and 5% CO_2, and included 100 μM picrotoxin, 20 μM bicuculline and 5-20 μM 2-Cl adenosine to block inhibition and suppress epileptiform activity. Transfected pyramidal cells were identified using fluorescence microscopy.

A bipolar tungsten stimulating electrode was placed in stratum radiatum approximately 100 μm from the cells. Recording electrodes were used to first establish cell-attached connections with both a transfected cell and an immediately adjacent untransfected cell under visual guidance (40x, DIC optics). Both cells were broken into simultaneously, and stimulation intensity was slowly increased until EPSCs were elicited from both cells. 50-100 trials were obtained at 0.33 Hz while holding the cells at –70 mV, followed by 50-100 trials while holding both cells at +40 mV. Series resistances were monitored during the experiment and typically ranged from 8-12 MΩ. A cell pair was discarded if the series resistances differed substantially between the two cells. AMPA-mediated whole cell currents were obtained from two cells simultaneously using a 10 minute bath perfusion of AMPA in the presence of 1 μM TTX. All statistics were obtained using paired t-tests.

A typical experiment is shown in Figure 2. All experiments involved simultaneous patch clamp recording from a transfected cell, in this case with GFP tagged PSD-95, and a neighboring untransfected cell. The relative magnitudes of the responses evoked by activating the same set of presynaptic afferents (associational/commissural fibers) were directly compared, allowing assessment of the effects of protein expression in the postsynaptic neuron on synaptic currents. The DIC image shows the two patch electrodes and a gold particle lodged in the nucleus of the successfully transfected cell on the right and fluorescence shows the punctate clustering of PSD-95 GFP.

Fixation and Confocal Microscopy

Slice cultures were fixed for use in confocal microscopy with 4% paraformaldehyde / 4% sucrose in phosphate-buffered saline overnight at 4 ^{O}C. Images were obtained by compiling Z-stacks of images made at 100x with 0.5 μm thick sections, using a Krypton-Argon laser and a BioRad MRC 1024 equipped with a 63x 1.4 NA oil-immersion objective attached to a Nikon microscope.

Figure 1. Determination of neuron type in dissociated culture recordings.

As hippocampal dissociated cultures are a mixture of excitatory and inhibitory neurons with distinct physiological properties, we determined the neurotransmitter phenotype of some neurons using post-hoc staining. To determine neurotransmitter phenotypes for all PSD-95-GFP transfected and untransfected cells, Lucifer yellow was injected during recording. Cultures were later stained for GAD-65. In this example, a PSD-95 GFP expressing cell (top image, taken before recording) was filled with Lucifer yellow (center image, during recording). Subsequent GAD-65 staining identified this cell as an inhibitory interneuron (bottom image).

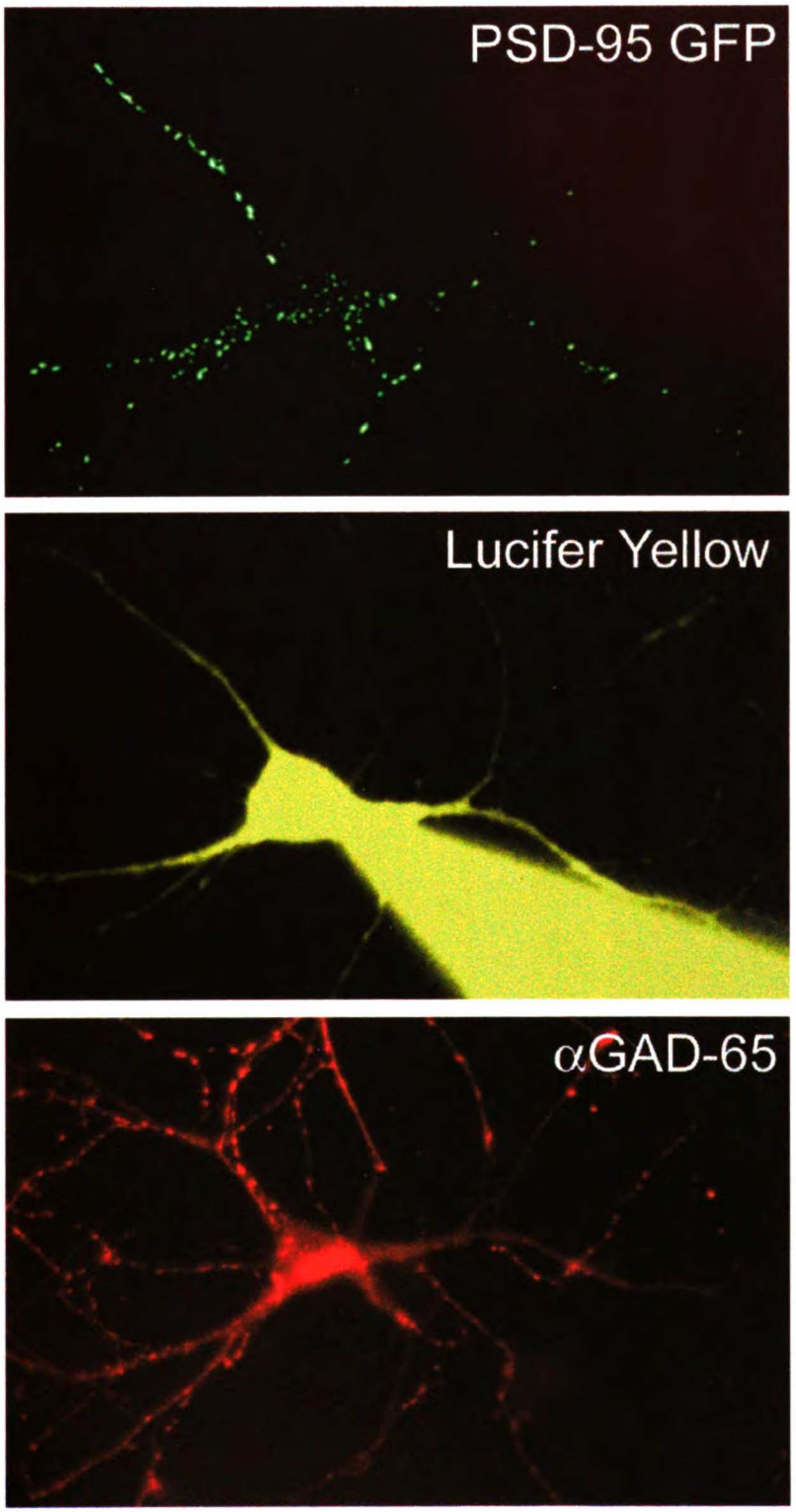
PSD-95 GFP
Lucifer Yellow
αGAD-65

Figure 2. Simultaneous paired recordings in hippocampal slice cultures.

Slice culture experimental configuration, involving simultaneous whole cell voltage-clamp recordings from both a transfected cell (PSD-95 GFP in this example, cell on right) and an immediately adjacent untransfected cell (on left). The left panel shows the DIC transmitted light image, with two pyramidal cells and two patch recording pipettes attached. A gold particle is visible in the nucleus of the transfected cell. The fluorescence image (center) shows the clusters of PSD-95 GFP in the spines of the transfected cell. The two images are overlaid on the right. Scale bar, 20 μm.

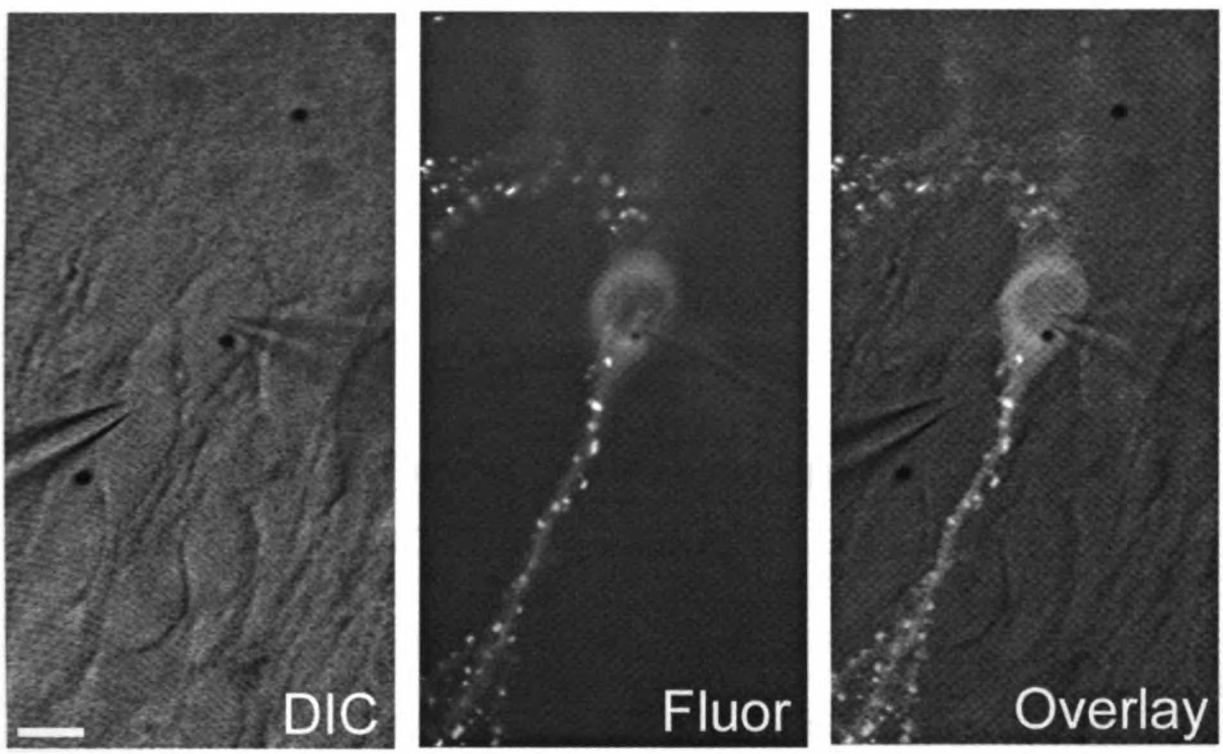
DIC
Fluor
Overlay

CHAPTER 3:

PSD-95 GFP Fusion Protein Construction and Analysis

Introduction

Rapid and efficient neurotransmission requires proper synaptic assembly of signal transducing protein networks. At excitatory synapses, glutamate receptors are clustered at the postsynaptic density (PSD), a thickening of the cytoskeleton beneath the plasma membrane. Also associated with the PSD are cytosolic enzymes including calcium calmodulin-dependent protein kinase II and neuronal nitric oxide synthase that modulate glutamatergic stimuli (Brenman et al., 1996a; Kennedy, 1998).

Although recent studies have helped to define the composition of the PSD (Craven and Bredt, 1998; Kornau et al., 1997; Sheng and Wyszynski, 1997), mechanisms for assembling protein complexes at postsynaptic sites are poorly understood. One attractive candidate is the postsynaptic density protein, PSD-95/SAP-90 (Cho et al., 1992; Kistner et al., 1993) that employs PDZ motifs to cluster proteins into complexes at synaptic sites (Brenman et al., 1996a; Kim et al., 1995; Kornau et al., 1995). PSD-95 has been hypothesized to act as a molecular scaffold to synaptically anchor Shaker type K+ channels, N-methyl-D-aspartate (NMDA) type glutamate receptors, and associated downstream signaling enzymes (Craven and Bredt, 1998; Kornau et al., 1997; Sheng and Wyszynski, 1997). Genetic analyses have highlighted these roles for MAGUK proteins in synaptic organization and function. Mutations of discs large (dlg), a MAGUK of Drosophila, perturb postsynaptic clustering of a Shaker type K+ channel at the larval

neuromuscular junction (Tejedor et al., 1997). Furthermore, targeted disruption of PSD-95 in mouse alters NMDA receptor mediated synaptic plasticity (Migaud et al., 1998).

Because postsynaptic protein clustering critically participates in both synaptogenesis and plasticity, mechanistic understanding of postsynaptic protein trafficking is an important goal. Some insight into mechanisms for protein sorting in neurons has been gained by comparison with polarized protein targeting in epithelial cells. Many transmembrane proteins that occur along the basolateral surface of epithelial cells have a somatodendritic or postsynaptic distribution in neurons whereas apical proteins of epithelial cells are typically found in neuronal axons (Dotti and Simons, 1990; Jareb and Banker, 1998; Rongo et al., 1998). Cellular analyses of epithelia have determined that targeting of transmembrane proteins to either the apical or basolateral membrane occurs in sorting endosomal compartments (Trowbridge et al., 1993). It is unclear whether similar sorting compartments mediate postsynaptic clustering in neurons or whether this type of processing would apply at all to a palmitoylated peripheral membrane protein, like PSD-95.

To clarify mechanisms for postsynaptic sorting and assembly of postsynaptic proteins, we constructed fluorescently labeled PSD-95 proteins and analyzed their trafficking in live cells. Strikingly, we found that PSD-95 is sorted with perinuclear vesicles in both heterologous cells and in developing neurons. Site-directed mutagenesis demonstrates that perinuclear vesicular sorting and ion channel clustering of PSD-95 in heterologous cells and its postsynaptic targeting in neurons all rely on palmitoylation of

cysteines 3 and 5. Replacing the palmitoylated NH2 terminus of PSD-95 with alternative palmitoylation motifs at either the NH2 or COOH terminus restores ion channel clustering and postsynaptic targeting. These data imply that PSD-95 is not merely a static cytoskeletal element but that PSD-95 is an itinerant vesicular protein and that initial targeting of PSD-95 to an intracellular membrane compartment may participate in postsynaptic ion channel clustering by PSD-95.

Results

PSD-95 Is Sorted with Perinuclear Vesicles in Heterologous Cells and in Neurons

To define cellular processes that mediate postsynaptic ion channel clustering by PSD-95, we first analyzed the subcellular distribution of exogenous PSD-95 expressed in various cell lines. 12 h after transfection of COS cells, wild-type or tagged versions of PSD-95 occur diffusely throughout the cytoplasm but are also conspicuously concentrated at a perinuclear compartment (Fig. 1A, top). To determine whether this transient perinuclear localization of PSD-95 corresponds to a specific organelle, transfected cells were double-stained for PSD-95 and either the mannose-6-phosphate receptor, Golgi 58K, TGN38, or DND-99 (Lysotracker). The perinuclear localization of PSD-95 corresponds to that of the mannose 6-phosphate receptor (M6PR; Fig. 1B and C), a well-characterized marker of late endosomes (Griffiths et al., 1988). PSD-95 localization only partially overlaps that of the Golgi markers, Golgi 58K, and TGN38;

PSD-95 does not overlap at all with the lysosomal marker DND-99 (Fig. 1B and data not shown).

As found in COS cells, PSD-95 expressed in either HEK293 or PC12 cells also coincides with the M6PR positive compartment (Fig. 1A, bottom, and data not shown). Furthermore, in developing hippocampal neurons we find that transfected PSD-95 GFP (not shown) and endogenous PSD-95 (Fig. 2) transiently colocalize with the M6PR during the first 2 d in culture. A similar perinuclear localization is observed for NMDA receptor subunits NR1 and NR2B (Fig. 2). By contrast, the microtubule-associated protein, MAP2, occurs in developing neurites and is not concentrated in the perinuclear domain. As the neurons mature, PSD-95 becomes less concentrated in this perinuclear domain and begins to accumulate in small clusters along the processes (Fig. 2).

Accumulation of PSD-95 at the Perinuclear Domain Is Brefeldin A- and Nocodazole-sensitive

To help to determine whether sorting of PSD-95 to the perinuclear domain requires active vesicular trafficking, we treated PSD-95–expressing heterologous cells with BFA. BFA has multiple and diverse effects on vesicular trafficking in cells including disassembly of the Golgi complex (Lippincott-Schwartz et al., 1991). 2 h after transfection, before PSD-95 accumulates in the perinuclear compartment, treatment with BFA completely prevents the accumulation of PSD-95 (Fig. 3A); instead PSD-95 protein occurs diffusely throughout the cytoplasm. However, addition of BFA after the perinuclear accumulation of PSD-95 does not alter the localization of PSD-95 or its

colocalization with M6PR even after prolonged (8 h) treatment (data not shown). These results indicate that accumulation of PSD-95 depends on trafficking through the secretory pathway, but that the perinuclear vesicular domain in which PSD-95 resides is a compartment distinct from the Golgi complex. In contrast, nocodazole, which depolymerizes microtubules and not only disperses Golgi-derived tubules but also endosomes (Cole et al., 1996), blocks accumulation of PSD-95 at the perinuclear compartment and disperses both PSD-95 and the M6PR to similar vesicular structures within the cell (Fig. 3A). These results suggest that PSD-95 accumulates in a perinuclear endosomal compartment rather than in the Golgi complex.

Vesicular Sorting of PSD-95 Requires a Short NH2-terminal Palmitoylated Motif

We next determined the region(s) of PSD-95 sufficient for its association with the perinuclear vesicular domain. We first transfected COS cells with a series of progressively larger deletion constructs encoding PSD-95 fused to GFP. This deletion analysis showed that a construct containing the first nine amino acids of PSD-95 fused to GFP occurs diffusely when expressed in COS cells, whereas constructs containing the first 13, 26, 46, or 64 amino acids all transiently accumulate at the perinuclear domain, just like full-length PSD-95 (Fig. 3B).

To determine whether association of PSD-95 with perinuclear vesicles requires NH2-terminal palmitoylation, we evaluated the distribution of palmitoylation-deficient mutants. Mutation of cysteine 3 or 5 of PSD-95 to serine prevents palmitoylation (Topinka and Bredt, 1998), and these mutations completely disrupt vesicular sorting of

PSD-95 in COS cells (Fig. 3C). Instead, the palmitoylation-deficient mutants occur diffusely throughout the cells. To determine if a dually palmitoylated motif is sufficient for vesicular trafficking of PSD-95, we replaced amino acids 1–13 of PSD-95 with the first 12 amino acids of growth-associated protein-43 (GAP-43), another dually palmitoylated motif. Indeed, this chimeric protein (GAP/PSD-95) was efficiently palmitoylated (Fig. 4C) and trafficked to the same perinuclear compartment as wild-type PSD-95 (Fig. 3B).

PSD-95 Localizes to Intracellular Membranes and to the PSD in Cortical Neurons

To determine whether PSD-95 also associates with membranous intracellular structures of neurons within intact brain, we performed electron microscopic immunocytochemical staining of the rat cerebral cortex, using a well characterized anti–PSD-95 antiserum (Brenman et al., 1996b) and established methods for immunocytochemical staining (Aoki et al., 1999b). Previous ultrastructural studies of PSD-95 in forebrain have been limited to a few studies focusing on the localization of PSD-95 at PSDs (Aoki et al., 1998; Hunt et al., 1996; Valtschanoff et al., 1999). Consistent with that work, we have found using the post-embedding gold method that labeling for PSD-95 occurs at the PSDs of >89% of cortical synapses (Aoki et al., 1999a). However, we also find, using a silver-intensified gold pre-embedding method (Chan et al., 1990), that PSD-95 localizes to nonsynaptic sites (Fig. 5A) and is often found in association with the cytosolic surface of membranous intracellular structures. Figure 5B shows an example of PSD-95 immunoreactivity associated with intracellular smooth endoplasmic reticulum in a dendritic shaft of a cortical neuron. In a nearby

synaptic spine PSD-95 immunoreactivity is associated with the spine apparatus adjacent to an unlabeled PSD of an asymmetric synapse (Figure 5B).

Postsynaptic Targeting of PSD-95 Requires Dual Palmitoylation

To evaluate the role of dual palmitoylation in postsynaptic sorting of PSD-95, we evaluated targeting of a series of NH2-terminal mutants in primary hippocampal neurons (at DIV 12). We found that the wildtype, dually palmitoylated PSD-95 GFP targeted appropriately to postsynaptic dendritic clusters (Figure 6A, also see (Craven et al., 1999)). By contrast, a nonpalmitoylated construct (Cys3Ser) occurred diffusely in dendrites of transfected neurons (Figure 6A, also (Craven et al., 1999)). Adding the NH2-terminal dually palmitoylated motif of GAP-43 or the COOH-terminal prenylated and dually palmitoylated motif of paralemmin to PSD-95(C3,5S) significantly restores postsynaptic targeting (Figure 6B).

Ion Channel Clustering by PSD-95 Requires Dual Palmitoylation

Certain aspects of channel clustering by MAGUK proteins can be reproduced in a coclustering experiment in heterologous cells (Kim et al., 1995). In this assay, cotransfection of PSD-95 with Shaker K+ channel Kv1.4 causes a striking redistribution of both proteins to raft-like clusters on the cell surface (Figure 7A).

To define the role for dual palmitoylation in ion channel clustering we analyzed a the non-palmitoylated PSD-95:C3,5S mutant. We found that PSD-95:C35S did not form

coclustered membrane patches when coexpressed with Kv1.4 (Figure 8A). Furthermore, the NH2-terminal palmitoylated motif of GAP-43 or the COOH-terminal palmitoylated motif of paralemmin can functionally substitute for the PSD-95 NH2 terminus to mediate ion channel clustering (Figure 8B).

Finally, minimal constructs of PSD-95 were designed to define the absolute requirements for ion channel clustering. Kv1.4 clustering is induced by the expression of a construct containing only the first 26 amino acids of PSD-95 fused to PDZ domains 1 and 2. In addition, a construct containing GAP-43, fused to only PDZ domains 1&2 of PSD-95 is capable of clustering Kv1.4 (Figure 8C). These experiments establish that ion channel clustering by PSD-95 requires (a) dual palmitoylation and (b) an appropriate PDZ domain.

Discussion

This work demonstrates that dual palmitoylation of PSD-95 mediates a transient association with perinuclear vesicles and that this lipid modification is also essential for ion channel clustering and postsynaptic targeting. Importantly, mutations that disrupt dual palmitoylation block perinuclear trafficking, postsynaptic targeting, and ion channel clustering activity of PSD-95.

Synaptic Targeting and Ion Channel Clustering by PSD-95 Require Dual Palmitoylation

This work emphasizes the central role for NH2-terminal palmitoylation in protein sorting by PSD-95. Previous studies noted essential roles for cysteines 3 and 5 in both receptor clustering (Hsueh et al., 1997) and postsynaptic targeting of PSD-95 (Craven et al., 1999). Although these cysteines were identified as sites of palmitoylation (Topinka and Bredt, 1998), it was unclear how this lipid modification participates in synaptic clustering. Several lines of evidence developed here indicate that palmitoylation may mediate ion channel clustering by initially targeting PSD-95 to the cytosolic surface of intracellular vesicles. First, localization of PSD-95 to perinuclear vesicles in heterologous cells and developing neurons requires an NH_2-terminal consensus that supports dual palmitoylation. Second, mutations that disrupt sorting of PSD-95 to the perinuclear domain prevent both ion channel clustering in heterologous cells and postsynaptic sorting in neurons. In addition, the palmitoylated NH_2 terminus of PSD-95 can functionally be replaced with other NH2- or COOH-terminal palmitoylation motifs to mediate ion channel clustering or postsynaptic targeting. Although these mutagenesis experiments can provide only indirect evidence, they do demonstrate a strict correlation between vesiculotubular trafficking and receptor clustering by PSD-95. Taken together, these results support a role for vesicular trafficking in sorting and clustering of PSD-95 at synaptic sites.

Implications for Synaptic Plasticity Regulated by MAGUK Proteins

Mice with mutant PSD-95 protein have a dramatic shift in NMDA receptor-dependent plasticity in hippocampus such that long-term depression (LTD) is blocked and long-term potentiation (LTP) is enhanced (Migaud et al., 1998). These abnormalities in synaptic plasticity presumably explain why the mutant mice are impaired in a spatial learning task. As postsynaptic signaling cascades downstream of NMDA receptors play critical roles in LTP and LTD, it seems likely that PSD-95 plays an essential role in linking NMDA receptors to these pathways.

How PSD-95 assembles these signaling complexes, however, remains uncertain. Previous models, based on the assumption that PSD-95 and other MAGUKs are static elements of the postsynaptic cytoskeleton suggested a passive role for these proteins in simply retaining receptor clusters and associated signaling enzymes at the synapse (Zito et al., 1997). The trafficking of PSD-95 with vesiculotubular intermediates here suggests an alternative mechanism, interaction of PSD-95 with the cytosolic tails of receptors residing in intracellular vesicles followed by insertion of these ion channel complexes into the plasma membrane. Such a model for interaction of PSD-95 with ion channels in sorting endosomes provides a mechanism to help explain recent work showing that PSD-95 regulates polarized trafficking of Kv1.4 (Arnold and Clapham, 1999). Interestingly, recent work suggests that other multi-PDZ domain proteins involved in synaptic organization including the glutamate interacting protein (GRIP) and LIN-10 also associate with post-Golgi vesicles (Rongo et al., 1998; Xia et al., 1999). This may

indicate a common role for PDZ proteins in transport of receptor-containing vesicles. Such a dynamic mechanism would allow for precise and regulated assembly of synaptic transduction machinery.

Figure 1. PSD-95 is sorted to a vesicular perinuclear domain.

(A) Exogenous PSD-95 accumulates at a perinuclear domain in transfected COS (top), HEK-293 and PC12 cells (bottom). Cells were transfected with either wild-type PSD-95 (PSD-95 WT), PSD-95 fused to GFP (PSD-95 GFP) or FLAG-epitope tagged PSD-95 (PSD-95 FLAG). (B) In COS cells, perinuclear staining for PSD-95 (green) partially overlaps with a Golgi marker Golgi 58K (red) and with a trans-Golgi marker TGN-38 (red), but extensively colocalizes with a late endosomal marker, mannose-6-phosphate receptor (red; M6PR). (C) High magnification shows colocalization of PSD-95 with M6PR. Merged images are shown in the right panels for B and C. Scale bars, 10 μm.

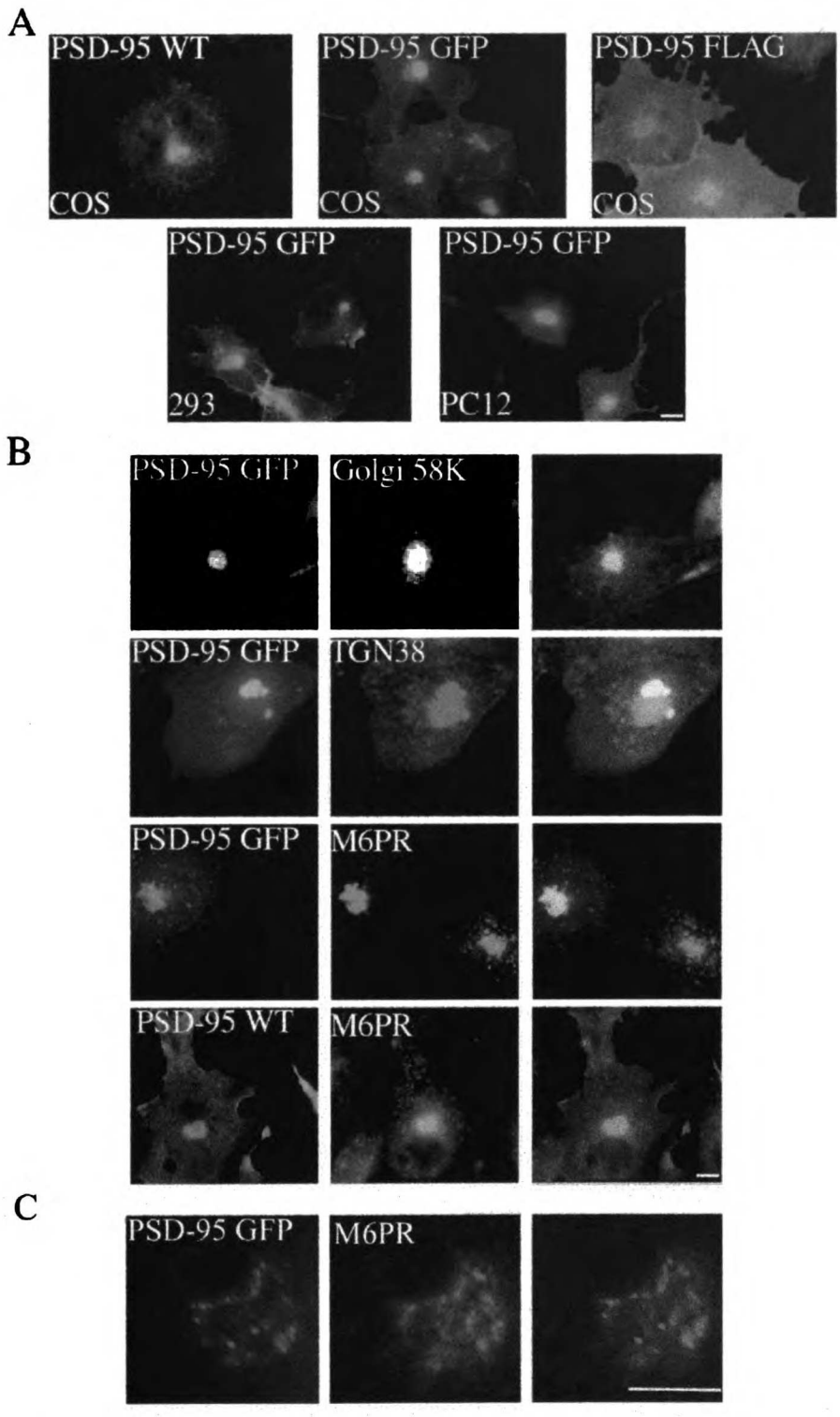
A
PSD-95 WT
COS
PSD-95 GFP
COS
PSD-95 FLAG
COS
PSD-95 GFP
293
PSD-95 GFP
PC12
B
PSD-95 GFP
Golgi 58K
PSD-95 GFP
TGN38
PSD-95 GFP
M6PR
PSD-95 WT
M6PR
C
PSD-95 GFP
M6PR

Figure 2. Accumulation of PSD-95 at a perinuclear domain precedes dendritic clustering in primary hippocampal neurons.

Endogenous PSD-95 expression in developing hippocampal neurons is shown at 1 d (DIV1) and 4 d (DIV4) in vitro. The expression pattern of PSD-95 (green) is compared with the endosomal marker M6PR (red) and merged images are shown in the right panels. At DIV1, PSD-95 shows strong perinuclear staining that coincides with M6PR. NMDA receptor subunits, NR1 and NR2B, colocalize with PSD-95 and M6PR at DIV1 whereas MAP2 shows diffuse staining in the soma and processes. By DIV4, PSD-95 occurs diffusely in the soma, and at this stage clusters begin to form in the neurites (arrowheads). Scale bar, 10 μm.

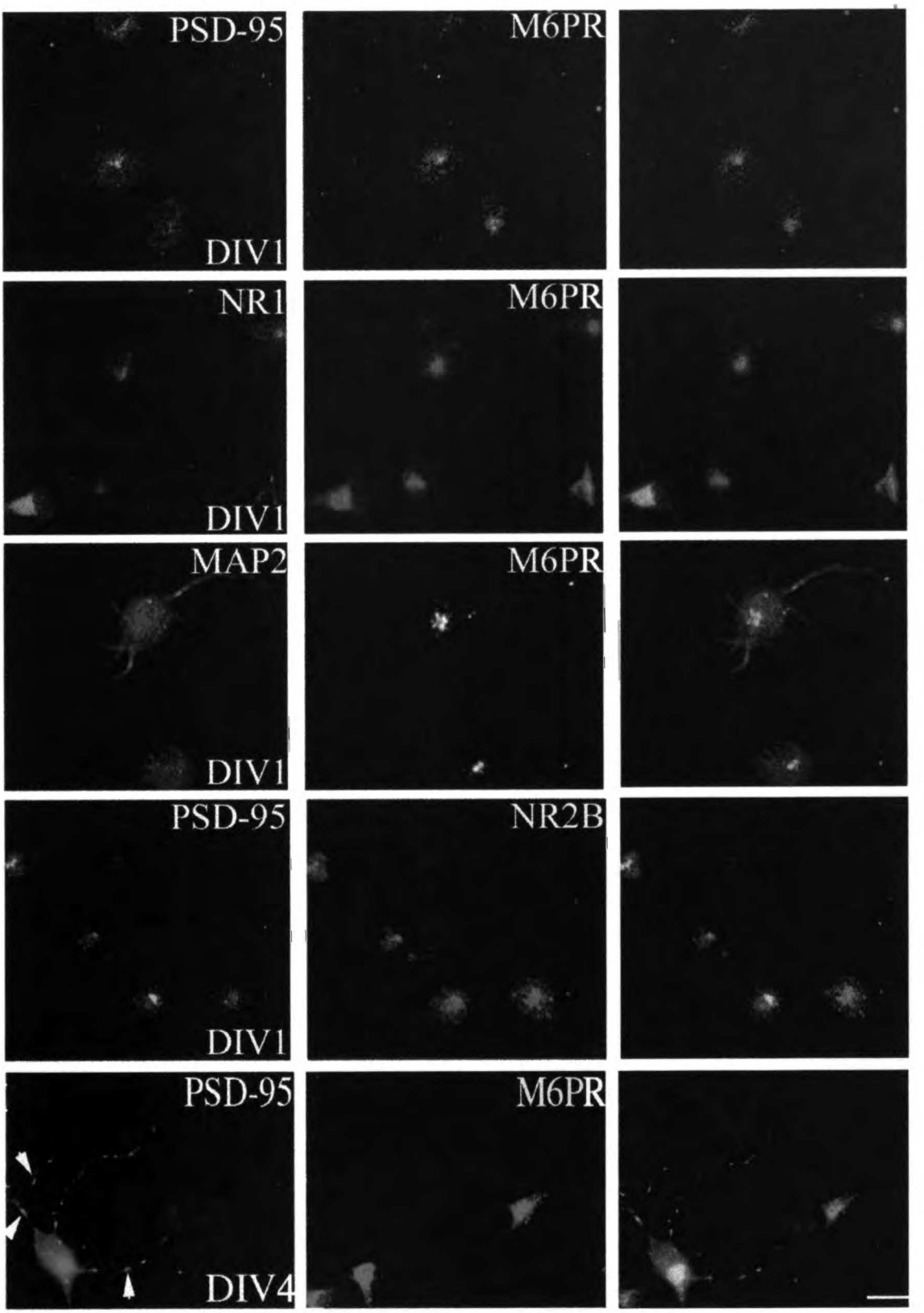
PSD-95
M6PR
DIV1
NR1
M6PR
DIV1
MAP2
M6PR
DIV1
PSD-95
NR2B
DIV1
PSD-95
M6PR
DIV4

Figure 3. Perinuclear accumulation of PSD-95 relies on the palmitoylation motif and requires a functional secretory pathway and intact microtubules.

(A) COS cells were transfected with PSD-95. 2 h after transfection, cells treated for 7 h with either vehicle or 10 μg/ml BFA, or 20 μg/ml nocodazole and were examined 8 h later for PSD-95 (green) and M6PR (red). For the nocodazole-treated cells, arrowheads point to the single cell in the field transfected with PSD-95 (bottom). (B) Targeting of PSD-95 to a M6PR-positive perinuclear compartment is mediated by an NH_2-terminal palmitoylated motif. Amino acids 1–13 but not 1–9 are sufficient for targeting GFP to the perinuclear, M6PR-positive compartment. Perinuclear accumulation is also observed with GFP-fusion constructs containing amino acids 1–26, 1–46,and 1–64. A chimera containing the first 12 amino acids of GAP-43 fused PSD-95 (GAP/PSD-95) is also sorted to the perinuclear domain. (C) Mutations in the palmitoylation motif dramatically affect perinuclear vesicular sorting. Mutations of Cys3 and/or 5 to Ser (C3,5S, C3S, C5S) disrupt vesicular sorting. (D) An enlarged image shows in greater detail the localization of PSD-95 along vesiculotubular structures that resemble Golgi-derived tubules (arrowheads) and also to a perinuclear region (arrows). Scale bar, 10 μm.

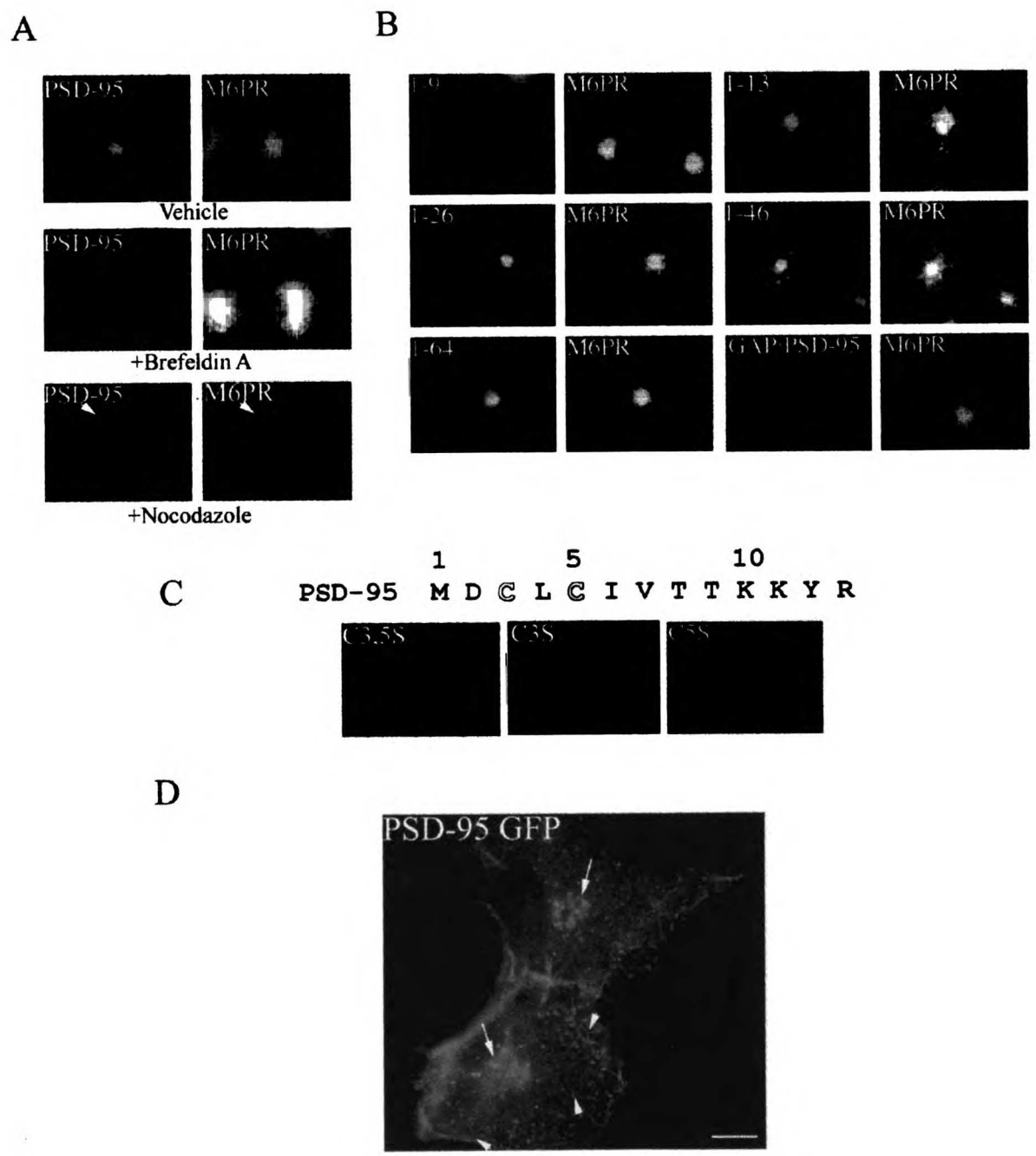
A
PSD-95
M6PR
Vehicle
PSD-95
M6PR
+Brefeldin A
PSD-95
M6PR
+Nocodazole
B
1-9
M6PR
1-13
M6PR
1-26
M6PR
1-46
M6PR
1-64
M6PR
GAP-PSD-95
M6PR
C
1 5 10
PSD-95 M D C L C I V T T K K Y R
C3,5S
C3S
C5S
D
PSD-95 GFP

Figure 4. Palmitoylation of PSD-95 and GAP-43.

(A) Schematic illustration of the domain structure of PSD-95 and sequence alignment of the NH2 terminus of PSD-95 with GAP-43. (B) Analysis of PSD-95 deletion mutants shows that amino acids 1–13 are sufficient for efficient palmitoylation. (C) Mutating Cys3 or 5 to Ser blocks palmitoylation. A chimera containing the first 12 amino acids of GAP-43 fused to PSD-95 (GAP/PSD-95) is efficiently palmitoylated.

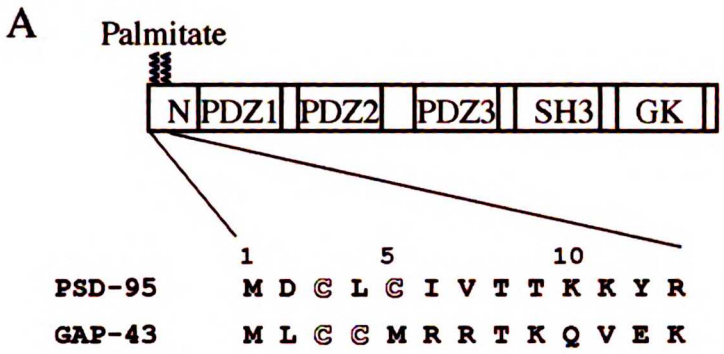
A
Palmitate
N
PDZ1
PDZ2
PDZ3
SH3
GK
1
5
10
PSD-95 M D C L C I V T T K K Y R
GAP-43 M L C C M R R T K Q V E K

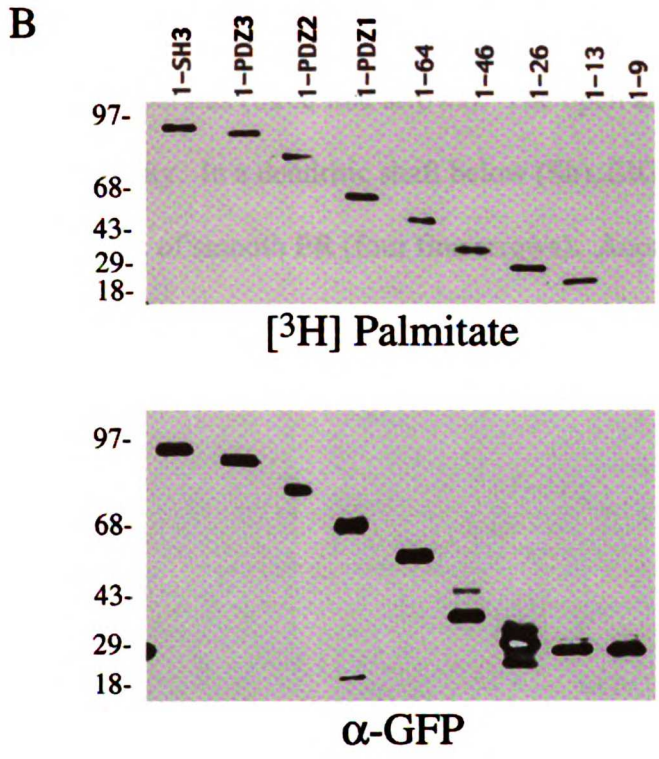
B
1-SH3
1-PDZ3
1-PDZ2
1-PDZ1
1-64
1-46
1-26
1-13
1-9
97-
68-
43-
29-
18-
[3H] Palmitate
97-
68-
43-
29-
18-
α-GFP

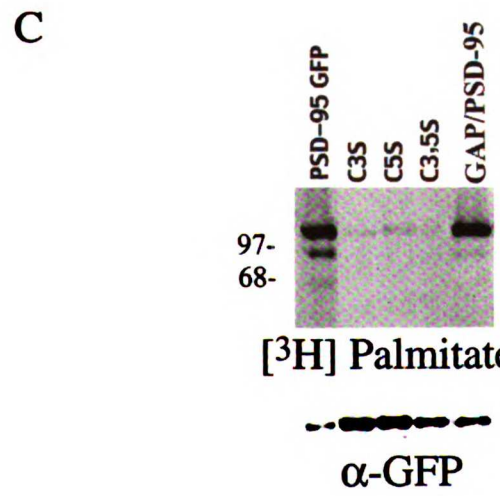
C
PSD-95 GFP
C3S
C5S
C3,5S
GAP/PSD-95
97-
68-
[3H] Palmitate
α-GFP

Figure 5. Ultrastructural localization of PSD-95 at synaptic and nonsynaptic sites. The silver-intensified colloidal gold (SIG) method was used for electron micrographic immunolabeling of PSD-95 in visual cortex. (A) Gold particles are associated with the PSD within a spine (arrowhead in Sp1) that opposes an unlabeled terminal, T. Two other spines (Sp2 and Sp3) are without SIG immunolabeling. Within the dendritic shaft (Sh), immunoreactivity is associated with the plasma membrane (curved arrow) and elsewhere. (B) Within a dendritic spine (Sp) of an asymmetric synapse, PSD-95 (dark arrow) is associated with the spine apparatus (three fine arrows). The open arrow points to the unlabeled postsynaptic density. In a dendritic shaft below (Sh), SIG label (curved arrow) is associated with a complex of smooth ER (four fine arrows). Another shaft, to the left of Sp, exhibits immunoreactivity in the cytoplasm, as is shown in A. Scale bar, 500 nm.

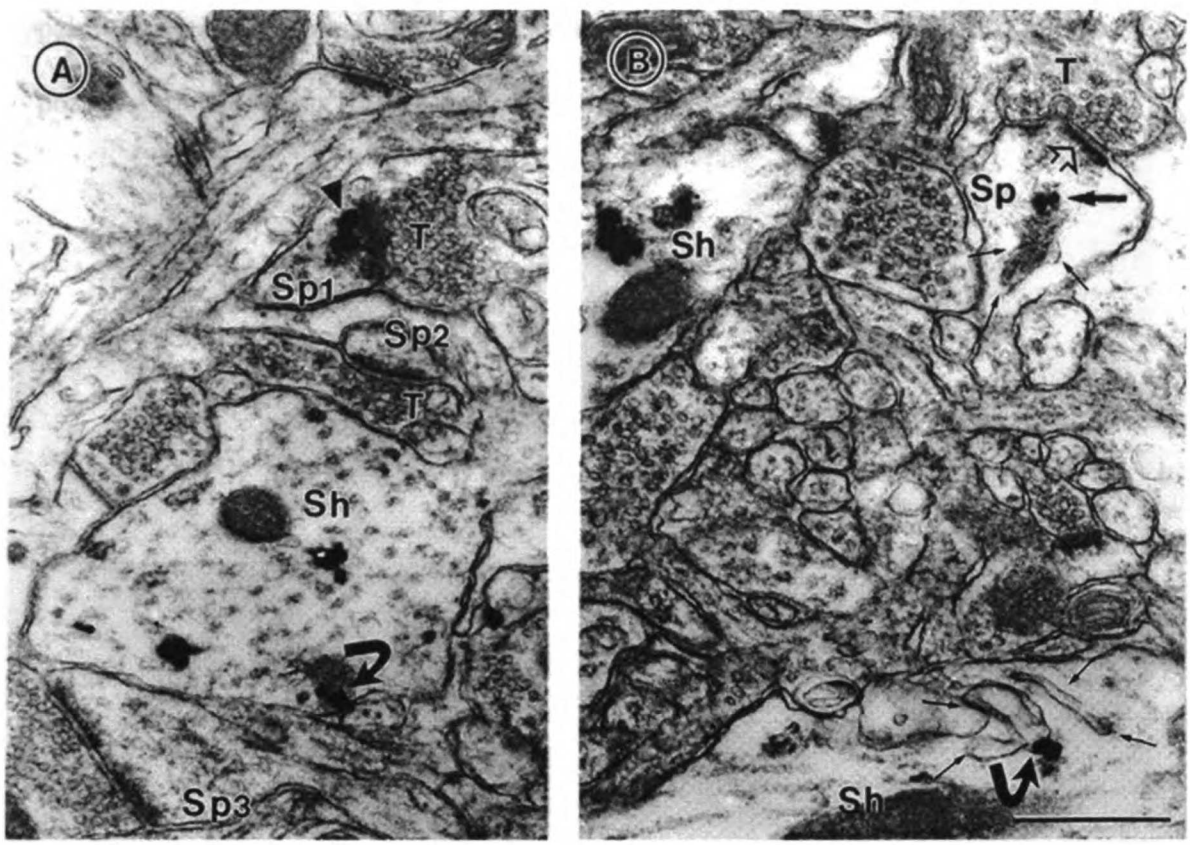
A
T
Sp1
Sp2
T
Sh
Sp3
B
T
Sp
Sh
Sh

Figure 6. Postsynaptic targeting of PSD-95 in hippocampal neurons requires the NH2-terminal dually palmitoylated motif.

(A) A mutation that blocks PSD-95 palmitoylation disrupts postsynaptic targeting of PSD-95. Mutation of Cys3 to Ser (C3S) abolishes protein palmitoylation and synaptic targeting. (B) A chimera containing the first 12 amino acids of GAP-43 fused to PSD-95 (GAP/PSD-95) is targeted to postsynaptic sites. The COOH-terminal 12–amino acid palmitoylated motif of paralemmin fused to PSD-95:C3,5S (PSD-95/Parlm) induces postsynaptic clustering of a PSD-95 (C3,5S) mutant. Scale bars, 10 μm.

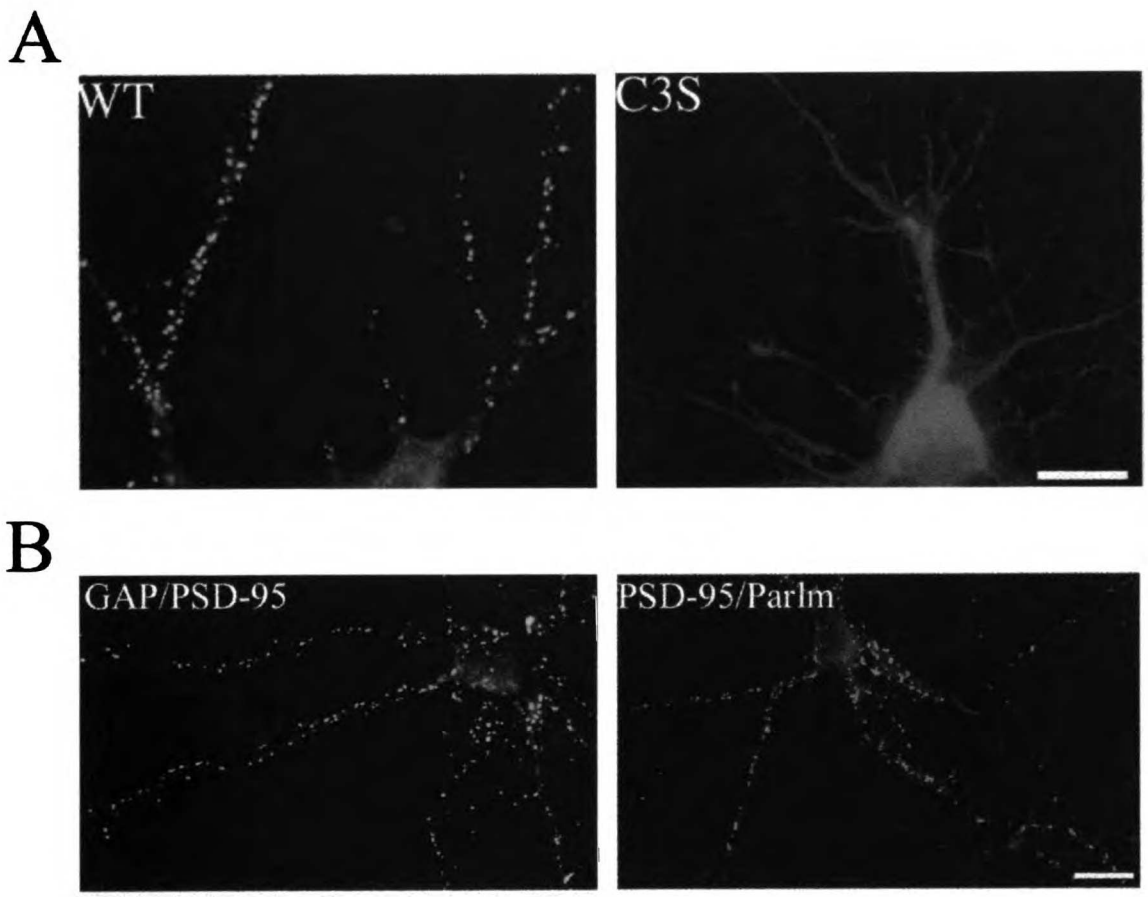
A
WT
C3S
B
GAP/PSD-95
PSD-95/Parlm

Figure 7. Ion channel clustering requires dual palmitoylation of PSD-95.

COS cells were cotransfected with Kv1.4 and PSD-95 (Wild-type or C3,5S). Cells were fixed 12 h (12h) after transfection and double-labeled with antibodies to PSD-95 (green) and Kv1.4 (red). Wildtype PSD-95 causes clustering of Kv1.4, while the palmitoylation-deficient PSD-95 (C3,5S) does not. (B) Chimeras containing the first 12 amino acids of GAP-43 fused to PSD-95 (GAP/PSD-95) or the last 12 amino acids of paralemmin fused to PSD-95 C3,5S (PSD-95/Parlm) mediate clustering of Kv1.4. (C) Cotransfection of Kv1.4 with a construct containing either the first 300 amino acids of PSD-95 (1-PDZ2) or amino acids 1-26 fused to PDZ1&2 (1-26-PDZ1&2) are sufficient for clustering Kv1.4. A construct containing full-length GAP-43 fused to PDZ domains 1 and 2 (GAP43-PDZ) but not GAP-43 itself also induces channel clustering. Scale bar, 10 μm.

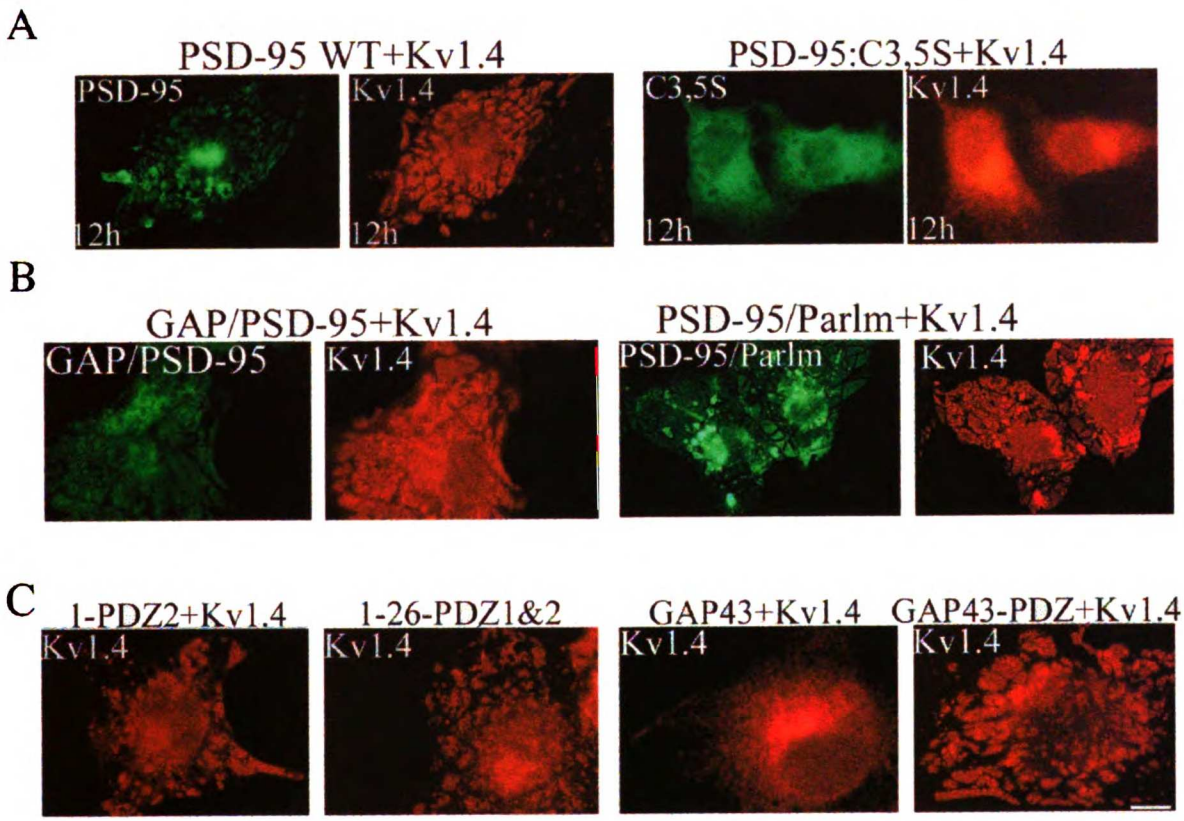
A
PSD-95 WT+Kv1.4
PSD-95
Kv1.4
12h
12h
PSD-95:C3,5S+Kv1.4
C3,5S
Kv1.4
12h
12h
B
GAP/PSD-95+Kv1.4
GAP/PSD-95
Kv1.4
PSD-95/Parlm+Kv1.4
PSD-95/Parlm
Kv1.4
C
1-PDZ2+Kv1.4
Kv1.4
1-26-PDZ1&2
Kv1.4
GAP43+Kv1.4
Kv1.4
GAP43-PDZ+Kv1.4
Kv1.4

CHAPTER 4:

PSD-95 Overexpression Drives Synapse Maturation

Introduction

Despite the central role for synapses in neuronal function, mechanisms underlying synapse formation remain incompletely understood. Recently, proteins containing PDZ motifs have been proposed as molecular scaffolds for receptors and cytoskeletal elements at synapses (Craven and Bredt, 1998; Garner et al., 2000; Kennedy, 1998; Lee and Sheng, 2000). The prototypical PDZ protein, postsynaptic density-95 (PSD-95 / SAP90) is a membrane-associated guanylate kinase (MAGUK) concentrated at glutamatergic synapses (Cho et al., 1992; Kistner et al., 1993). PSD-95 may participate in synapse development because it clusters at synapses before other postsynaptic proteins (Rao et al., 1998), and because *discs large*, a PSD-95 homolog in *Drosophila*, is necessary for proper development of larval neuromuscular junctions (Lahey et al., 1994). Despite numerous studies it remains uncertain whether PSD-95 participates in synapse development in mammals. Targeted disruption of PSD-95 in mice does not alter synaptic structure (Migaud et al., 1998) possibly because three other MAGUKs and dozens of other PDZ proteins occur at brain synapses. This molecular redundancy has obscured understanding of functions for PSD-95 and other PDZ proteins in brain.

We overexpressed PSD-95 to help define its roles. GFP-tagged versions of PSD-95 target faithfully to postsynaptic sites in hippocampal neurons, despite being overexpressed 5-10 times above endogenous levels (Arnold and Clapham, 1999; Craven et al., 1999). We used lipid-mediated gene transfer techniques to introduce PSD-95 GFP into dissociated neuronal cultures at an early stage (day 0-1 in vitro), to assess how a prolonged increase in PSD-95 level affects synaptic structure and function.

Results

PSD-95 Overexpression Enhances GluR1, but not NR1, staining

To evaluate influences of PSD-95 on synaptic development, we analyzed cultures at early developmental stages, day *in vitro* (DIV) 10-12, and noted an increase of glutamate receptor subunit-1 (GluR1) immunofluorescence at postsynaptic sites of neurons transfected for PSD-95 (Fig. 1A). This increase was detected both in permeabilized cells with an antibody to a cytosolic GluR1 epitope (Fig. 1A) and in live cells with an antibody to an extracellular site (Fig. 2B). When compared to neighboring untransfected cells, neurons overexpressing PSD-95 exhibited synaptic GluR1 labeling approximately 250% of control. By contrast, PSD-95 overexpression did not alter synaptic clustering of N-methyl-D-aspartate receptor-1 (NR1) (Fig. 1B). These results are surprising because PSD-95 directly binds to NMDAR but not to GluR (Kennedy, 1998; Lee and Sheng, 2000). This suggests that PSD-95 may have an unexpected role in synaptic assembly.

We wondered whether these postsynaptic effects of PSD-95 overexpression occur in both excitatory pyramidal neurons and inhibitory interneurons. Glutamic acid decarboxylase- (GAD-) negative pyramidal neurons had a punctate distribution for PSD-95 and GluR1 at spiny protrusions of the dendritic membrane, whereas the GAD-positive interneurons showed more linear clustering along the dendritic shaft (Fig. 1C, D). Quantitating the intensity of synaptic staining showed that PSD-95 transfection selectively enhanced GluR1 clustering in both pyramidal cells and interneurons (Fig. 1D, E) and the synaptic GluR1 fluorescence intensity correlated with the PSD-95 expression

(Fig. 3). Overexpression of other postsynaptic proteins including CaMKII and nNOS did not influence GluR1 clustering (Fig. 2; data not shown).

PSD-95 Overexpression Enhances mEPSC Amplitude

To determine whether this PSD-95 mediated enhancement of GluR1 clustering augments postsynaptic function, we measured miniature excitatory postsynaptic currents (mEPSCs). Each recorded cell was identified as excitatory or inhibitory by injecting with Lucifer Yellow and double labeling for GAD-65 (Chapter 2; Fig. 1). GAD-positive interneurons in our cultures had larger and more numerous mEPSCs than GAD-negative pyramidal neurons (Figs. 4A, 5A), consistent with differences in GluR1 clustering detected anatomically (Fig. 1C). For both pyramidal cells and interneurons, transfection with PSD-95 augmented the amplitude of mEPSCs, indicating that the additional GluRs recruited by PSD-95 are functional (Figs. 4, 5). The frequency of mEPSCs was also enhanced by PSD-95 transfection (Figs. 4, 5).

We compared mEPSC amplitudes and frequencies of PSD-95 transfected and untransfected cells at various ages after plating. For both pyramidal cells (Fig. 6) and interneurons (Fig. 7), the mEPSC enhancement mediated by PSD-95 overexpression was observed at both early and late time-points. For untransfected pyramidal cells, mEPSC amplitude and frequency increased as development *in vitro* progressed (Fig. 6), as has been noted previously (Gomperts et al., 2000). PSD-95 transfected cells recorded at DIV 11-13 had a similar mEPSC amplitude as untransfected cells recorded at DIV 21-22 (Fig. 6A), suggesting that PSD-95 transfection accelerated synaptic development. Untransfected interneurons, on the other hand, did not show an increase in mEPSC

amplitude as development progressed (Fig. 7A), but did show a gradual increase in mEPSC frequency (Fig. 7B). At various timepoints during development, PSD-95 GFP expression increased both mEPSC amplitude and frequency in interneurons (Fig. 7).

PSD-95 Overexpression Enhances Presynaptic Size and Function

Although increases in mEPSC frequency typically reflect increased probability of transmitter release, an enlarged mEPSC amplitude can also increase apparent frequency, because very small events can be amplified to the detection threshold. To determine whether a change in mEPSC detection might account for the increase in frequency, we made additional recordings from cultured neurons at different holding potentials to manipulate mEPSC amplitude. In these conditions, mEPSC amplitude was changed by altering the ionic driving force without altering the actual presynaptic release frequency. Thus, all changes in frequency could be attributed to changes in mEPSC amplitude and detectability.

In these experiments, an increase of mEPSC amplitude which corresponded to the observed difference between untransfected and PSD-95 transfected pyramidal cells (from 8.4 ± 0.3 pA to 11.4 ± 0.2 pA, n = 4) was associated with a 2.9 ± 0.6 fold increase in the mEPSC frequency (Fig. 8). As the transfected neurons had a 9.8 ± 2.9 fold greater mEPSC frequency, a change in mEPSC detection is unable to account for the increase in frequency, suggesting that either a change in presynaptic function or an increase in the number of AMPA-receptor containing synapses had occurred.

An increase in mEPSC frequency can result from an increase in the probability of transmitter release from an individual synapse and / or from an increase in the number of synapses. It has been reported that the probability of release is related to the size of the vesicle pool (Murthy et al., 1997). Given a lack of change in the number of synapses contacting PSD-95 transfected cells in DIV 12 neurons (untransfected, GluR1 puncta 0.614 ± 0.054 μm^{-1}, PSD-95-GFP, 0.714 ± 0.054 μm^{-1}, $p>0.05$), we concluded that much of the change in mEPSC frequency was due to an increase in release probability.

We therefore assessed the possibility that postsynaptic expression of PSD-95 might alter the presynaptic terminal. Staining for synaptophysin and SV-2 were enhanced in axon terminals contacting postsynaptic sites of PSD-95 transfected pyramidal cells (Figs. 9A, 10) as well as interneurons (synaptophysin density = 203 ± 6% of control). We also labeled transfected cultures with FM4-64, which marks sites of synaptic vesicle endocytosis (Cochilla et al., 1999). Labeling by FM4-64 was strikingly enhanced at presynaptic sites that oppose postsynaptic sites labeled by PSD-95-GFP (FM4-64 intensity = 184 ± 17% of control; Fig. 9B, 10B), suggesting a larger presynaptic vesicle pool size and supporting our physiological data of increased presynaptic release (Figs. 4, 5).

PSD-95 Overexpression Enhances Spine Maturation

Given that PSD-95 enhances a number of pre- and postsynaptic markers at early developmental stages, we wondered if there might be associated morphological changes at later stages. We therefore allowed neurons to develop in culture for three weeks, filled

them with Lucifer Yellow, and compared the morphology of transfected cells with their neighbors. Dendritic spines detected in PSD-95 transfected neurons were both more numerous and larger than those in untransfected neurons (Fig. 11). The modest increase in spine count may have resulted from a proliferation of spines or from the inclusion of enlarged spines that would otherwise have been undetectable. Most remarkable was the increased density of large spines >1 μm in diameter (Fig. 11C).

Requirements for PSD-95 Mediated Enhancement

Does the enhancement of synaptic function by PSD-95 require its targeting to synaptic sites? We transfected dissociated cultured neurons with a PSD-95 mutant (PSD-95:C3,5S) lacking N-terminal palmitoylation, which is required for synaptic clustering (Craven et al., 1999). PSD-95:C3,5S occurred diffusely in hippocampal neurons (Fig. 12A). It did not enhance GluR1 clustering but rather appeared to partially disrupt GluR1 clustering in pyramidal cells (Fig. 12A). Neurons transfected with this mutant also failed to display augmented mEPSC amplitude and frequency (Fig. 12B-D). The palmitoylation-deficient mutant of PSD-95 thus failed to enhance GluR1 clustering or presynaptic maturation, demonstrating the importance of palmitoylation to PSD-95 function.

Overexpression of PSD-95 also augmented postsynaptic clustering of a PSD-95 associated protein, guanylate kinase associated protein (GKAP) (Kim et al., 1997), but clustering of a non-interacting protein, Ca^{++} / calmodulin-dependent protein kinase II (CaMKII), was not influenced (Fig. 13A, B). We wondered whether the increase in

synaptic GKAP might mediate enhanced GluR clustering by PSD-95, as GKAP binds to an actin-associated postsynaptic complex containing Shank (Naisbitt et al., 1999). However, neurons transfected with PSD-95 lacking the GK domain still showed enhanced postsynaptic clustering of GluR1 and presynaptic aggregation of synaptophysin in the absence of augmented GKAP clustering (Fig. 14D-F). The GKAP / Shank complex does not, therefore, appear necessary for enhanced synaptic development by PSD-95.

Discussion

PSD-95 can drive maturation of synapses, not only of postsynaptic components but also of presynaptic terminals. The selective enhancement of GluR1 versus NR1 clustering correlates with previous anatomical studies showing that the number of NMDARs remains relatively constant, whereas the number of synaptic GluRs increases during development (Nusser et al., 1998; Petralia et al., 1999) and the magnitude of GluR quantal response increases as synapses mature (Gomperts et al., 2000). It is not clear whether the increase in size of synaptic spines and the increase in GluR1 clustering induced by PSD-95 are parallel processes or if one triggers the other (see (McKinney et al., 1999)). Also unclear is the mechanism underlying the enhanced GluR1 clustering, which presumably involves an intermediary protein(s), as PSD-95 does not bind GluR1 (Leonard et al., 1998).

The enhanced size of axon terminals contacting neurons transfected with PSD-95 and the increased frequency of mEPSCs could be explained by the hypothesis that PSD-95 conveys a retrograde signal for presynaptic development. The increased frequency of

mEPSCs presumably reflects the increased probability of release associated with an increased vesicle pool size. This result may explain why the PSD-95 knockout mouse has augmented paired pulse facilitation (Migaud et al., 1998), which would be consistent with a decreased probability of release in the mutant. The trans-synaptic influence of PSD-95 is reminiscent of rapsyn, a nicotinic acetylcholine receptor clustering protein essential for differentiation of motor neuron terminals (Gautam et al., 1995). PSD-95 may communicate with the axon through neuroligin, a PSD-95 associated cell adhesion molecule that links to the nerve terminal via neurexins (Ichtchenko et al., 1995; Irie et al., 1997). Very recent studies show that neuroligin expression in heterologous cells can trigger presynaptic development (Scheiffele et al., 2000).

In addition to sculpting developing synapses, PSD-95 may contribute to synapse stabilization and remodeling in adult brain (Maletic-Savatic et al., 1999). Targeted disruption of PSD-95 alters activity dependent synaptic plasticity and learning (Migaud et al., 1998). As PSD-95 clustering is controlled by its PDZ domains, palmitoylation, and intramolecular SH3 / GK domain interaction (Craven et al., 1999; McGee and Bredt, 1999; Shin et al., 2000), it will be of interest to determine whether these sites are regulated by neural activity to modulate synaptic structure and plasticity.

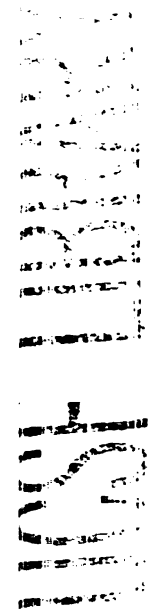

Figure 1. Expression of PSD-95 enhances synaptic clustering of AMPA but not NMDA receptors.

(A) Hippocampal neurons were transfected with PSD-95 GFP, fixed at DIV 12 and stained for GluR1 or NR1. Higher magnification micrographs of the boxed regions are shown in the panels to the right. Clusters of GluR1 are more intense in spines from the neuron transfected with PSD-95 (arrowheads) than in spines from the neighboring untransfected neuron (arrows). (B) NR1 staining is equally intense in spines from transfected (arrowheads) and untransfected (arrows) neurons. (C) GluR1 shows spiny clusters (arrowheads) in GAD- pyramidal cells and forms shaft clusters (arrows) in GAD+ interneurons. (D, E) GluR1 clustering is selectively enhanced both in pyramidal cells and in interneurons overexpressing PSD-95 GFP whereas NR1 is not. Scale bars, 10 μm. (*** $p < 0.001$)

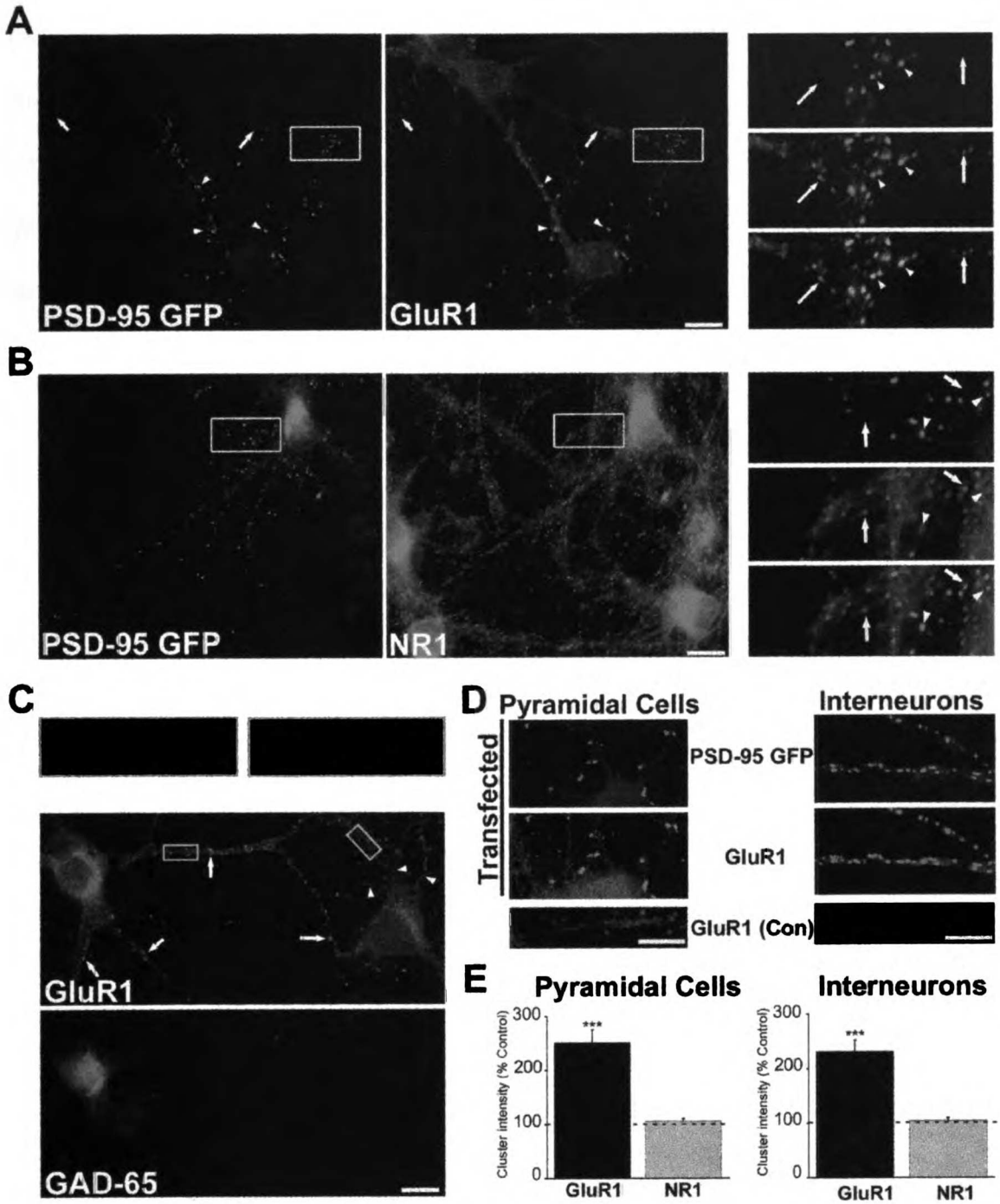
A
PSD-95 GFP
GluR1
B
PSD-95 GFP
NR1
C
GluR1
GAD-65
D
Pyramidal Cells
Interneurons
Transfected
PSD-95 GFP
GluR1
GluR1 (Con)
E
Pyramidal Cells
Interneurons
Cluster intensity (% Control)
300
200
100
0
***
GluR1
NR1

Figure 2. Overexpression of PSD-95 but not CaMKII enhances synaptic clustering of AMPA receptors.

(A) Hippocampal neurons were transfected with CaMKII GFP, fixed at DIV 12 and stained for GluR1. Clusters of GluR1 are of similar intensity in spines from transfected (arrowheads) and untransfected (arrows) neurons. Images are overlaid on right. (B) Surface GluR1 clustering was assessed using non-permeabilized staining conditions and an antibody recognizing an extracellular epitope of GluR1 (N-term GluR1). Clustering is selectively enhanced in neurons overexpressing PSD-95 GFP (arrowheads) as compared to neighboring untransfected neurons (arrows). Higher magnification micrographs of the boxed regions are shown in the panels to the right. Scale bars, 10 μm. (C) Quantification of the effects of CaMKII GFP expression on GluR1 and synaptophysin (Syn) cluster intensity, expressed as percent of control cluster intensity. (D) Quantification of surface GluR1 cluster intensity in PSD-95 GFP transfected cells relative to untransfected cells. The data from permeabilized cells (total GluR1) are included for comparison.

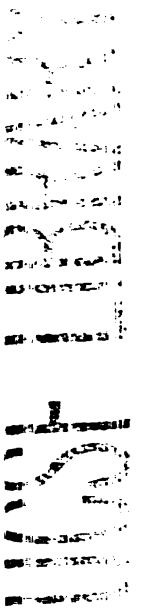

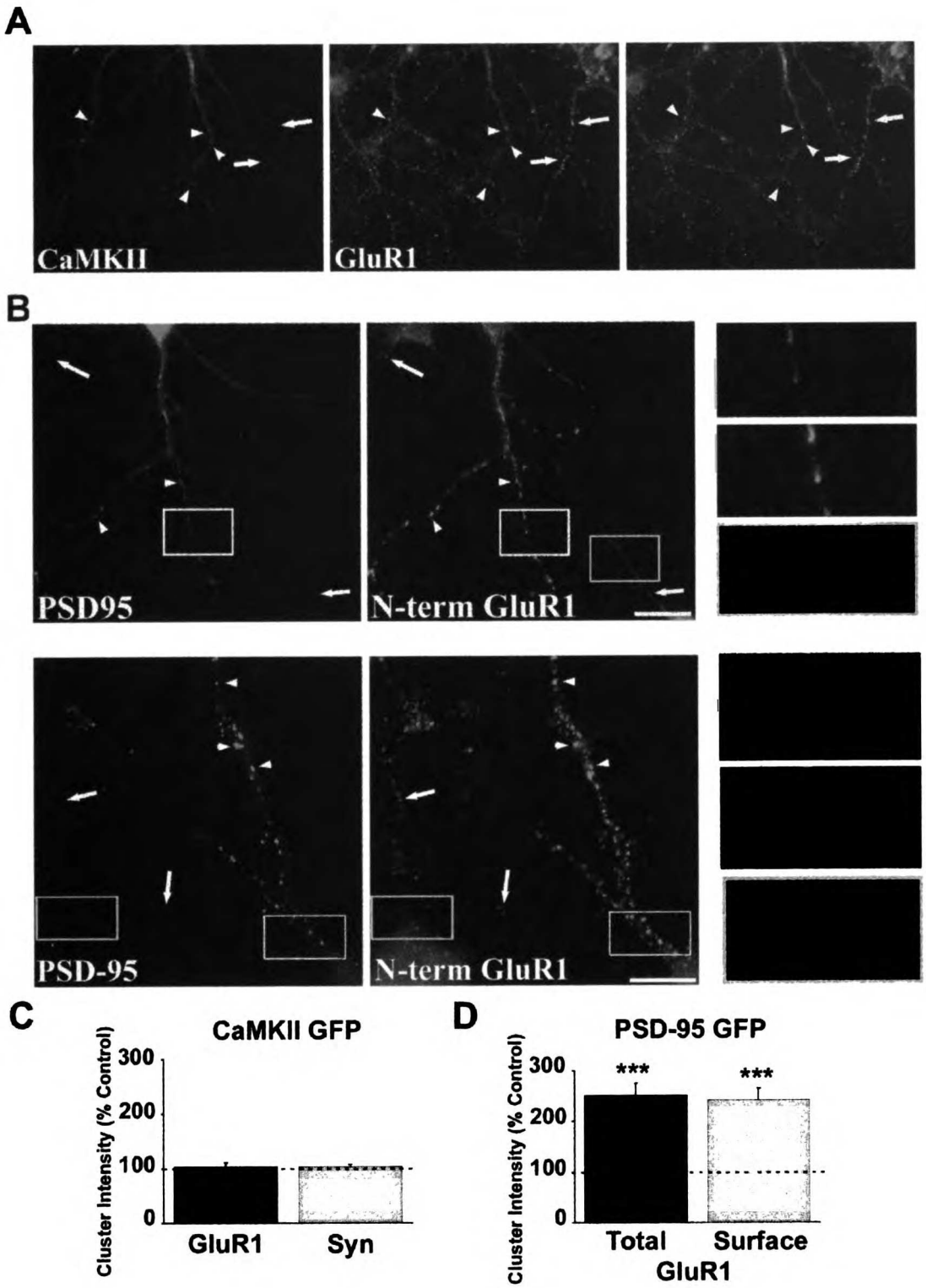
A
CaMKII
GluR1
B
PSD95
N-term GluR1
PSD-95
N-term GluR1
C
CaMKII GFP
Cluster Intensity (% Control)
300
200
100
0
GluR1
Syn
D
PSD-95 GFP
Cluster Intensity (% Control)
300
200
100
0
***
***
Total
Surface
GluR1

Figure 3. PSD-95 GFP intensity at individual spines correlates with GluR1 staining intensity.

The intensity of each individual PSD-95 cluster in three separate transfected neurons was plotted against the GluR1 staining intensity. Linear regression yielded a strong correlation between the two measurements.

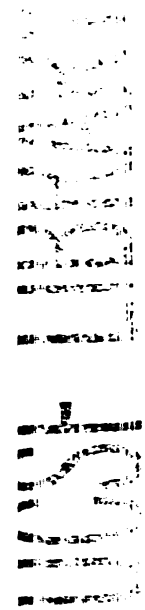

Correlation: PSD-95 and GluR1 Cluster Intensity

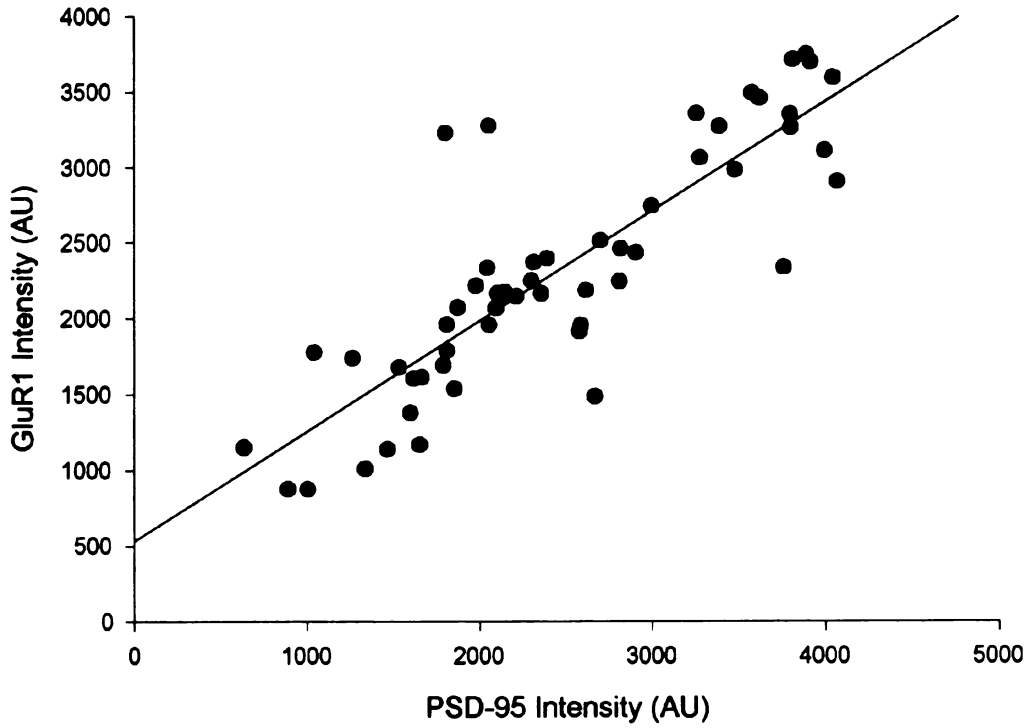

Figure 4. PSD-95 overexpression increases the amplitude and frequency of AMPA-mediated miniature synaptic currents in pyramidal cells.

(A) Summary data showing the increased mEPSC amplitudes and frequencies in PSD-95 overexpressing pyramidal cells (n = 13, 16, **p < 0.01). (B) PSD-95-transfected cells have increased mEPSC amplitude when compared to neighboring untransfected cells. Each pair of points represents the average mEPSC amplitude from both a transfected pyramidal cell and an untransfected pyramidal cell on the same coverslip. (C) Sample current traces from a neighboring untransfected (top) and PSD-95-GFP expressing (bottom) pyramidal cell. mEPSCs in untransfected pyramidal cells are marked with an asterisk (*).

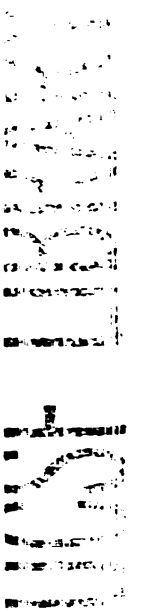

Pyramidal Cells

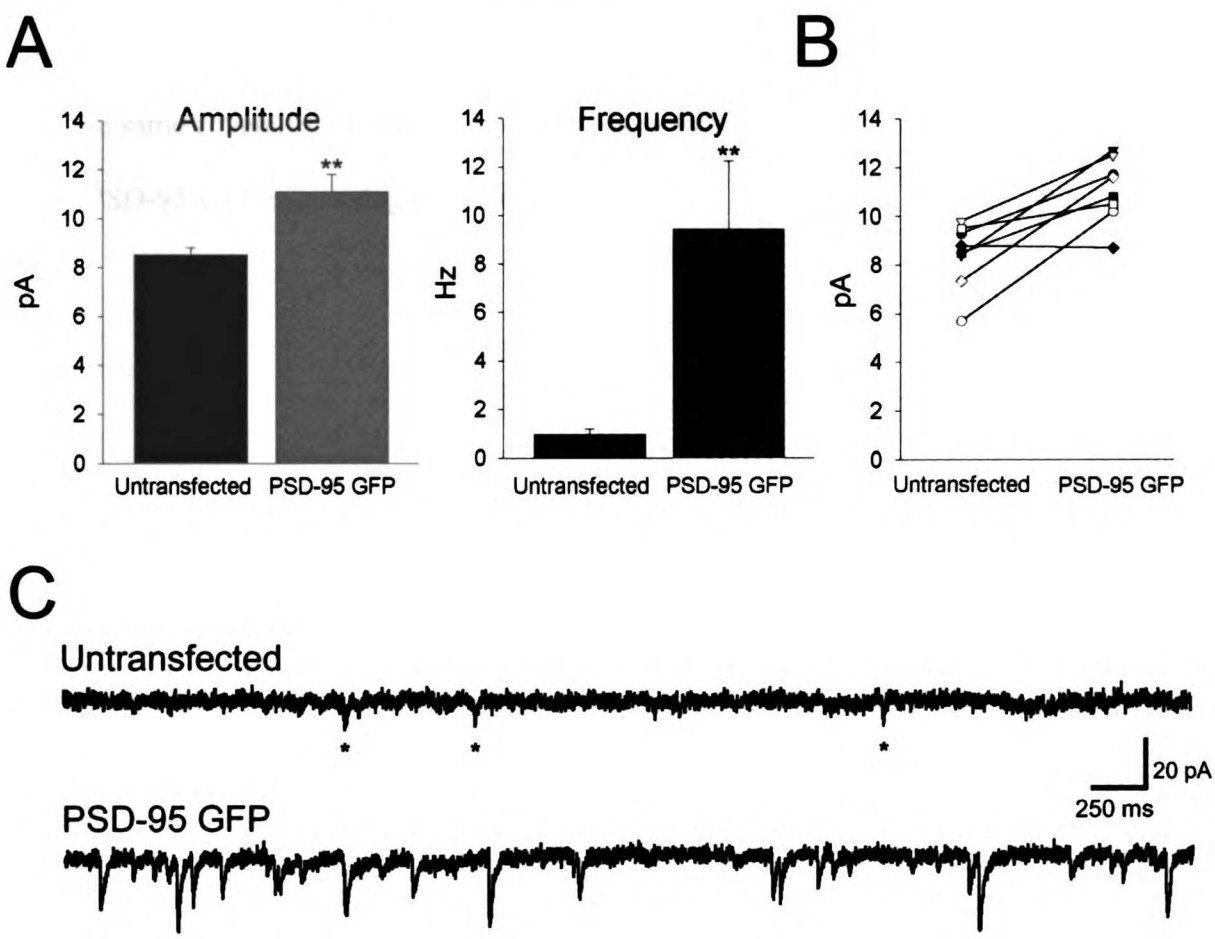

Figure 5. PSD-95 overexpression increases the amplitude and frequency of AMPA-mediated miniature synaptic currents in interneurons.

(A) Summary data showing the increased mEPSC amplitudes and frequencies in PSD-95 overexpressing interneurons (n = 10, 19; **p < 0.01, ***p < 0.001). (B) PSD-95-transfected interneurons have increased mEPSC amplitude when compared to neighboring untransfected interneurons. Each pair of points represents the average mEPSC amplitude from both a transfected interneuron and an untransfected interneuron on the same coverslip. (C) Sample current traces from a neighboring untransfected (top) and PSD-95-GFP expressing (bottom) interneuron.

Interneurons

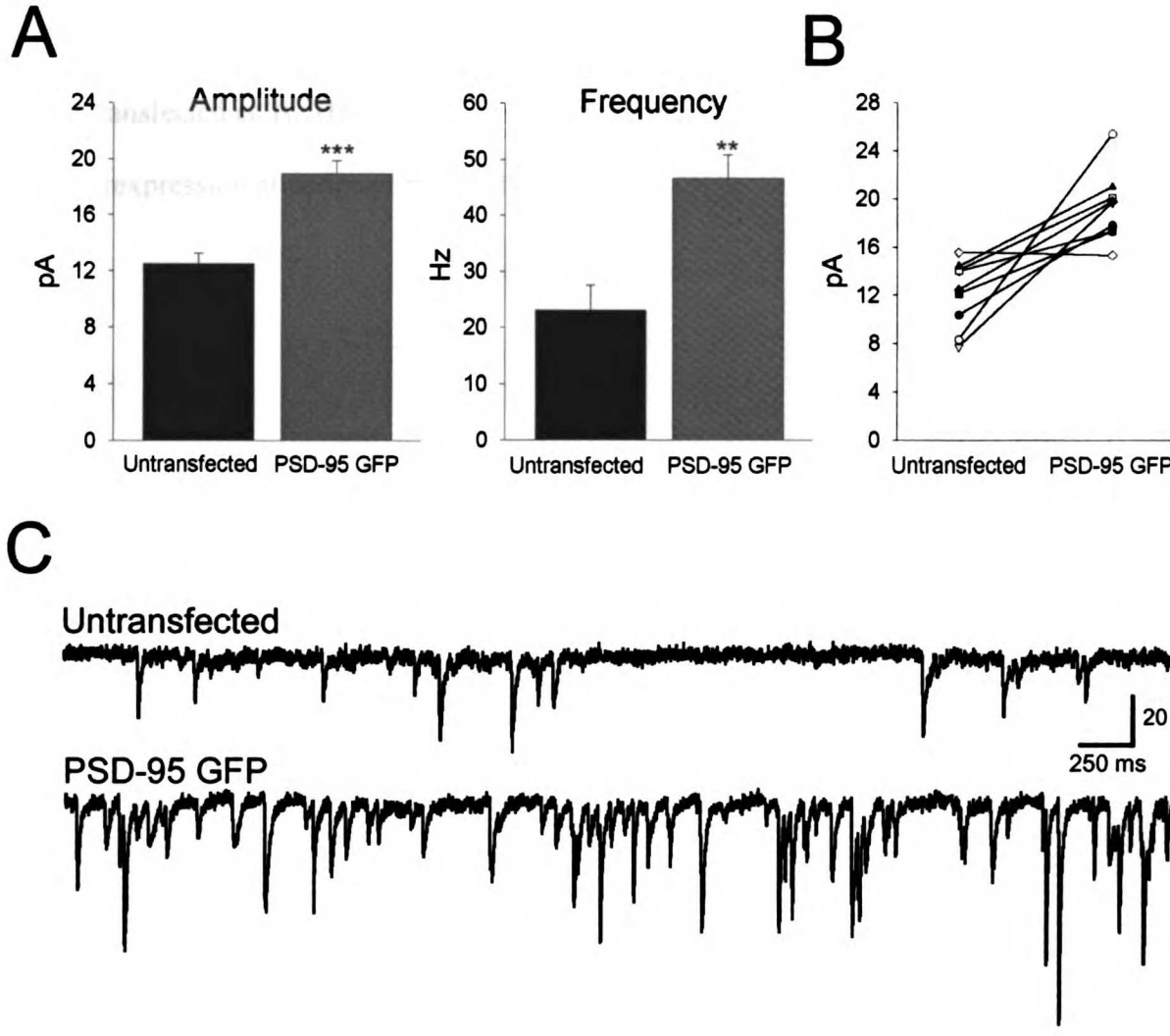

Figure 6. Summary data showing the results obtained from PSD-95 transfected pyramidal cells at various times during development.

(A) Summary mEPSC amplitude data obtained from cultures at various timepoints after preparation. In untransfected pyramidal cells, mEPSC amplitudes gradually increase with increasing time *in vitro*. Recordings were made at DIV 7, DIV 11-13, and DIV 21-22. At each age, PSD-95 GFP expressing cells had larger mEPSC amplitudes than untransfected cells. (B) mEPSC frequencies were also increased by PSD-95 overexpression at various timepoints.

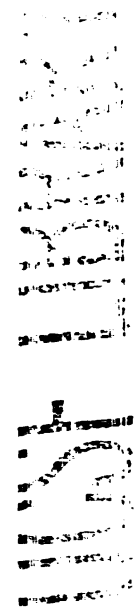

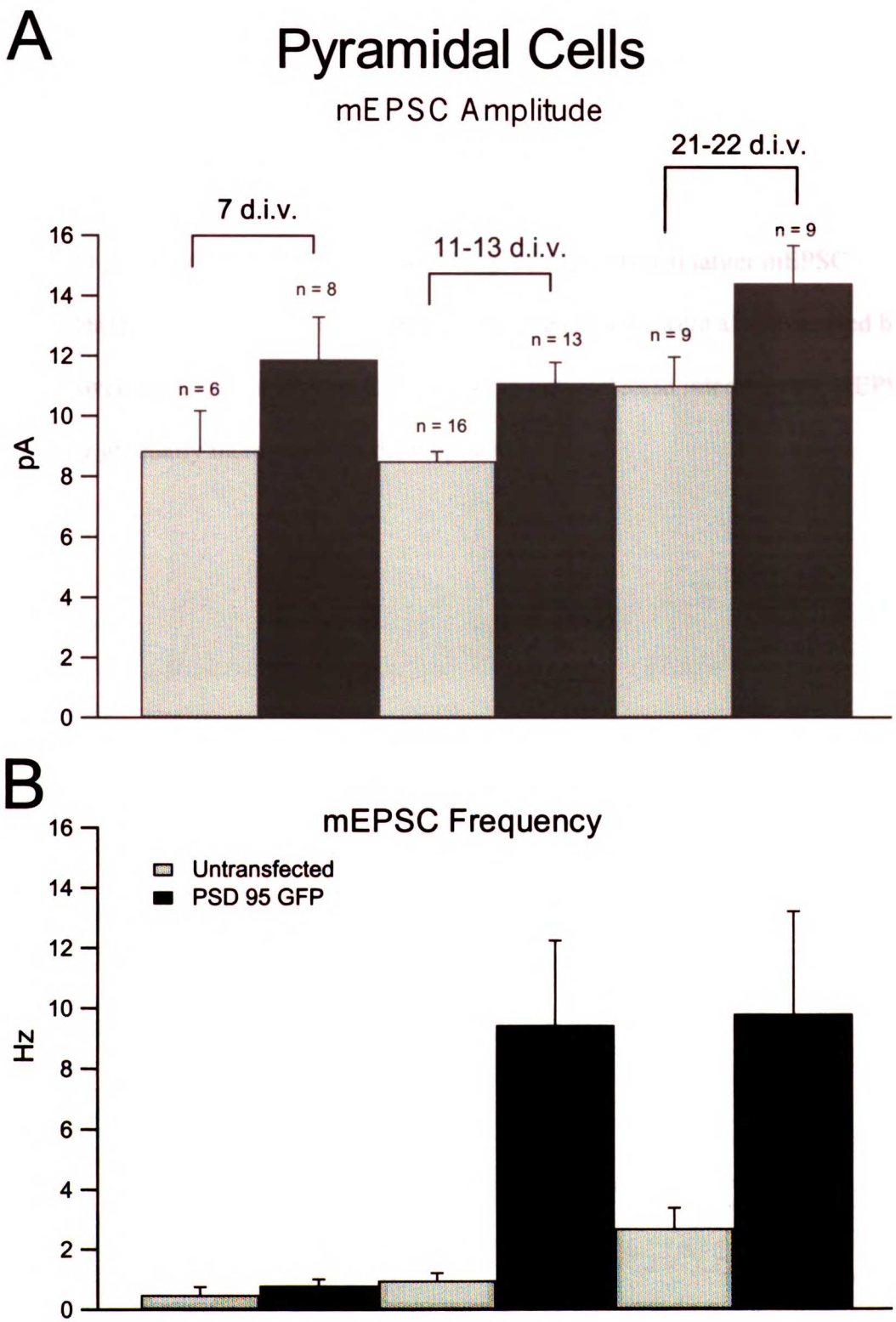
A
Pyramidal Cells
mEPSC Amplitude
7 d.i.v.
11-13 d.i.v.
21-22 d.i.v.
pA
16
14
12
10
8
6
4
2
0
n = 6
n = 8
n = 16
n = 13
n = 9
n = 9
B
mEPSC Frequency
Untransfected
PSD 95 GFP
Hz
16
14
12
10
8
6
4
2
0

Figure 7. Summary data showing the results obtained from PSD-95 transfected interneurons at various times during development.

(A) Summary mEPSC amplitude data obtained from cultures at various timepoints after preparation. In untransfected interneurons, mEPSC amplitude remained constant with increasing time *in vitro*. Recordings were made at DIV 7, DIV 10, DIV 12-13, and DIV 21-22. At each age analyzed, PSD-95 GFP expressing cells had larger mEPSC amplitudes than untransfected cells. (B) mEPSC frequencies were also increased by PSD-95 overexpression at various timepoints. In untransfected interneurons, mEPSC frequency gradually increases with development.

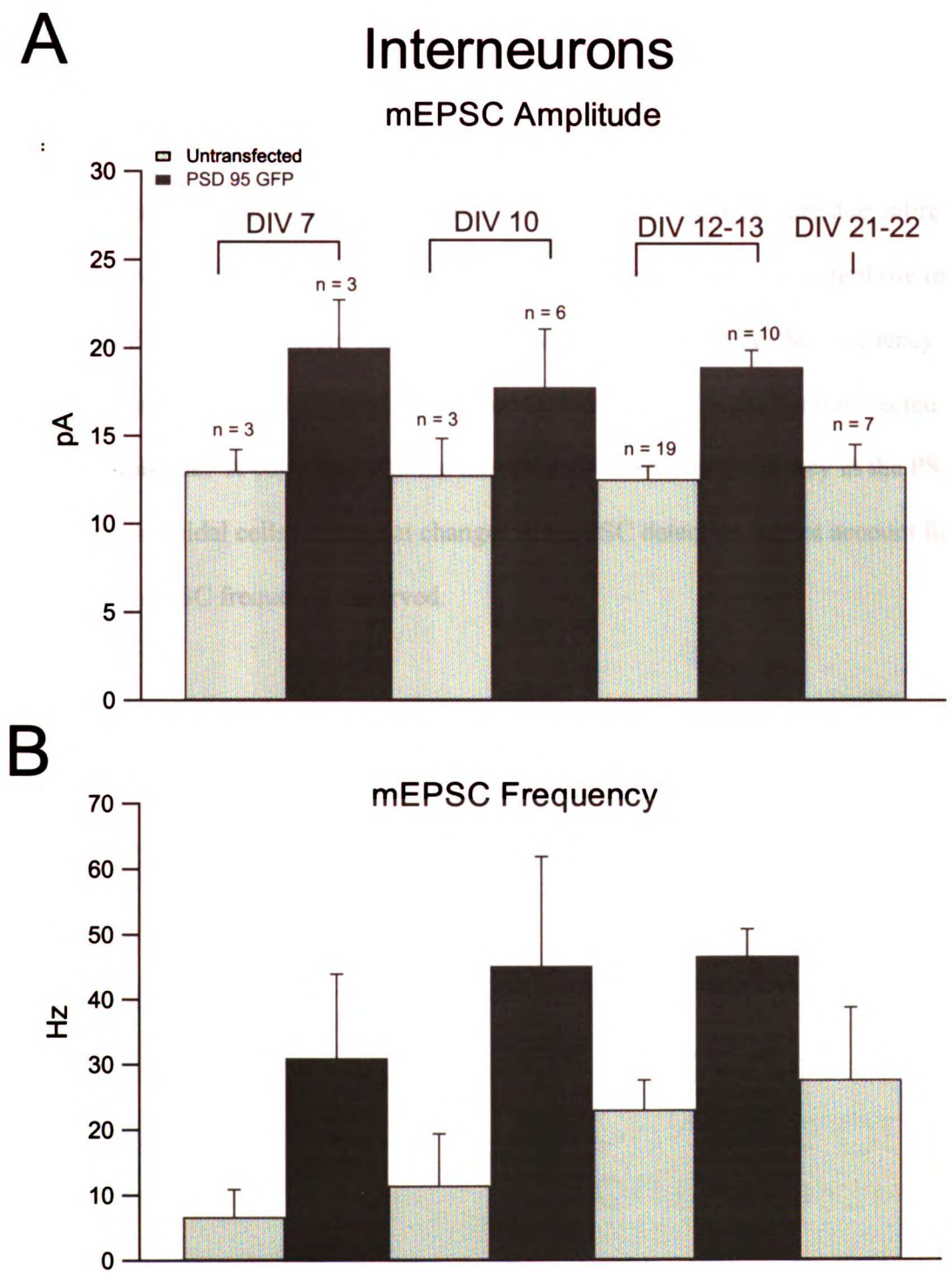
A
Interneurons
mEPSC Amplitude
Untransfected
PSD 95 GFP
DIV 7
DIV 10
DIV 12-13
DIV 21-22
pA
30
25
20
15
10
5
0
n = 3
n = 3
n = 3
n = 6
n = 19
n = 10
n = 7
B
mEPSC Frequency
Hz
70
60
50
40
30
20
10
0

Figure 8. Changes in mEPSC detection does not account for increased mEPSC frequency in pyramidal cells.

In a series of control experiments, mEPSC recordings were obtained from untransfected neurons while holding them at different membrane potentials. Altering the membrane potential alters only mEPSC amplitude; changes in mEPSC frequency are due entirely to changes in event detection. Control cells with mEPSC amplitudes matching those in the PSD-95 GFP experiments were analyzed for changes in detected mEPSC frequency. For these cells, mEPSC frequency was normalized to that obtained at the "untransfected" mEPSC amplitude. A comparison to the normalized increase in frequency in the PSD-95 tranfected pyramidal cells shows that changes in mEPSC detection do not account for the increase in mEPSC frequency observed.

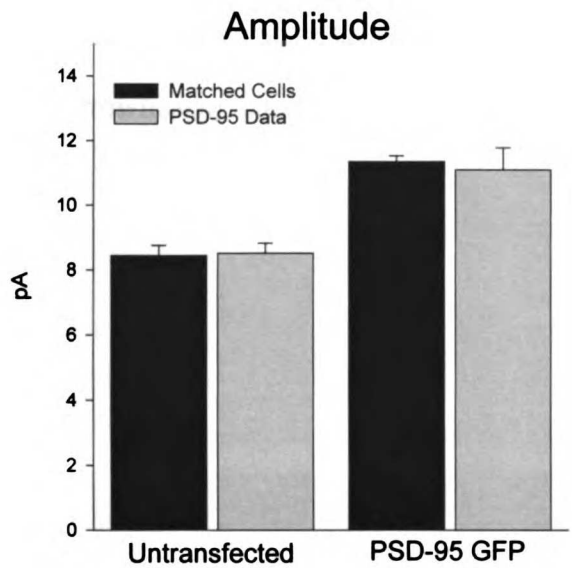
Amplitude
Matched Cells
PSD-95 Data
pA
14
12
10
8
6
4
2
0
Untransfected
PSD-95 GFP

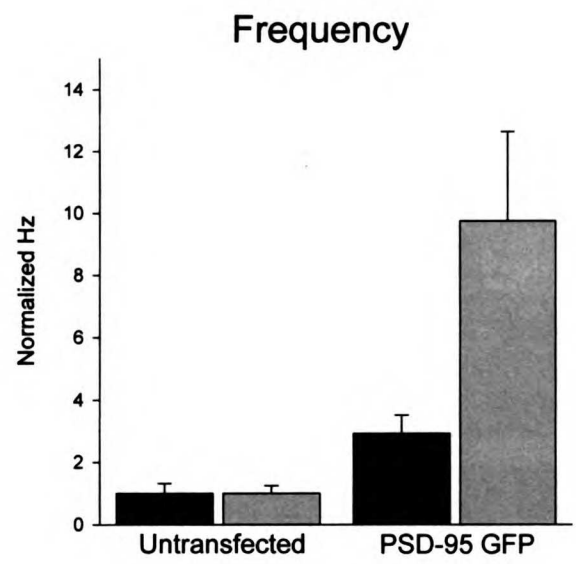
Frequency
Normalized Hz
14
12
10
8
6
4
2
0
Untransfected
PSD-95 GFP

Figure 9. Postsynaptic expression of PSD-95 enhances presynaptic development.

(A) PSD-95 GFP transfected hippocampal neurons were fixed at 10 DIV and stained for GluR1 and synaptophysin. At synapses onto neurons transfected with PSD-95 (arrowheads) both GluR1 and synaptophysin (syn) staining are more intense than at synapses onto untransfected neurons (arrows). (B) Hippocampal neurons transfected with PSD-95 GFP and incubated with 15 μM FM4-64 in the presence of 90 mM KCl for 45 sec show enhanced staining of FM4-64 at sites opposing PSD-95 GFP clusters (arrowheads) than at untransfected synapses (arrows).

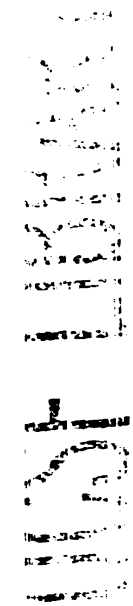

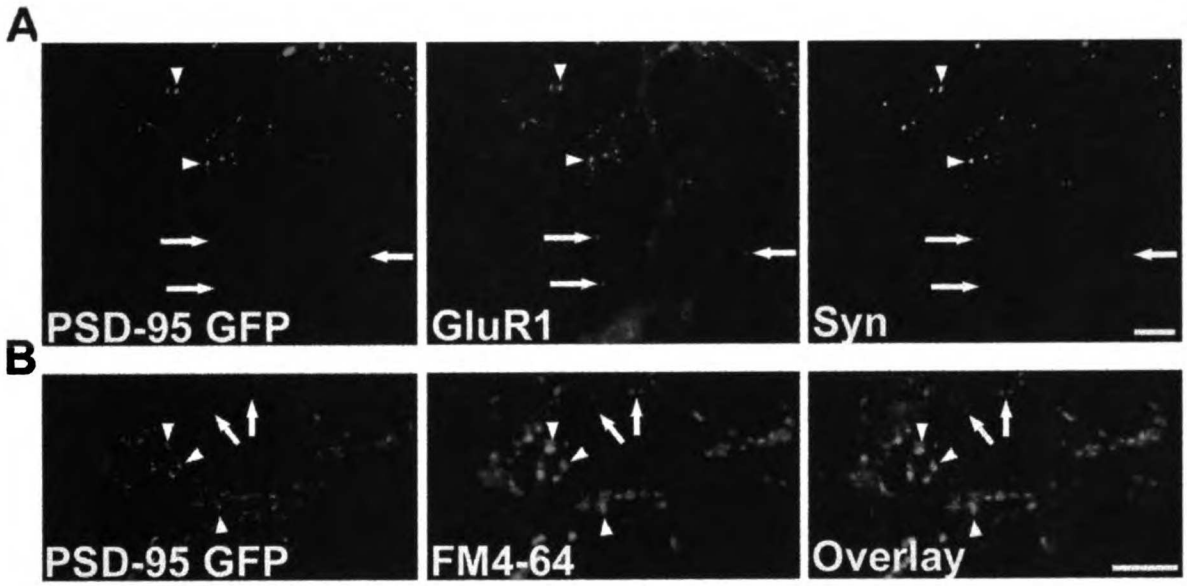
A
PSD-95 GFP
GluR1
Syn
B
PSD-95 GFP
FM4-64
Overlay

Figure 10. Postsynaptic expression of PSD-95 enhances presynaptic SV2 staining.

(A) PSD-95 GFP transfected hippocampal neurons were fixed at 10 DIV and stained for SV2. At synapses onto neurons transfected with PSD-95, SV2 staining is more intense than at synapses onto untransfected neurons. Overlaid images are shown on right, an additional untransfected neuron from a neighboring field is shown below (Control). Staining is selectively enhanced at synaptic sites of neurons overexpressing PSD-95 GFP (arrowheads) as compared to neighboring untransfected neurons (arrows). (B) Quantification of presynaptic staining data. Cluster intensity of presynaptic markers SV2, synaptophysin (Syn), and FM4-64 are presented for comparison.

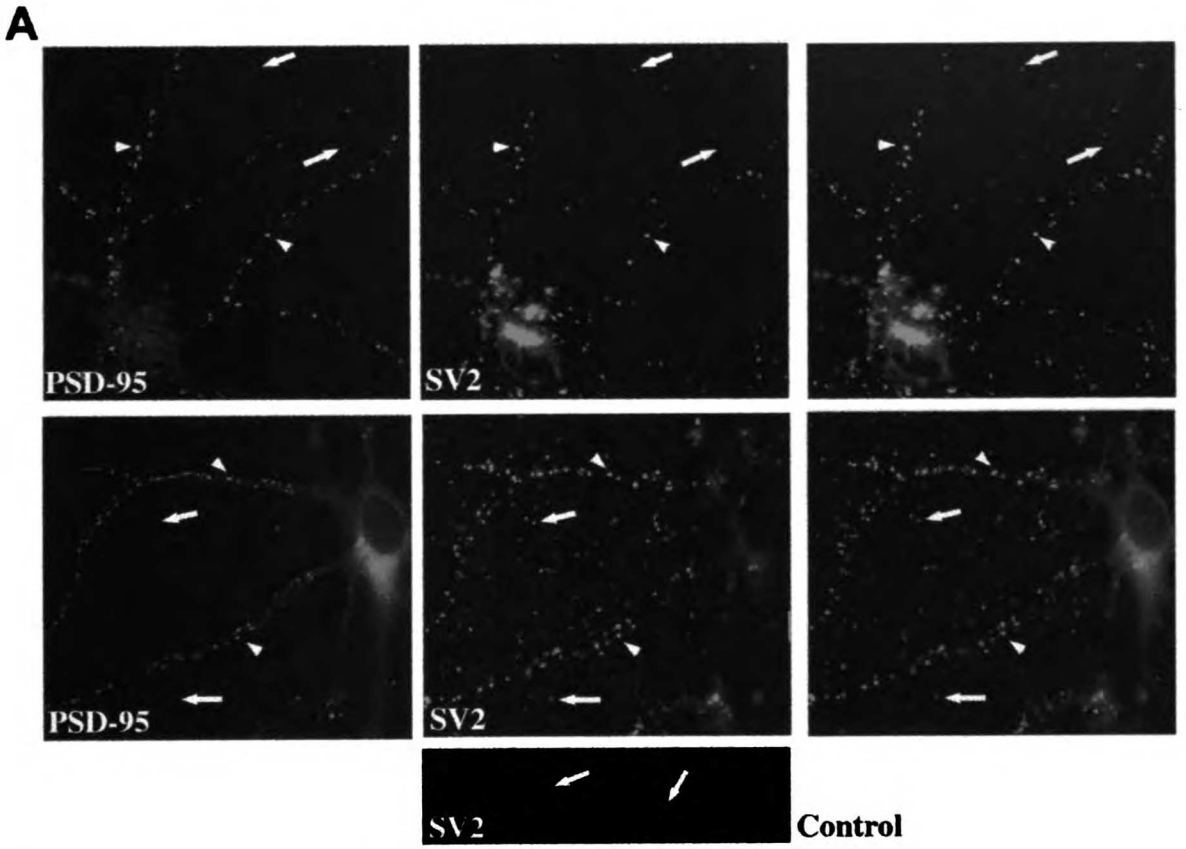
A
PSD-95
SV2
PSD-95
SV2
SV2
Control

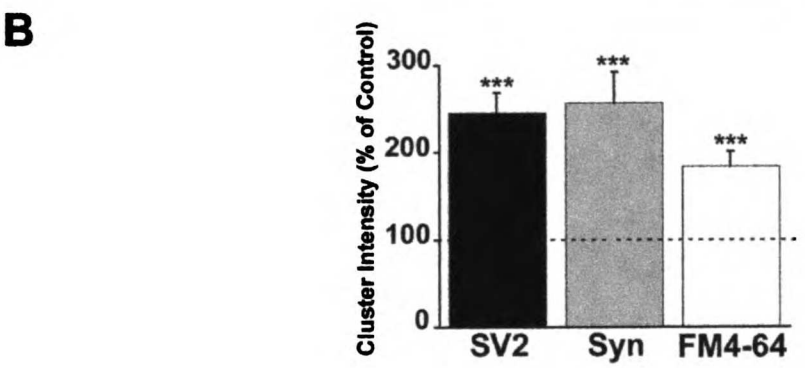
B
Cluster Intensity (% of Control)
300
200
100
0
***
***
***
SV2
Syn
FM4-64

Figure 11. PSD-95 overexpression enhances spine maturation.

Hippocampal neurons (DIV 21) expressing PSD-95 GFP were filled with Lucifer yellow, fixed and analyzed for number and size of spines. Nearby untransfected cells were chosen randomly and filled as controls. (A) Two filled pyramidal cells from the same coverslip demonstrate the increased spine size and density in the transfected cells. Scale bars 10 μm, above; 2 μm, below. (B) The density of spines was augmented in cells expressing PSD-95 GFP (n = 17 each). (C) Neurons expressing PSD-95 GFP showed an increased density of spines >1 μm in diameter. (**$p < 0.01$, ***$p < 0.001$)

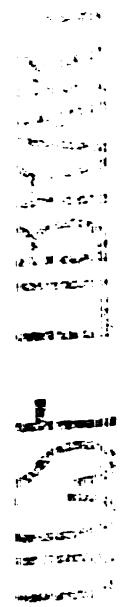

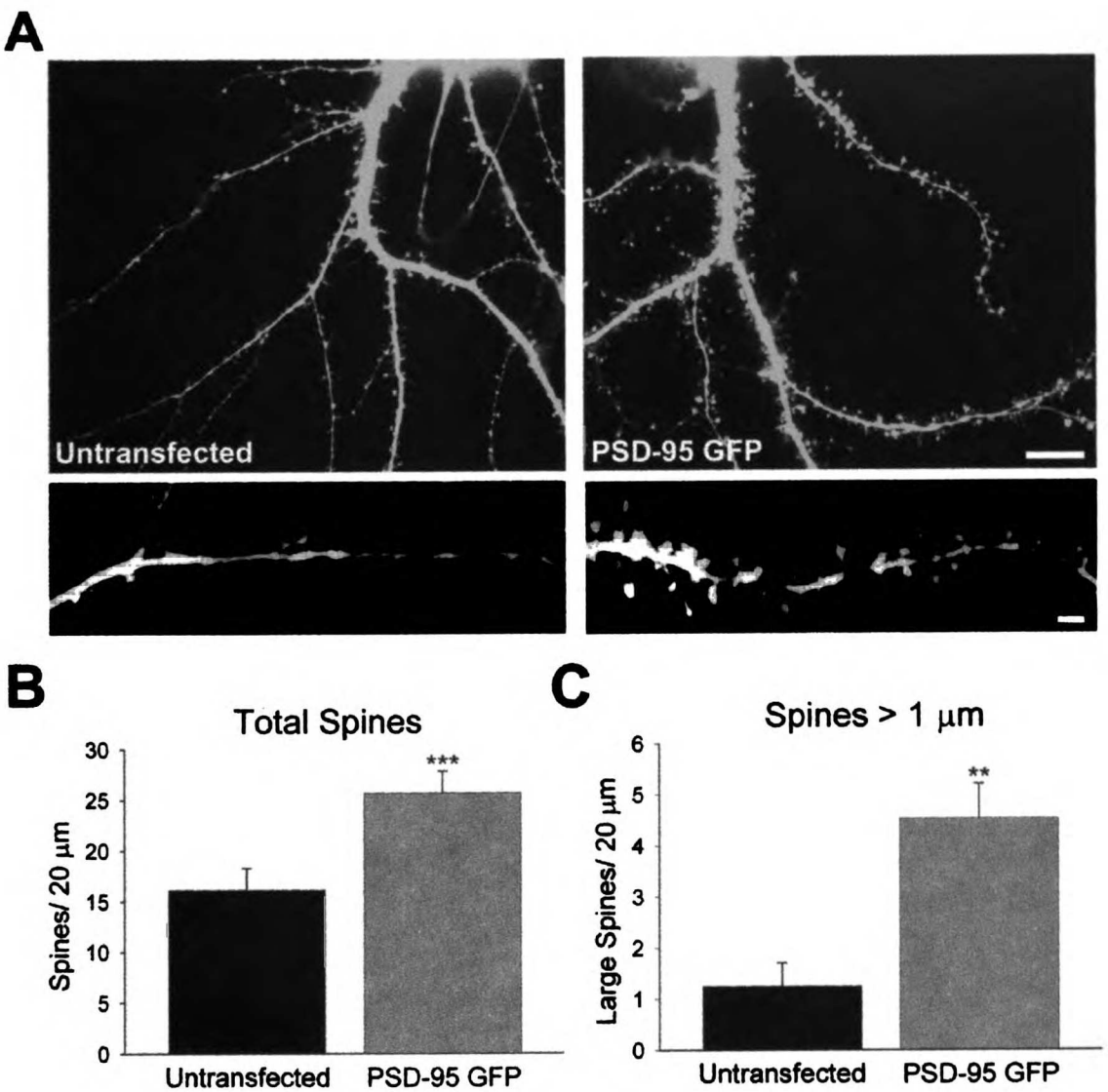
A
Untransfected
PSD-95 GFP
B
Total Spines
Spines/ 20 µm
30
25
20
15
10
5
0
***
Untransfected
PSD-95 GFP
C
Spines > 1 µm
Large Spines/ 20 µm
6
5
4
3
2
1
0
**
Untransfected
PSD-95 GFP

Figure 12. PSD-95 palmitoylation is required to enhance synaptic maturation.

(A) Expression of the palmitoylation-deficient mutant form of PSD-95 (PSD-95:C3,5S) reduces clustering of GluR1. Scale bars, 10 μm. (B) Summary data showing the mEPSC amplitudes and frequencies in PSD-95:C3,5S expressing pyramidal cells ($n = 10, 11, p > 0.4$). (C) PSD-95:C3,5S transfected pyramidal cells show no change in mEPSC amplitude when compared to neighboring untransfected pyramidal cells. Each pair of points represents the average mEPSC amplitude from both a transfected pyramidal cell and an untransfected pyramidal cell on the same coverslip. (D) Sample current traces from a neighboring untransfected (top) and PSD-95:C3,5S GFP expressing (bottom) pyramidal cell.

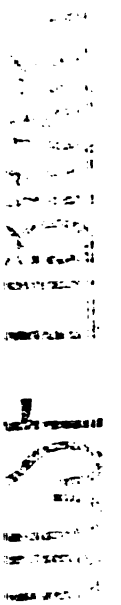

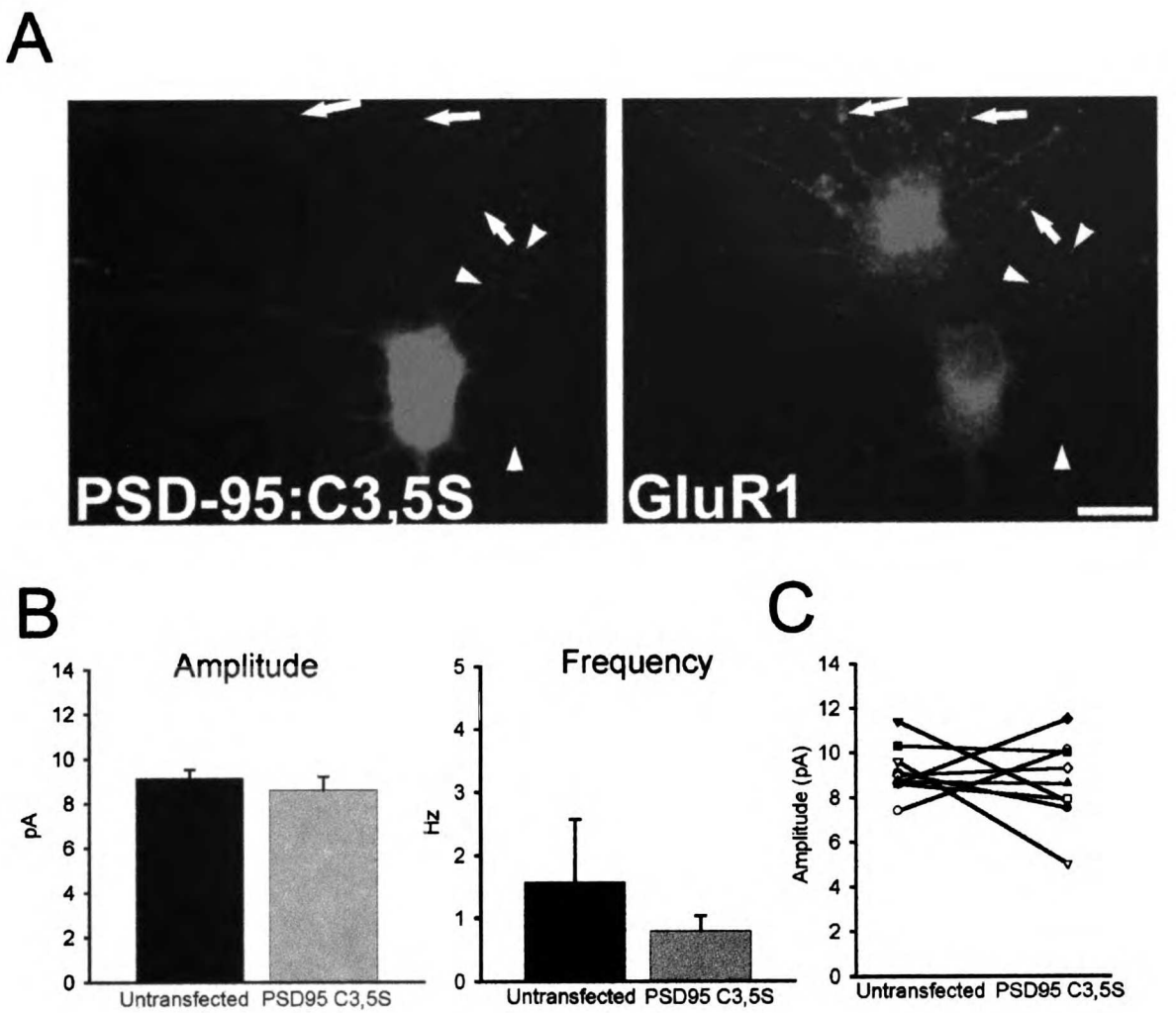
A
PSD-95:C3,5S
GluR1
B
Amplitude
pA
14
12
10
8
6
4
2
0
Untransfected
PSD95 C3,5S
Frequency
Hz
5
4
3
2
1
0
Untransfected
PSD95 C3,5S
C
Amplitude (pA)
14
12
10
8
6
4
2
0
Untransfected
PSD95 C3,5S
D
Untransfected
10mV
50 msec
PSD-95:C3,5S GFP

Figure 13. Synaptic enhancement by PSD-95 does not require the guanylate kinase domain.

(A, B, C) PSD-95 GFP expression induces clustering of a PSD-95 interacting protein, GKAP, but does not alter synaptic clustering of CaMKII. Overexpression of PSD-95-GFP in one of two adjacent pyramidal cells shows that GKAP but not CaMKII labeling is enhanced in the spines from the transfected neuron (arrowhead) as compared to those from the untransfected neuron (arrows). (C) Quantitative analysis of synaptic changes resulting from PSD-95 transfections. (D) The GK domain of PSD-95 is not required for enhanced clustering of GluR1 or presynaptic maturation. (D, E) Expression of a truncated form of PSD-95 lacking the GK domain (PSD-95 ΔGK) enhances postsynaptic GluR1 clustering and presynaptic synaptophysin (syn) but does not alter GKAP synaptic localization. (F) Quantitative analysis of synaptic changes resulting from transfections with PSD-95 ΔGK. Scale bar, 10 μm. (*$p<0.02$, ***$p<0.001$)

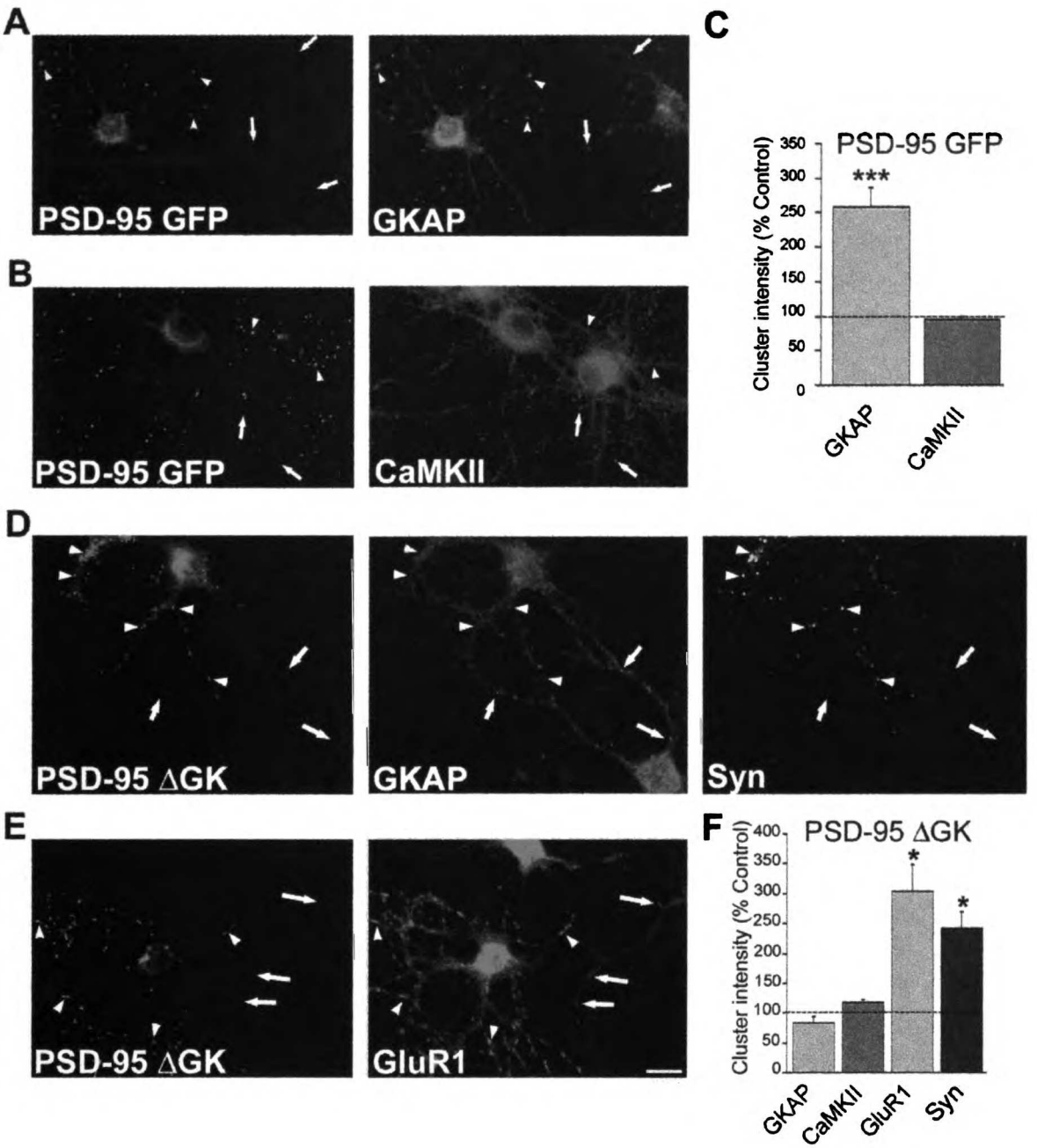
A
PSD-95 GFP
GKAP
B
PSD-95 GFP
CaMKII
C
PSD-95 GFP
Cluster intensity (% Control)
350
300
250
200
150
100
50
0
***
GKAP
CaMKII
D
PSD-95 ΔGK
GKAP
Syn
E
PSD-95 ΔGK
GluR1
F
PSD-95 ΔGK
Cluster intensity (% Control)
400
350
300
250
200
150
100
50
0
*
*
GKAP
CaMKII
GluR1
Syn

CHAPTER 5:

PSD-95 interacts directly with stargazin to mediate synaptic AMPAR targeting

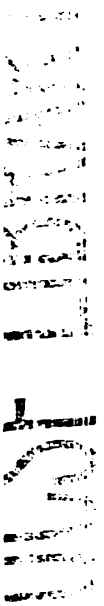

Excitatory synapses in the brain release the transmitter glutamate, which acts primarily on two subtypes of ionotropic receptors, the AMPA and NMDA receptors. Recent studies establish that AMPA receptors (AMPARs), in contrast to NMDA receptors (NMDARs), turn over rapidly at synapses (Beattie et al., 2000; Ehlers, 2000; Lin et al., 2000; Lüscher et al., 1999; Man et al., 2000; Nishimune et al., 1998; Ziff, 1999) and that synaptic plasticity involves rapid regulation of AMPAR number in the postsynaptic membrane (Daw et al., 2000; Lu et al., 2001; Malenka and Nicoll, 1999; Malinow et al., 2000; Xia et al., 2000; Zamanillo et al., 1999). However, little is known about the underlying mechanisms that localize AMPARs to synapses.

Previous attempts to explore these mechanisms have focused on PDZ-domain containing proteins that might regulate the number of synaptic AMPARs by binding them directly (Daw et al., 2000; Dong et al., 1997; Srivastava et al., 1998; Xia et al., 1999). However, recent evidence suggests that a tetraspanning membrane protein, stargazin, can bridge the interaction between AMPARs and a separate family of synaptic PDZ-domain proteins referred to as membrane-associated guanylate kinases (MAGUKs) (Chen et al., 2000). This finding expands the pool of PDZ proteins that potentially regulate synaptic localization of AMPARs. One particular MAGUK, PSD-95/SAP90 (Cho et al., 1992; Kistner et al., 1993), has been intensively studied for its possible role in the clustering of receptors and channels (El-Husseini et al., 2000c; Tiffany et al., 2000). Indeed, PSD-95 overexpression in developing neurons enhances synaptic maturation, including an increase in synaptic GluR1 accumulation (El-Husseini et al., 2000b). However, because over 20 synaptic proteins have been identified which bind to the PDZ domains of PSD-95, it is unclear which of these interactions are functionally relevant at the synapse and might mediate the enhanced maturation.

In this study, we designed experiments to circumvent this redundancy and show that PSD-95 and stargazin acting together directly regulate synaptic AMPAR number. Rather than generally enhancing maturation, we show that increasing PSD-95 levels rapidly and selectively increases the number of synaptic AMPARs. Our results also demonstrate differential regulation of synaptic and extrasynaptic AMPARs by stargazin.

Results

Control of Synaptic AMPARs by PSD-95

We used organotypic slice cultures in conjunction with biolistic transfections to express GFP tagged proteins in hippocampal pyramidal neurons. All experiments involved simultaneous patch clamp recording from a transfected cell and a neighboring untransfected cell. A stimulating electrode placed in stratum radiatum activated excitatory afferents. The relative response magnitudes evoked by activating the same presynaptic afferents were directly compared, allowing assessment of the effects of protein expression in the postsynaptic neuron on synaptic currents. A typical experiment, in this case with GFP tagged PSD-95, is shown in Chapter 2, Figure 2. The DIC image shows the two patch electrodes and a gold particle lodged in the nucleus of the successfully transfected cell on the right and fluorescence shows the punctate clustering of PSD-95 GFP. Confocal microscopy of fixed slices (Fig. 1A) allowed for high-resolution localization of PSD-95 to dendritic spines, the contact site for excitatory synapses.

In all experiments we measured the amplitude of the AMPAR-mediated excitatory postsynaptic current (AMPAR EPSC) at –70 mV and measured the amplitude of the NMDAR-mediated EPSC at +40 mV and at a latency when the AMPAR EPSC had fully decayed (60 msec). Representative traces of averaged AMPAR and NMDAR

EPSCs simultaneously recorded from a control and transfected cell (Fig. 1C) show that PSD-95 dramatically enhanced the AMPAR EPSC, while the NMDAR EPSC was unchanged. There was no change in the kinetics of the EPSCs. Data from 27 such experiments are plotted in scatter graphs (Fig. 1B). Each simultaneously recorded pair is plotted as an open circle representing the amplitude of the EPSC in the transfected cell (abscissa) compared to the amplitude of the EPSC in the untransfected cell (ordinate); the larger filled circle represents the average (± SEM) of all experiments. The data in Fig. 1B are also summarized in bar graphs (Fig. 1D), which are used to present the data for the remainder of this chapter. These findings indicate that overexpression of PSD-95 markedly and specifically enhanced AMPAR-mediated synaptic transmission. The enhancement was rapid; we observed increases within 12 hours of transfection, which correlated with the rapid synaptic clustering of transfected PSD-95.

We showed previously that overexpressing PSD-95 in dissociated neuronal cultures for many days during neuronal development accelerated synapse maturation (El-Husseini et al., 2000b). PSD-95 transfection enhanced AMPAR responses, enlarged dendritic spines, and increased presynaptic glutamate release. The enhancement of the AMPAR EPSC observed here occurred without a change in the NMDAR EPSC, implying no increase in glutamate release. This conclusion was supported by the lack of change in paired pulse facilitation, a sensitive assay for changes in release probability (untransfected = 1.75 ± 0.17; PSD-95 GFP = 1.83 ± 0.25; n = 5). Presumably the presynaptic changes (El-Husseini et al., 2000b) require prolonged expression of PSD-95. In a number of pairs we simultaneously recorded the response to bath applied AMPA, which activated both synaptic and extrasynaptic AMPARs. No enhancement was detected in neurons expressing PSD-95 (Fig.1E), even though in these same cells the AMPAR EPSCs were strongly enhanced.

Which domains of PSD-95 are important for the enhancement of AMPAR EPSCs? The N-terminal palmitoylation of PSD-95 that is essential for its synaptic clustering was also necessary for enhancement of synaptic responses, as the PSD-95 C3,5S mutant did not enhance AMPAR EPSCs (Fig. 2). Removing the guanylate kinase (GK), SH3 and third PDZ domains of PSD-95 did not disrupt the robust enhancement of the AMPAR EPSC (Figs. 3, 4C-D), suggesting that the first two PDZ domains were sufficient. Deletion of the first two PDZ domains completely abolished the enhancement (Fig. 4A). However, it is unclear whether this was an indirect consequence of the reduced synaptic localization of this construct (data not shown), as PDZ3, which also binds stargazin (SK, unpublished observation), remained intact. For all PSD-95 mutants no change was seen in the simultaneously recorded NMDAR EPSC (Figs. 1-4,6). While we were unable to observe any effects of PSD-95 overexpression on NMDAR EPSCs, our results do not exclude effects of PSD-95 expression on other NMDAR-mediated signaling (Sattler et al., 1999). These results demonstrate the importance of the synaptic clustering of PSD-95 and the involvement of the first two PDZ domains in the selective enhancement of the AMPAR EPSC.

We also examined other MAGUKs to see if they shared the AMPAR enhancing properties of PSD-95. SAP97 binds the C-terminus of GluR1 (Leonard et al., 1998). Recent evidence suggests that this interaction occurs primarily in the ER and may play a role in the trafficking of AMPARs (Sans et al., 2001). Overexpressed SAP97, which lacks N-terminal palmitoylation, exhibited a diffuse fluorescence, with only slight clustering (data not shown, also see (Craven et al., 1999)) and had no significant effect on either AMPAR or NMDAR EPSCs (Fig. 5A-B). Insertion of the PSD-95 palmitoylation motif onto the N-terminus of SAP97 resulted in a high degree of clustering (Craven et al., 1999) and enhanced AMPAR EPSCs (Fig. 5C-D), demonstrating the correspondence between synaptic localization of MAGUKs and their effects on synaptic AMPARs. This

95/97 construct was the only one to cause a significant increase in the NMDAR EPSC (Fig. 5D); the functional significance of this is unclear. SAP102 overexpression also selectively enhanced the AMPAR EPSC (Fig. 5E-F).

For each of the constructs examined, we examined the degree of synaptic clustering and the degree of enhancement of AMPAR EPSCs. Our results with clustering (data not shown) generally agreed with previous findings (Arnold and Clapham, 1999; Craven et al., 1999). Taken together, we found that the level of clustering correlated with the degree of enhancement of the AMPAR EPSC. A summary of our physiology data is presented in Figure 6.

Control of Synaptic AMPARs by Stargazin

As PSD-95 has not been shown to interact directly with AMPARs, we performed a similar set of slice culture experiments with a putative adaptor protein, stargazin. Stargazin-GFP showed a punctate expression pattern, with most of the puncta present in dendritic spines (Fig. 7A). In striking contrast to PSD-95, overexpression of stargazin did not affect the AMPAR or NMDAR EPSC (Fig. 7C), suggesting that stargazin is not limiting for synaptic AMPARs. However, removing the PDZ binding region at the C-terminus of stargazin (stargazinΔC), reduced both its clustering (Fig. 7B) and the AMPAR EPSC (Fig. 7D). These data extend previous results obtained in dissociated cell culture (Chen et al., 2000) and further demonstrated that this effect was selective for the AMPAR EPSC, as the NMDAR EPSC did not change. The depression of the AMPAR EPSC caused by stargazinΔC indicated that this PDZ binding domain is critical for synaptic targeting of not only stargazin, as evidenced by the diffuse expression pattern, but also AMPARs. This construct appeared to act as a dominant negative to suppress the trafficking of AMPARs to the synapse.

Previous work demonstrated that stargazin is required for the delivery of AMPARs to the cell surface in cerebellar granule cells (Chen et al., 2000). We therefore examined pyramidal cell responses to the bath application of AMPA, which activates both synaptic and extrasynaptic AMPARs. Remarkably we found that both stargazin (Fig. 8B) and stargazinΔC (Fig. 8A,C) caused a 5 fold increase in the response to bath-applied AMPA, suggesting a dramatic increase in the number of surface AMPARs. This result indicates that, in contrast to synaptic AMPARs, stargazin is limiting for expression of extrasynaptic surface AMPARs. Intriguingly, stargazinΔC had two opposing actions; it simultaneously depleted the synapse of AMPARs while loading the extrasynaptic membrane with AMPARs (Figs. 7D,8C). The increased response to bath-applied AMPA was not due to an effect of stargazin on AMPAR desensitization, as it was still observed in the presence of cyclothiazide, which blocks desensitization (100 nM AMPA + 100 M cyclothiazide; untransfected = 377 ± 78 pA verses transfected = 1210 ± 227 pA; n = 7, p = 0.01). The effect of stargazin was specific to extrasynaptic AMPARs, because responses to bath applied NMDA (5 μM) were unaffected (untransfected = 496 ± 65 pA verses transfected = 419 ± 147 pA; n = 3). Together, these results highlight the critical role of stargazin and, in particular, its PDZ-binding C-terminus, in controlling delivery of extrasynaptic AMPARs to the synapse.

A Direct Interaction Between Stargazin and PSD-95 Mediates the Synaptic Delivery of AMPARs

Might the effects of PSD-95 and stargazin be interdependent? We designed two types of experiments to address this possibility. First, if the enhancement of the AMPAR EPSC by PSD-95 required an interaction with stargazin, overexpressing the C-terminus of stargazin might interfere with the enhancement and on its own depress AMPAR EPSCs. Expression of a GFP-tagged stargazin C-terminus significantly depressed

AMPAR EPSCs (Fig. 9A-B) and when coexpressed with PSD-95 significantly attenuated the enhancement caused by PSD-95 (Fig. 9C). While these results supported our model, expression of the C-terminus of stargazin could have displaced other ligands that bind PSD-95 and/or perturbed interactions involving other PDZ-domain containing proteins. Indeed, this construct depressed NMDAR EPSCs (Fig. 9A-B), confirming that this approach lacked specificity.

To determine more decisively whether stargazin and PSD-95 interact physically and functionally at the synapse to control AMPAR localization, we generated compensatory mutations in the PDZ domains of PSD-95 and the C-terminus of stargazin (Kaech et al., 1998). Crystallographic and NMR structures of PSD-95 PDZ domains (Doyle et al., 1996; Piserchio et al., 2002; Tochio et al., 2000) identified key residues that should interact with the stargazin C-terminus. Conserved histidine residues in the PSD-95 PDZ domains (which are Class I) are predicted to form hydrogen bonds with the threonine at the -2 position in the C-terminus of stargazin, as is typical of most Class I PDZ-domains and their ligands (Songyang et al., 1997). Class II PDZ domains often contain a valine at this position, and bind ligands with a large hydrophobic residue such as tyrosine or phenylalanine at their –2 position (Daniels et al., 1998). Thus, we made mutations in both stargazin and PSD-95 to convert the PDZ/ligand interaction from a Class I to a Class II (Kaech et al., 1998). In the case of stargazin, we mutated the –2 position threonine to phenylalanine (= Stargazin T321F), and for PSD-95, we mutated histidines 130 and 225 (corresponding to PDZs 1 and 2, respectively) to valines (= PSD-95 H130V or H225V).

The results of these mutations on PSD-95/stargazin interactions were examined biochemically using GST-fusion constructs terminating with the last 12 amino acids of either wildtype or T321F stargazin. The T321F point mutation completely disrupted

stargazin binding to PSD-95 (Fig. 10A). By contrast, this mutant stargazin clearly bound PSD-95 bearing a compensatory mutation (Fig. 10A). We then tested the effects of these mutations on protein function in neurons.

When stargazin T321F was transfected into neurons alone, it had a diffuse, membrane-associated pattern (Fig. 10B, top), reminiscent of the expression pattern of stargazinΔC (Fig 7B). The expression pattern of stargazin T321F was unaffected by co-transfection with PSD-95 (Fig. 10B, center). In striking contrast, co-transfection of PSD-95 with a compensatory mutation in PDZ1 (data not shown) or PDZ2 (Fig. 10B, bottom) restored the synaptic localization of the stargazin mutant. This demonstrated that an appropriate, synaptically localized PSD-95 PDZ domain is sufficient for the synaptic targeting of stargazin.

We next examined whether the reconstitution of synaptic clustering was associated with changes in synaptic transmission. Transfection of stargazin T321F strongly depressed AMPAR EPSCs, without any change in the NMDAR EPSC (Fig. 11A). Again, this result was identical to that obtained with stargazinΔC, as would be predicted if the mutation interfered with the binding of stargazin to its endogenous PDZ partner. In addition, co-expression of stargazin T321F with wild type PSD-95 prevented the typical enhancement of the AMPAR EPSC, and the AMPAR EPSC was actually depressed (Fig 11B). By contrast, co-expression of stargazin T321F with PSD-95 bearing a compensatory mutation reversed the depressant effect of stargazin T321F. AMPAR EPSCs were significantly enhanced (Fig. 11C), in a manner reminiscent of the over-expression of wild type PSD-95 (Fig. 1B-D). This occurred both for PSD-95 constructs bearing a compensatory point mutation in PDZ1 (untransfected AMPAR average = 31.9 ± 3.6 pA; star T321F + PSD-95 H130V transfected = 71.5 ± 9.7 pA; n = 21 pairs, p = 0.001) or PDZ2 (untransfected AMPAR average = 21.4 ± 2.9 pA; star

T321F+ PSD-95 H225V transfected = 50.2 ± 6.1 pA; n = 14 pairs, p = 0.001), with neither causing a change in the NMDAR EPSC. These data show that direct interactions between PSD-95 and stargazin mediate the synaptic targeting of AMPARs.

Discussion

This study used hippocampal slice cultures in conjunction with biolistics to address the roles of PSD-95 and stargazin in controlling synaptic AMPAR targeting. Our data agree with previous results in dissociated culture (El-Husseini et al., 2000b), showing that expression of PSD-95 enhanced AMPAR EPSCs. In that study, the enhancement required a week of PSD-95 expression. However, in transfected slice culture, the enhancement is apparent within a day and is much more dramatic. Furthermore, we now demonstrate that the enhancement is selective to the AMPAR EPSC, with no change in NMDAR EPSC. The rapidity and selectivity of this effect implies that overexpression of PSD-95 in mature neurons works not by globally enhancing synapse maturation, but by rapidly recruiting AMPARs to synapses. Overexpression of PSD-95 does not alter responses to exogenously applied AMPA, suggesting that PSD-95 shifts extrasynaptic AMPARs to the synapse, with no net change in total surface AMPARs. However, we cannot exclude the possibility that PSD-95 inserts new AMPARs at the synapse, if synaptic AMPARs represent a small fraction of the response to exogenous AMPA.

Previous studies in dissociated culture (Craven et al., 1999) showed that synaptic clustering of PSD-95 relies on three elements of PSD-95: N-terminal palmitoylation, the first two PDZ domains, and a C-terminal targeting motif. Generally similar results were reported in slice culture (Arnold and Clapham, 1999). Our data now show that the synaptic targeting of the PDZ-domains of PSD-95 is sufficient to increase synaptic AMPAR number.

We also examined other MAGUKs to investigate their ability to enhance AMPAR EPSCs. SAP102, which is highly homologous to PSD-95, is synaptically clustered and enhances AMPAR EPSCs. Although SAP102 contains N-terminal cysteines, it is not palmitoylated in heterologous cells (El-Husseini et al., 2000a). Thus it remains unclear whether the synaptic targeting of SAP102 occurs because palmitate transferases in neurons have alternate specifities to those present in non-neuronal cells, or whether SAP102 traffics to synapses via an alternative mechanism. In contrast, SAP97 lacks these cysteines entirely and is not palmitoylated (El-Husseini et al., 2000a). We find that overexpressed SAP97 is poorly clustered at synapses and fails to affect synaptic currents. However, if we place the N-terminal palmitoylation site of PSD-95 onto SAP97, both the synaptic clustering and the enhancement of the AMPAR EPSC are similar to that seen with PSD-95. This suggests that MAGUKS might be functionally interchangeable, apart from differences in their synaptic targeting. Different MAGUKS are highly homologous, particularly in their PDZ domains (for example, 96% sequence identity between PDZ1 of PSD-95 and SAP97); it will be interesting to elucidate the structural differences and functional relevance of instances in which MAGUKs differentially bind particular proteins (e.g., GluR1).

Remarkably, we found that expression of either stargazin or stargazinΔC greatly increased the response to exogenously applied AMPA, indicating a large increase in the number of extrasynaptic AMPARs. This result contrasts with our previous data in dissociated neuronal cell cultures (Chen et al., 2000), where stargazin did not affect whole-cell AMPA currents. A difference in the processing of AMPARs between dissociated and slice cultured pyramidal cells has been noted previously (Shi et al., 1999), as the slice culture preparation retains many more physiological properties of the intact hippocampus, such as its spatial anatomy and robust long-term potentiation. The differential regulation of synaptic and extrasynaptic AMPARs is particularly striking for

stargazinΔC, where in the same cell the AMPAR EPSC was severely depressed while the extrasynaptic response was greatly enhanced. These results indicate that dramatic changes in the expression of extrasynaptic AMPARs can go undetected at the synapse (see also (Zamanillo et al., 1999)).

What might account for the privileged access to the postsynaptic membrane? Perhaps a limited number of positions or slots are available for AMPARs at the synapse (Malinow et al., 2000). When the number of slots changes, the number of synaptic AMPARs will change accordingly. We propose that PSD-95 and other MAGUKs play the role of slot at the postsynaptic membrane and via their interaction with stargazin bring AMPARs to the synapse. Thus, even when the number of surface AMPARs is increased by overexpressing stargazin, the amount of synaptic MAGUK protein imposes a limit on the number of synaptic AMPARs.

To determine if a direct interaction between PSD-95 and stargazin can control synaptic AMPAR number we mutated both PSD-95 and stargazin in a complementary manner, allowing them to interact uniquely with each other. A point mutation in the PDZ-binding region of stargazin created a dominant negative construct that reversed the enhancement normally observed with wild type PSD-95. However, when this mutant was co-expressed with PSD-95 constructs bearing compensatory point mutations that reconstituted stargazin binding, the enhancement was fully rescued. This identifies the interaction between PSD-95 (or other synaptic MAGUKs) and stargazin as a crucial aspect in the function of both proteins. Given the complexity and redundancy of many synaptic protein-protein interactions, this compensatory mutation approach seems essential for defining their roles.

Figure 1. PSD-95 GFP expression enhances AMPAR, but not NMDAR, EPSCs.

(A) Confocal image of a cell expressing PSD-95 GFP. Scale bar, 20 μm. (B) Scatter-plots of data obtained from 27 cell pairs, in which the EPSC amplitude in the PSD-95 transfected cell is plotted against the EPSC amplitude in the untransfected cell. AMPAR EPSCs are significantly enhanced ($p < 1 \times 10^{-6}$), while NMDAR EPSCs are unchanged ($p = 0.81$). (C) Averaged EPSCs recorded simultaneously from a pair of cells, showing the responses at -70 mV and +40 mV. Scale bars, 10 pA, 10 msec. (D) Bar graph representations of the data obtained from the paired recordings. (E) PSD-95 expressing cells do not show a change in the whole-cell response to bath applied AMPA (1 μM).

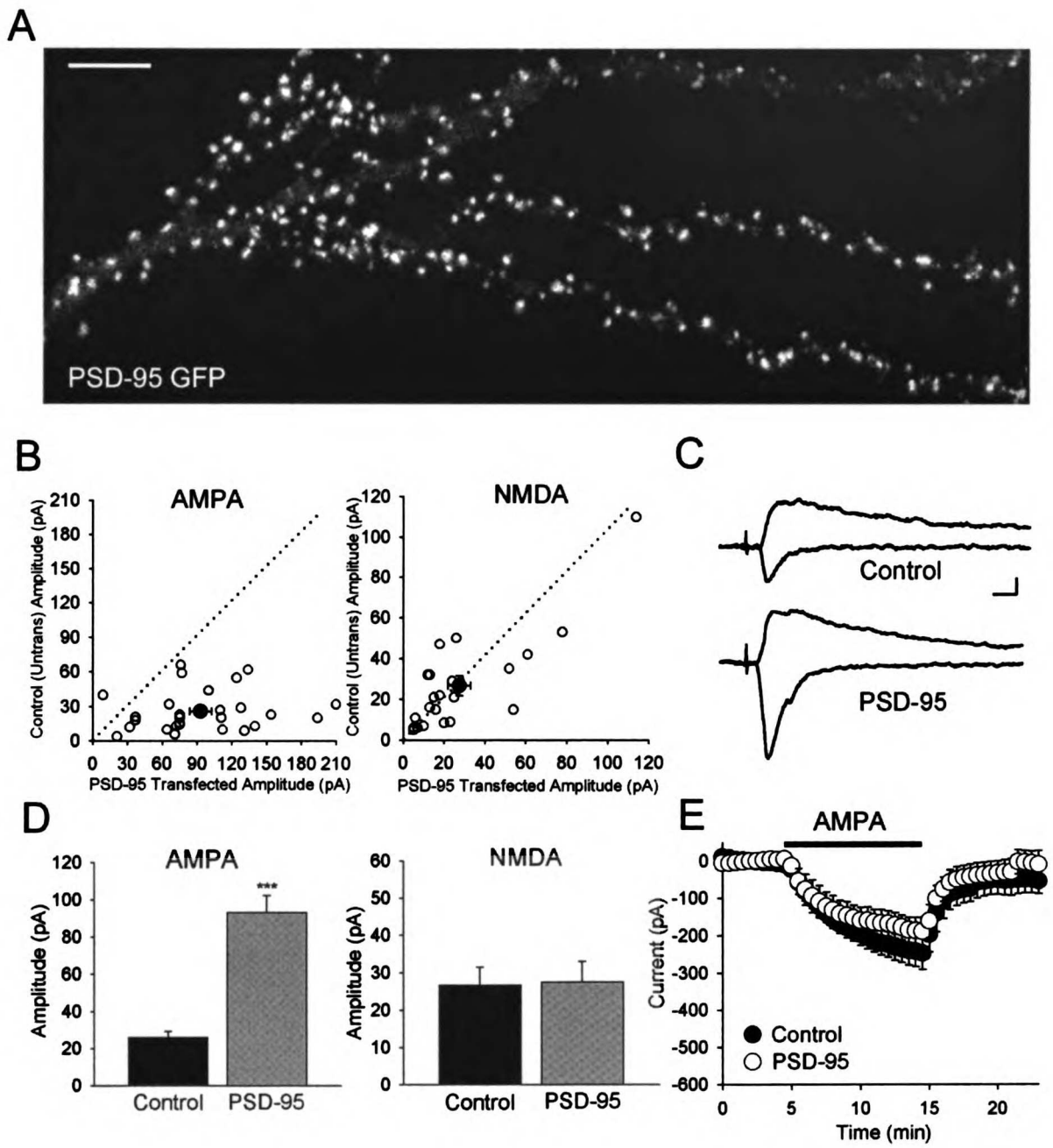
A
PSD-95 GFP
B
AMPA
NMDA
Control (Untrans) Amplitude (pA)
PSD-95 Transfected Amplitude (pA)
C
Control
PSD-95
D
AMPA
NMDA
Amplitude (pA)
***
Control
PSD-95
E
AMPA
Current (pA)
Control
PSD-95
Time (min)

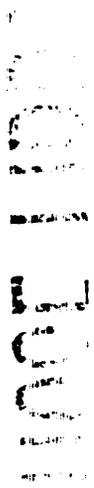

Figure 2. PSD-95 palmitoylation is required to enhance synaptic AMPAR EPSCs.

(A) Averaged EPSCs recorded simultaneously from a pair of cells, showing the responses at -70 mV and +40 mV in a PSD-95 C3,5S transfected cell and a neighboring untransfected cell. Scale bars, 10 pA, 20 msec. (B) Bar graph representations of the data obtained from the paired recordings showing no change in the evoked AMPAR or NMDAR EPSC (AMPAR EPSC, n = 20 pairs, p = 0.08; NMDAR EPSC, n = 12 pairs; p = 0.79).

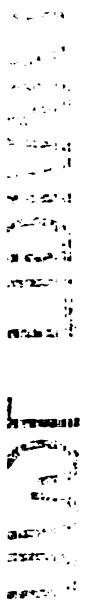

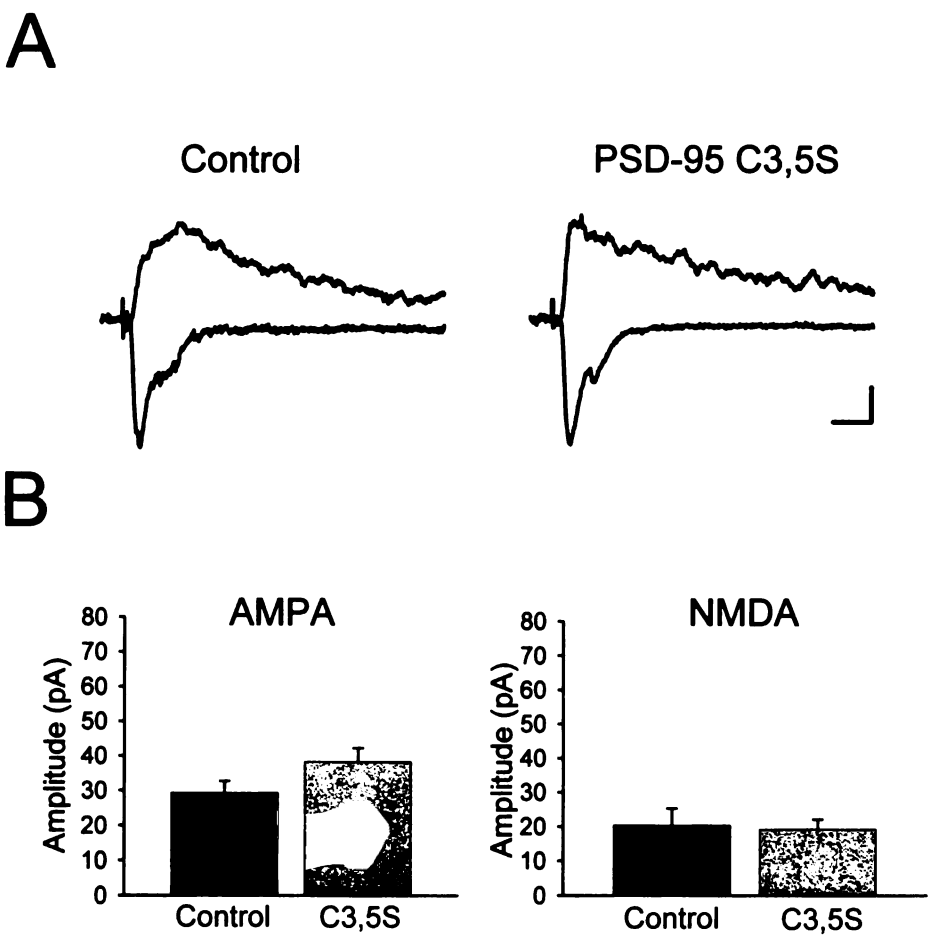
A
Control
PSD-95 C3,5S
B
AMPA
NMDA
Amplitude (pA)
80
70
60
50
40
30
20
10
0
Control
C3,5S

Figure 3. The SH3 and GK domains of PSD-95 are not required to enhance AMPAR EPSCs.

(A) Averaged EPSCs recorded simultaneously from a pair of cells, showing the responses at -70 mV and +40 mV in a PSD-95 ΔGK transfected cell and a neighboring untransfected cell. Scale bars, 10 pA, 20 msec. (B) Bar graph representations of the data obtained from the paired recordings showing a large increase in the AMPAR EPSC without a change in the evoked NMDAR EPSC (AMPAR EPSC, n = 10 pairs, p = 0.003; NMDAR EPSC, n = 10 pairs; p = 0.30). (C) Averaged EPSCs recorded simultaneously from a pair of cells, showing the responses at -70 mV and +40 mV in a PSD-95 ΔSH3,GK transfected cell and a neighboring untransfected cell. Scale bars, 10 pA, 20 msec. (D) Bar graph representations of the data obtained from the paired recordings showing a large increase in the AMPAR EPSC without a change in the evoked NMDAR EPSC (AMPAR EPSC, n = 10 pairs, p = 0.02; NMDAR EPSC, n = 10 pairs; p = 0.56).

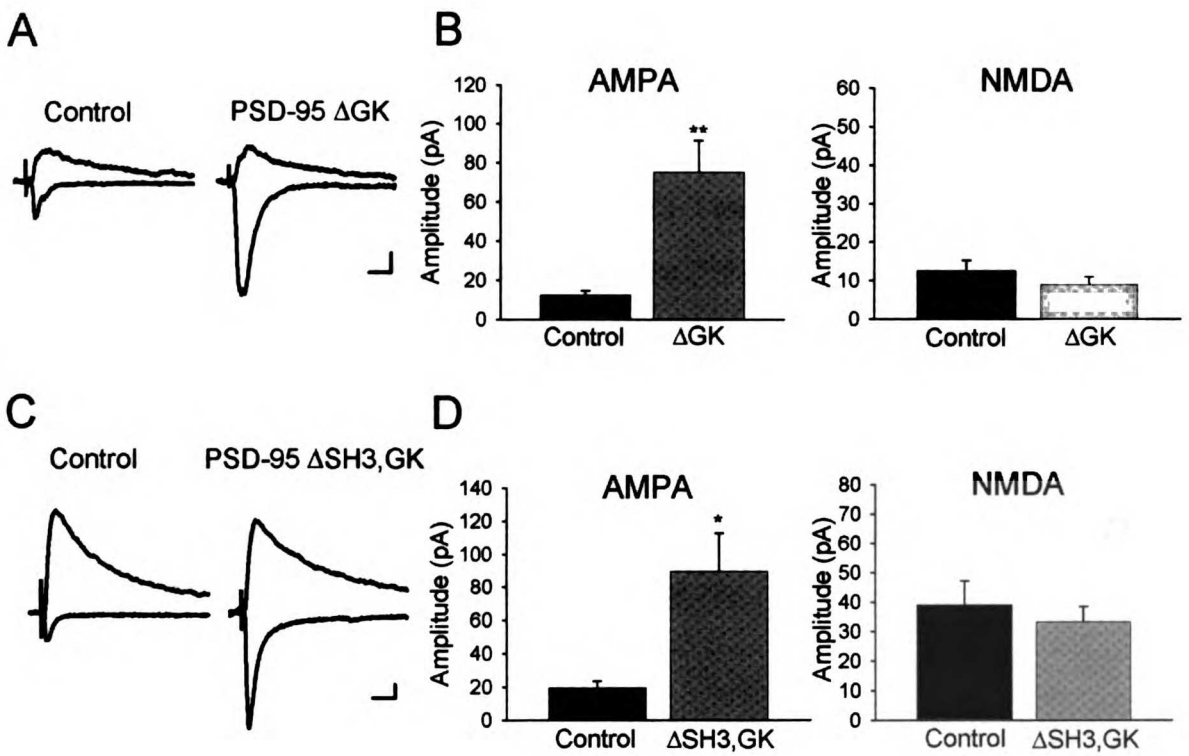
A
Control
PSD-95 ΔGK
B
AMPA
NMDA
Amplitude (pA)
120
100
80
60
40
20
0
**
Control
ΔGK
60
50
40
30
20
10
0
Control
ΔGK
C
Control
PSD-95 ΔSH3,GK
D
AMPA
NMDA
Amplitude (pA)
140
120
100
80
60
40
20
0
*
Control
ΔSH3,GK
80
70
60
50
40
30
20
10
0
Control
ΔSH3,GK

Figure 4. The first two PDZ domains are necessary and sufficient to enhance synaptic AMPAR EPSCs.

(A) Averaged EPSCs recorded simultaneously from a pair of cells, showing the responses at -70 mV and +40 mV in a PSD-95 ΔPDZ1-2 transfected cell and a neighboring untransfected cell. Scale bars, 10 pA, 20 msec. (B) Bar graph representations of the data obtained from the paired recordings showing no change in the evoked AMPAR or NMDAR EPSC (AMPAR EPSC, n = 25 pairs, p = 0.21; NMDAR EPSC, n = 25 pairs; p = 0.10). (C) Averaged EPSCs recorded simultaneously from a pair of cells, showing the responses at -70 mV and +40 mV in a PSD-95 PDZ1-2 transfected cell and a neighboring untransfected cell. This constuct consisted of the first 309 amino acids of PSD-95, including the palmitoylation motif and first two PDZ domains, with addition of the 25 amino acid C-terminal targeting motif. Scale bars, 10 pA, 20 msec. (D) Bar graph representations of the data obtained from the paired recordings showing an increase in the AMPAR EPSC without a change in the evoked NMDAR EPSC (AMPAR EPSC, n = 23 pairs, p = 0.0001; NMDAR EPSC, n = 19 pairs; p = 0.12).

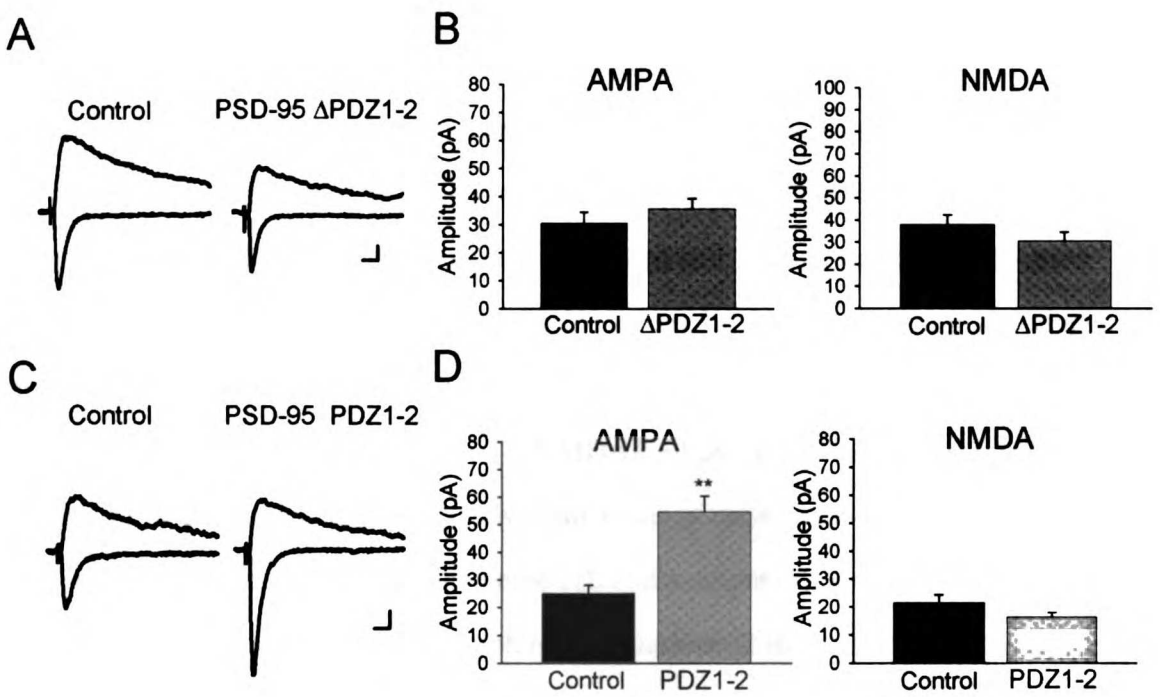
A
Control
PSD-95 ΔPDZ1-2
B
AMPA
NMDA
Amplitude (pA)
Control
ΔPDZ1-2
C
Control
PSD-95 PDZ1-2
D
AMPA
NMDA
**
Amplitude (pA)
Control
PDZ1-2

Figure 5. Effects of other MAGUK proteins on synaptic transmission.

(A) Averaged EPSCs recorded simultaneously from a pair of cells, showing the responses at -70 mV and +40 mV in a SAP97 transfected cell and a neighboring untransfected cell. Scale bars, 10 pA, 20 msec. (B) Bar graph representations of the data obtained from the paired recordings showing no change in the evoked AMPAR or NMDAR EPSC (AMPAR EPSC, n = 23 pairs, p = 0.52; NMDAR EPSC, n = 18 pairs; p = 0.30). (C) Appending the palmitoylation motif from the N-terminus of PSD-95 onto SAP97 results in a protein that enhances synaptic transmission. Averaged EPSCs recorded simultaneously from a pair of cells, showing the responses at -70 mV and +40 mV in a 95/97 transfected cell and a neighboring untransfected cell. Scale bars, 10 pA, 20 msec. (D) Bar graph representations of the data obtained from the paired recordings showing a large increase in the AMPAR EPSC with a modest change in the evoked NMDAR EPSC (AMPAR EPSC, n = 19 pairs, $p = 4 \times 10^{-6}$; NMDAR EPSC, n = 17 pairs; p = 0.01). (E) Averaged EPSCs recorded simultaneously from a pair of cells, showing the responses at -70 mV and +40 mV in a SAP102 transfected cell and a neighboring untransfected cell. Scale bars, 10 pA, 20 msec. (F) Bar graph representations of the data obtained from the paired recordings showing an increase in the AMPAR EPSC without a change in the evoked NMDAR EPSC (AMPAR EPSC, n = 27 pairs, p = 0.002; NMDAR EPSC, n = 23 pairs; p = 0.61).

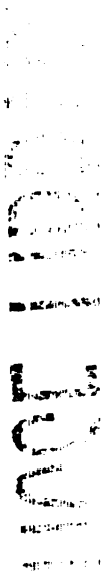

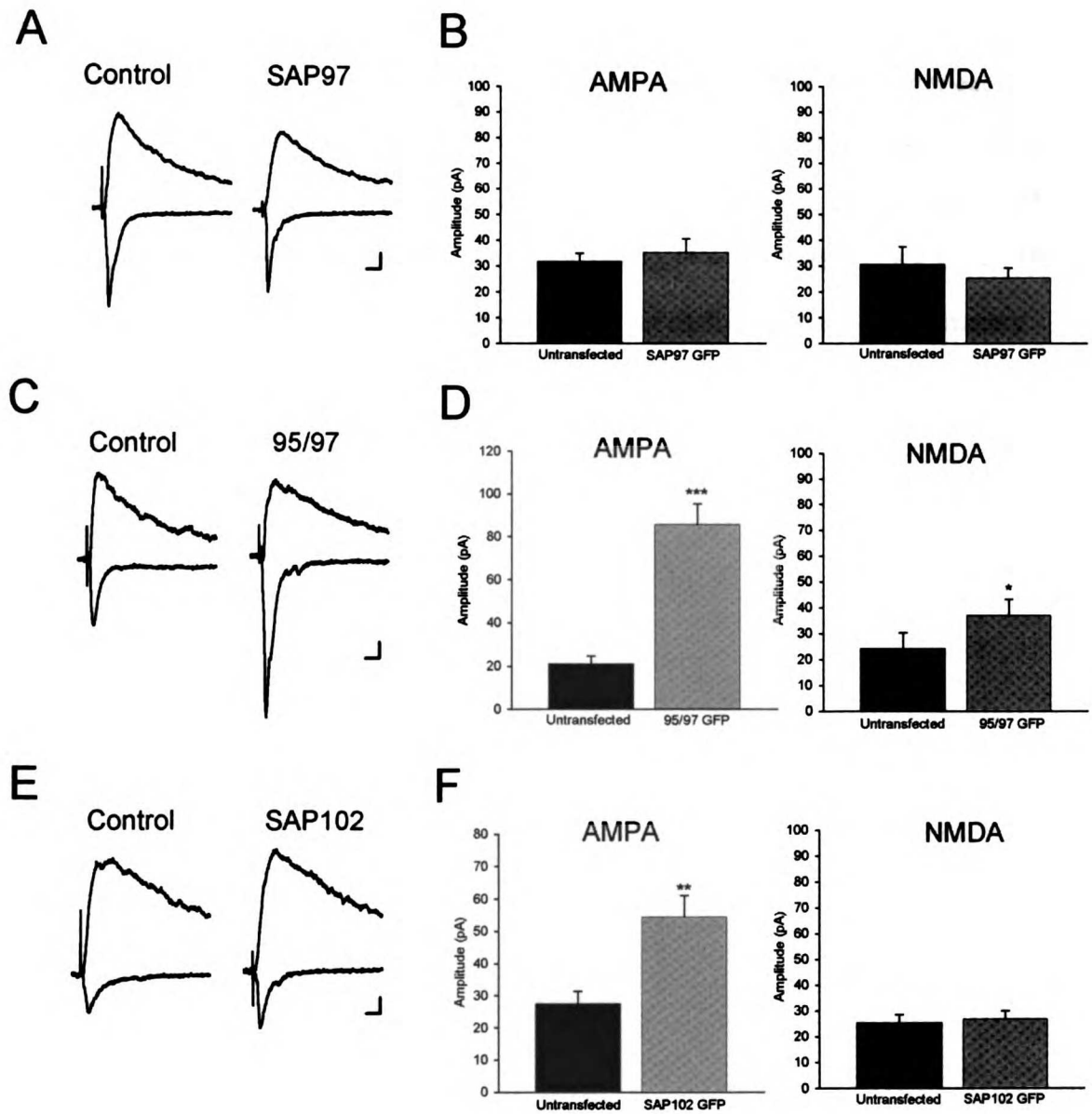
A
Control
SAP97
B
AMPA
NMDA
Amplitude (pA)
Untransfected
SAP97 GFP
C
Control
95/97
D
AMPA
NMDA
***
*
Untransfected
95/97 GFP
E
Control
SAP102
F
AMPA
NMDA
**
Untransfected
SAP102 GFP

Figure 6. Data summary from PSD-95 and MAGUK transfected neurons.

(A) Diagrams showing the domain structure of the various PSD-95 and MAGUK constructs. (B) Summary graph showing the effects of overexpressing the various constructs on the evoked AMPAR EPSC in simultaneously recorded pairs. For each construct, the normalized response was obtained by dividing the average AMPAR EPSC amplitude in the transfected cells by the average amplitude in paired, untransfected cells. Statistically significant values are marked with asterisks (* = $p < 0.05$; ** $p < 0.01$; *** $p < 0.001$), the number of paired recordings is listed for each construct. (C) Summary graph showing the effects of these constructs on the NMDAR EPSC.

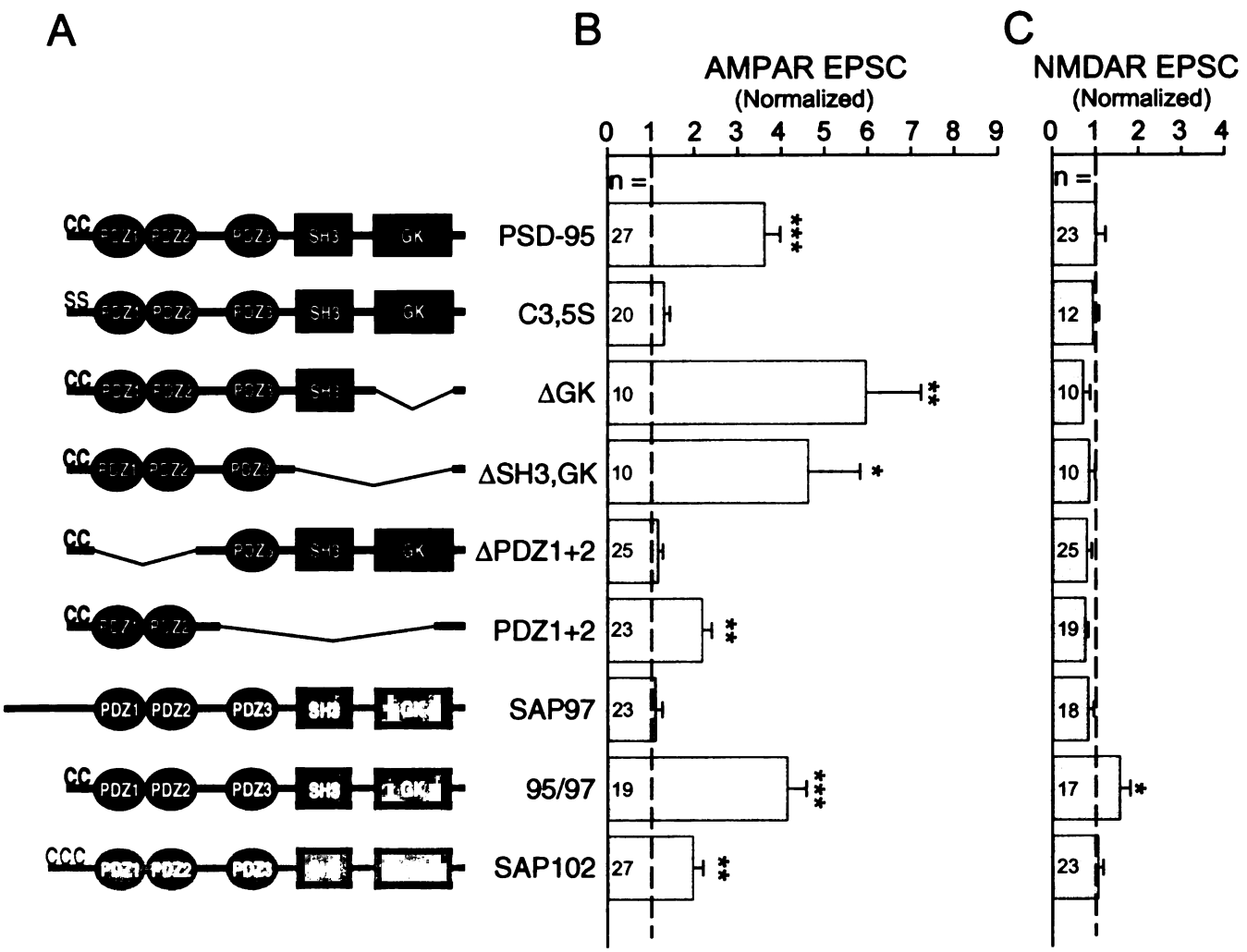
A
B
C
AMPAR EPSC
(Normalized)
NMDAR EPSC
(Normalized)
0 1 2 3 4 5 6 7 8 9
0 1 2 3 4
n =
CC
SS
CCC
PDZ1
PDZ2
PDZ3
SH3
GK
PSD-95
C3,5S
ΔGK
ΔSH3,GK
ΔPDZ1+2
PDZ1+2
SAP97
95/97
SAP102
27
20
10
10
25
23
23
19
18
17
23
23
12
10
25
19
17

Figure 7. Stargazin regulates synaptic AMPARs.

(A,B) Confocal images of pyramidal cells expressing stargazin-GFP (A) or stargazinΔC-GFP (B). Whereas stargazin GFP is clustered in synaptic spines, deletion of the last 4 amino acids (stargazinΔC) causes a diffuse localization. Scale bar, 5 μm. (C) Overexpression of stargazin has no effect on evoked synaptic responses (AMPAR EPSCs, n = 26 pairs, p = 0.48; NMDAR EPSCs, n = 14 pairs, p = 0.99). (D) Overexpression of stargazinΔC strongly reduces AMPAR EPSCs (n = 54 pairs, $p < 1x10^{-9}$) while having no effect on NMDAR EPSCs (n = 37 pairs, p = 0.43). Scale bars (traces) 10 pA, 20 msec.

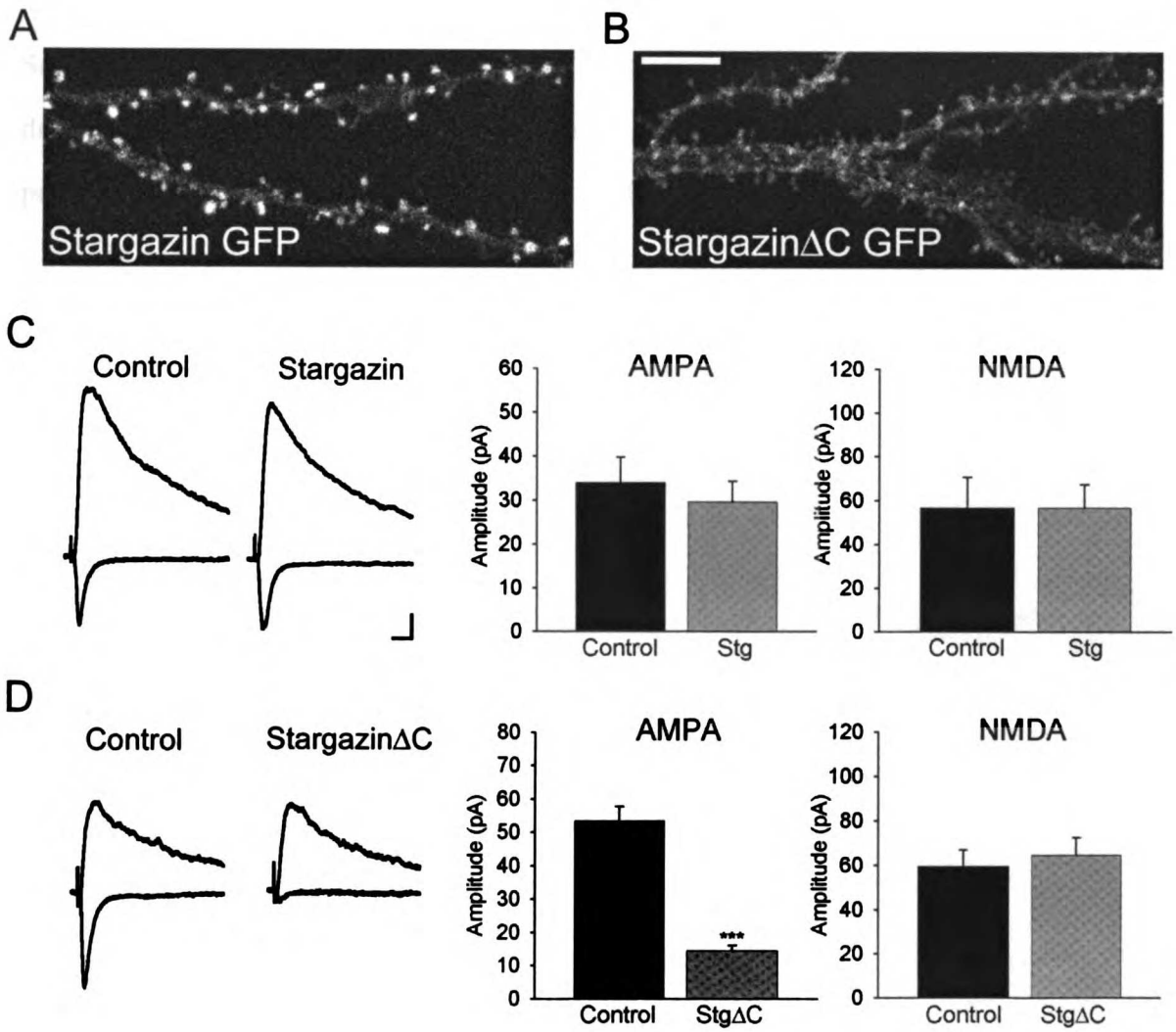
A
Stargazin GFP
B
StargazinΔC GFP
C
Control
Stargazin
AMPA
NMDA
Amplitude (pA)
Control
Stg
D
Control
StargazinΔC
AMPA
NMDA
***
Control
StgΔC

Figure 8. Stargazin regulates extrasynaptic AMPARs.

(A) Representative experiment showing the effect of bath-perfused AMPA on holding currents in a pair of simultaneously recorded pyramidal cells. Transfection with stargazinΔC increased the response to both concentrations of AMPA several fold. (B,C) Summary data showing that overexpression of stargazin (B) or stargazinΔC (C) dramatically increases responses to bath application of 500 nM AMPA (stargazin, n = 7 pairs, p = 0.003; stargazinΔC, n = 9 pairs, p = 0.0006).

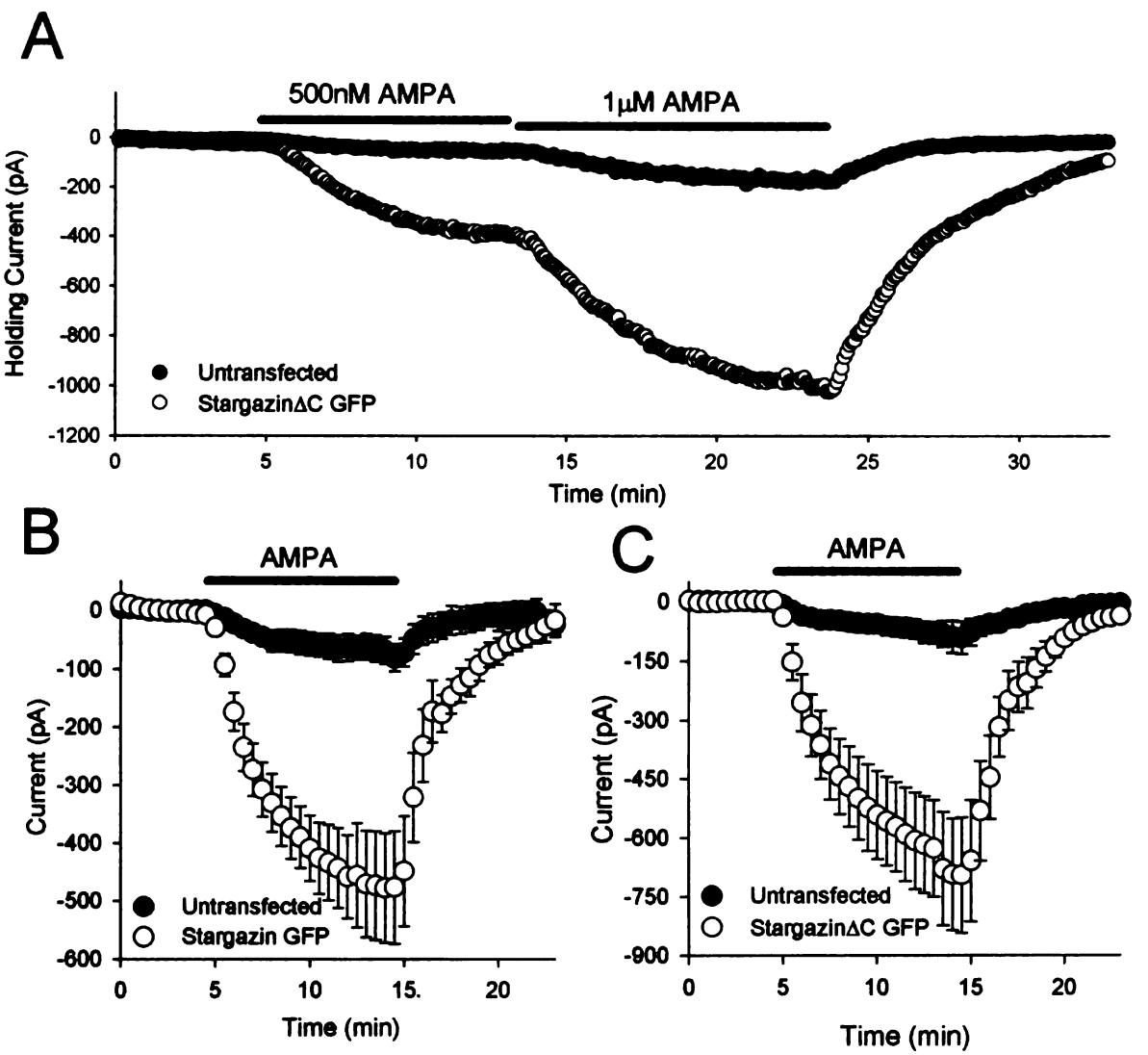
A
500nM AMPA
1μM AMPA
Holding Current (pA)
0
-200
-400
-600
-800
-1000
-1200
Untransfected
StargazinΔC GFP
0
5
10
15
20
25
30
Time (min)
B
AMPA
Current (pA)
0
-100
-200
-300
-400
-500
-600
Untransfected
Stargazin GFP
0
5
10
15.
20
Time (min)
C
AMPA
Current (pA)
0
-150
-300
-450
-600
-750
-900
Untransfected
StargazinΔC GFP
0
5
10
15
20
Time (min)

Figure 9. Overexpression of the stargazin C-terminus reduces synaptic AMPAR accumulation.

(A) Expression of GFP fused to the C-terminal 120 amino acids of stargazin reduces AMPAR and NMDAR EPSCs. Averaged EPSCs recorded simultaneously from a pair of cells, showing the responses at -70 mV and +40 mV in a GFP-StarCterm transfected cell and a neighboring untransfected cell. Scale bars, 20 pA, 20 msec. (B) Bar graph representations of the data obtained from the paired recordings showing a reduction in both the evoked AMPAR and NMDAR EPSC (AMPAR EPSC, n = 47 pairs, p = 0.002; NMDAR EPSC, n = 16 pairs; p = 0.009). (C) Co-transfection of GFP-StarCterm attenuates the enhancement of the AMPAR EPSC by PSD-95. PSD-95 was co-transfected with either GFP or GFP-StarCterm. Co-expression of GFP-StarCterm resulted in significantly less enhancement by PSD-95 than co-transfection with GFP (GFP + PSD-95 = 202 ±13% increase, n = 15 pairs; GFP-StarCterm + PSD-95 = 72 ± 19 % increase, n = 14 pairs, $p < 0.05$).

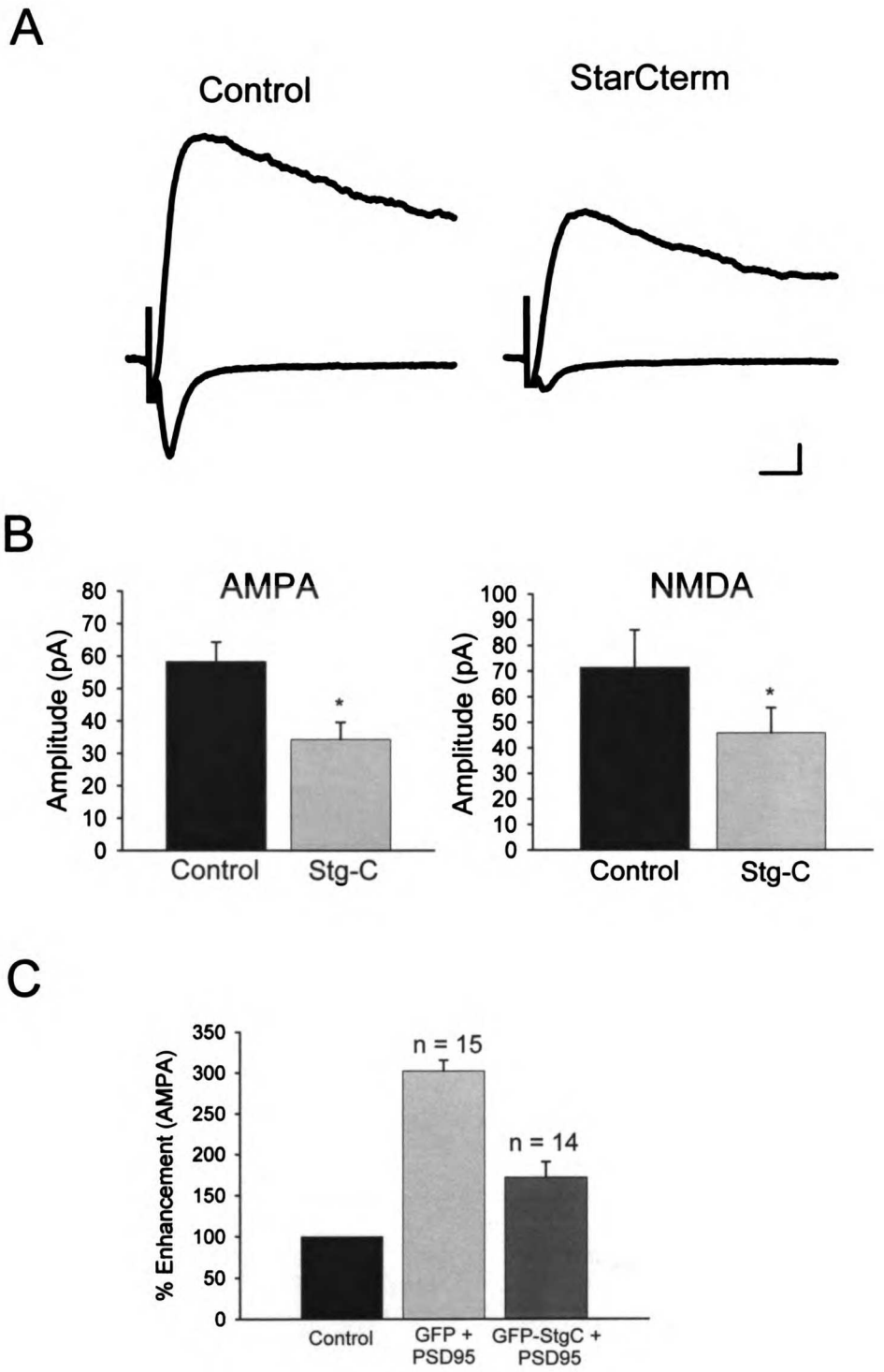
A
Control
StarCterm
B
AMPA
NMDA
Amplitude (pA)
80
70
60
50
40
30
20
10
0
100
90
80
70
60
50
40
30
20
10
0
*
*
Control
Stg-C
Control
Stg-C
C
% Enhancement (AMPA)
350
300
250
200
150
100
50
0
n = 15
n = 14
Control
GFP + PSD95
GFP-StgC + PSD95

Figure 10. Compensatory mutations to PSD-95 and stargazin reconstitute binding and clustering.

(A) GST fusion proteins show that stargazin with a point mutation in its PDZ-binding region (T321F) does not bind wildtype PSD-95, but does bind PSD-95 bearing a compensatory point mutation (H225V) in its second PDZ domain. (B) Confocal images of pyramidal cells expressing stargazin T321F GFP. Stargazin T321F GFP alone expressed diffusely (top), reminiscent of the stargazinΔC expression pattern. Co-expression of untagged PSD-95 did not alter the diffuse localization of stargazin T321F (center). Co-transfection of an untagged compensatory PSD95 (PSD-95 H225V) caused robust synaptic localization of stargazin T321F GFP (bottom). Scale bar, 5 μm.

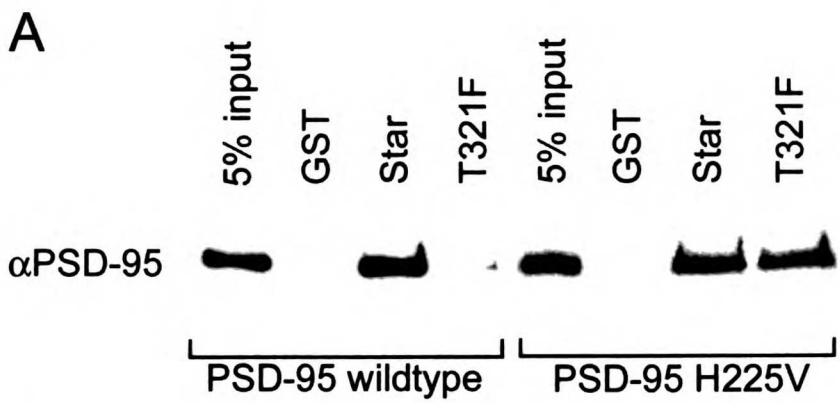
A
5% input
GST
Star
T321F
5% input
GST
Star
T321F
αPSD-95
PSD-95 wildtype
PSD-95 H225V

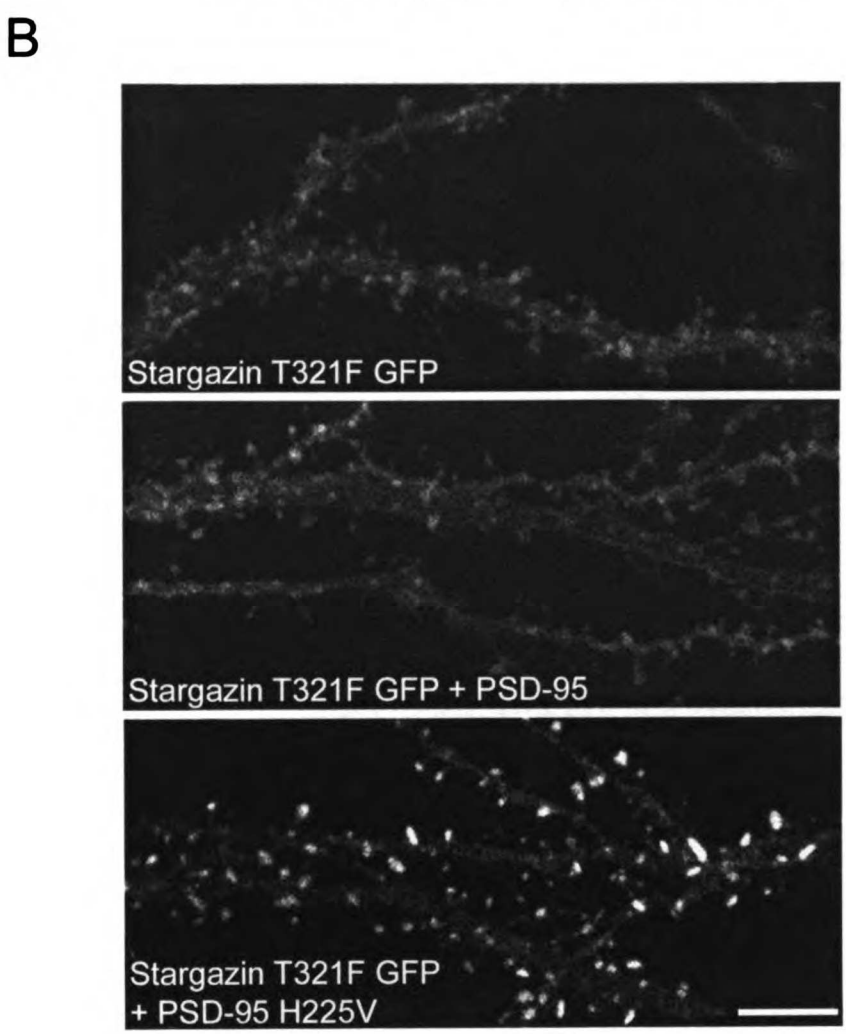
B
Stargazin T321F GFP
Stargazin T321F GFP + PSD-95
Stargazin T321F GFP
+ PSD-95 H225V

Figure 11. PSD-95 and stargazin directly interact to mediate synaptic AMPAR delivery.

(A) Stargazin T321F overexpression dramatically reduces AMPAR EPSCs (n = 14 pairs, $p < 0.00001$) but does not change NMDAR EPSCs (n = 13 pairs, p = 0.52). (B) The enhancement mediated by PSD-95 overexpression is reversed by a non-interacting stargazin mutant. Co-expression of stargazin T321F with PSD-95 still results in a significant reduction of the AMPAR EPSC (n = 30 pairs, p = 0.035). (C) Co-expression of stargazin T321F with a PSD-95 construct bearing a compensatory mutation rescues and significantly enhances the AMPAR EPSC. PSD-95 mutants bearing a complementary mutation in either PDZ1 (H130V) or PDZ2 (H225V) were co-transfected with the stargazin mutant. In the bar graphs, results from both co-transfections were combined as the results were identical (see text) (AMPAR EPSCs, p = 0.00001, n = 35 pairs; NMDAR EPSCs, p = 0.43, n = 31 pairs). Scale bars: 10 pA, 20 msec.

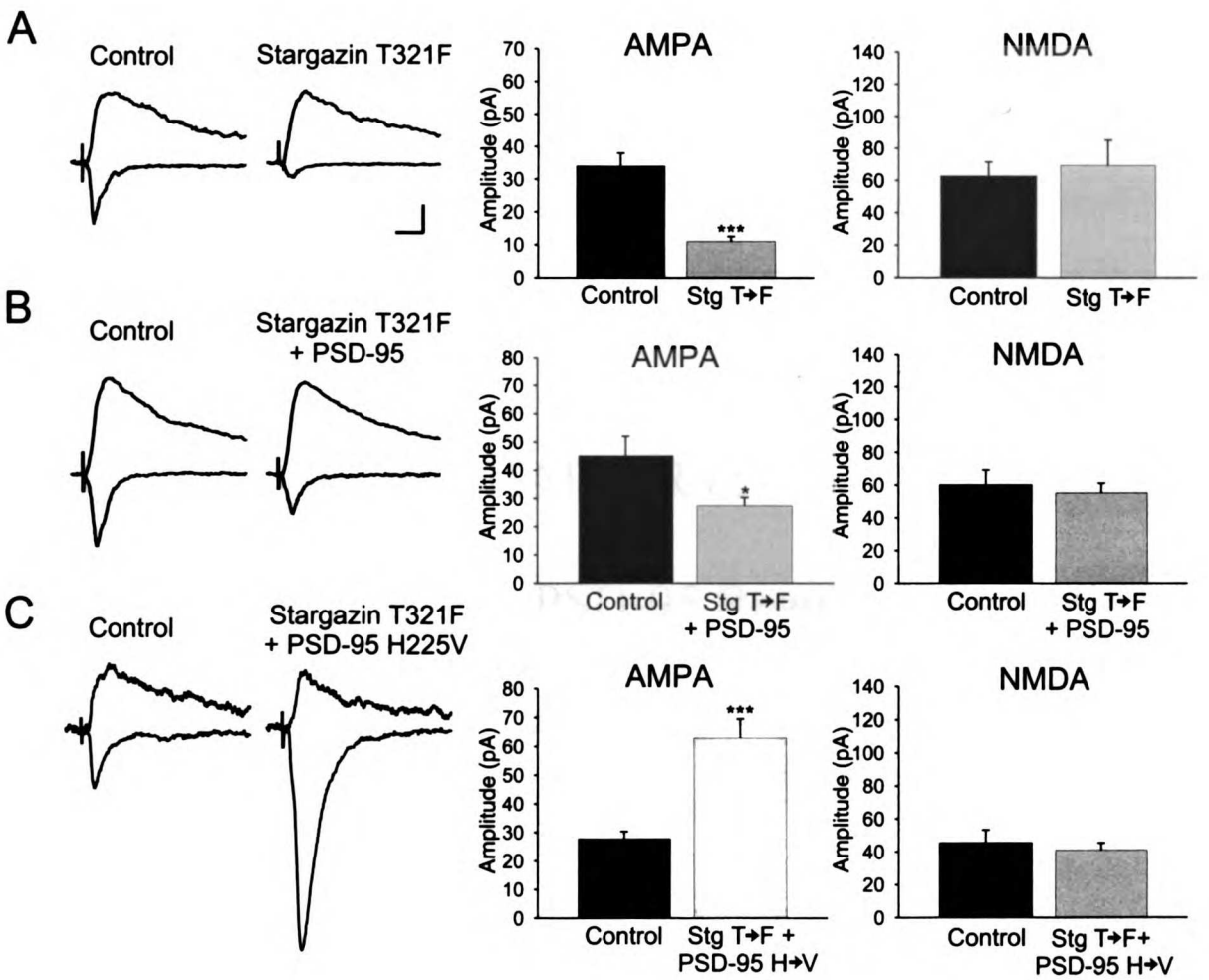
A
Control
Stargazin T321F
AMPA
NMDA
Amplitude (pA)
***
Control
Stg T→F
B
Control
Stargazin T321F
+ PSD-95
AMPA
NMDA
*
Control
Stg T→F
+ PSD-95
C
Control
Stargazin T321F
+ PSD-95 H225V
AMPA
NMDA
***
Control
Stg T→F +
PSD-95 H→V
Stg T→F+
PSD-95 H→V

CHAPTER 6:

Palmitate Cycling on PSD-95 Regulates Synaptic Strength

Introduction

Excitatory signaling in brain occurs primarily at synapses that employ glutamate as a neurotransmitter. The ionotropic glutamate receptors are clustered with associated downstream signaling enzymes in the postsynaptic density (PSD), a thickening of the cytoskeleton beneath the plasma membrane (Kennedy, 1997; Walters and Matus, 1975). This clustered arrangement facilitates rapid and efficient transmission; however, the PSD is also a dynamic structure. Changes in glutamate receptor number at the PSD provide a critical mechanism for rapidly altering synaptic strength (Malenka and Nicoll, 1999; Malinow et al., 2000). Interestingly, the two principle classes of ionotropic glutamate receptors are differentially anchored at the PSD. The NMDARs are firmly tethered to the PSD (Moon et al., 1994), whereas the AMPARs are more loosely attached (Malenka and Nicoll, 1999; Malinow et al., 2000). Dynamic cycling of AMPARs on and off the synaptic membrane occurs in an activity-dependent fashion and appears to underlie aspects of synaptic plasticity (Beattie et al., 2000; Ehlers, 2000; Lin et al., 2000; Lüscher et al., 1999; Man et al., 2000).

By interacting with glutamate receptors, cell adhesion molecules, and cytoskeletal elements (Irie et al., 1997; Kim et al., 1997; Kornau et al., 1997), MAGUK proteins regulate synapse development and plasticity. Disruption of *discs large* (*dlg*), a *Drosophila* MAGUK, perturbs postsynaptic structure and blocks clustering of *Shaker* type K^+ channels that normally associate with DLG (Tejedor et al., 1997). In cultured hippocampal neurons, overexpression of PSD-95 accelerates development of excitatory

synapses and selectively enhances clustering of AMPARs (El-Husseini et al., 2000b). On the other hand, targeted disruption of PSD-95 causes severe abnormalities of synaptic plasticity such that long-term potentiation (LTP) is enhanced and long-term depression (LTD) is eliminated (Migaud et al., 1998). These abnormalities in synaptic plasticity presumably explain why PSD-95 mutant mice are impaired in spatial learning (Migaud et al., 1998).

How might PSD-95 dynamically regulate synaptic glutamate receptors and synaptic plasticity? Phosphorylation of DLG within PDZ1 by calcium / calmodulin dependent protein kinase regulates clustering at the *Drosophila* neuromuscular junction (Koh et al., 1999), but it is uncertain whether this mechanism applies for PSD-95 in brain. In addition to its PDZ motifs, PSD-95 contains several other domains that could help explain its role. The C-terminal half of PSD-95 comprises an SH3 and a guanylate kinase domain, which both function as protein-protein interaction motifs (Craven and Bredt, 1998; Garner et al., 2000; Lee and Sheng, 2000). Interestingly, these domains also can bind each other in both intra- and intermolecular orientations (McGee and Bredt, 1999; Shin et al., 2000). However, it is not yet clear how the SH3 or GK domains might be regulated in an activity-dependent fashion.

PSD-95 also contains two critical cysteine residues at positions 3 and 5, which are sites of protein palmitoylation (Topinka and Bredt, 1998). This post-translational modification involves addition of palmitate, a 16-carbon fatty acid, via a labile thioester linkage (Dunphy and Linder, 1998; Resh, 1999). Palmitoylation of PSD-95 is essential

for receptor clustering at the PSD (Craven et al., 1999). Akin to protein phosphorylation, palmitoylation is a reversible process that is dynamically regulated by specific cellular stimuli (Milligan et al., 1995; Mumby, 1997). We therefore asked whether this lipidation of PSD-95 is activity-dependent at the synapse and whether this might regulate glutamate receptor function.

Here, we identify palmitate turnover on PSD-95 at the synapse. This palmitate cycling occurs in an activity-dependent fashion, and acutely disrupting palmitoylation with 2-bromopalmitate disperses synaptic clusters of PSD-95. This activity-dependent dispersion of PSD-95 results in a selective loss of AMPAR subunits and AMPAR activity at synapses. Preventing depalmitoylation of PSD-95 blocks glutamate-mediated internalization of AMPARs. Surface clusters of PSD-95, stargazin and AMPAR subunits that form in transfected heterologous cells also require on-going palmitoylation of PSD-95 at the plasma membrane. These studies suggest that protein palmitoylation is regulated in an activity-dependent fashion at the synapse and suggest mechanisms for plasticity regulated by palmitate cycling on PSD-95.

Results

Dynamic Turnover of Palmitate on PSD-95 at the Synapse

Previous studies have shown that palmitoylation of PSD-95 is essential for its clustering at synapses (Craven et al., 1999). To determine whether palmitoylation of

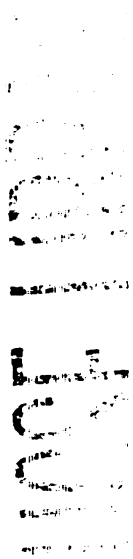

PSD-95 is a dynamic process at the synapse, we treated cultured hippocampal neurons (DIV 14) with 2-bromopalmitate, a drug that potently blocks palmitoylation by blocking protein acyl-transfer (Webb et al., 2000). We found that incubation of neurons with 10 μM 2-bromopalmitate dispersed synaptic clusters of PSD-95 (Fig. 1A, B) and blocked palmitoylation of PSD-95 (Fig. 1C). This treatment did not affect clustering of synaptophysin, a presynaptic marker used as a control (Fig. 1A). This effect was also seen with 2-bromopalmitoyl-CoA (Fig. 1B), which also inhibits protein palmitoylation (data not shown). Synaptic clusters of PSD-93 (Brenman et al., 1996b; Kim et al., 1996), a palmitoylated MAGUK (El-Husseini et al., 2000c) related to PSD-95 are also dispersed by 2-Br palmitate (Fig. 2). As a control we found that palmitate at a 10 times higher dose significantly enhanced clustering of PSD-95 (Fig. 1A, B). The effects of 2-Br palmitate on clustering are not simply due to disrupting palmitoylation of newly synthesized PSD-95, as cycloheximide, which effectively blocks synthesis of PSD-95 (Fig. 3C), does not disperse PSD-95 synaptic clusters (Fig. 1A, B).

Many palmitoylated proteins, including PSD-95, are insoluble in non-ionic detergents (Cho et al, 1992, Kistner et al, 1993). As a surrogate assay for palmitoylation, we monitored the solubility of PSD-95 in neurons treated with 2-bromopalmitate. Neurons were homogenized, lysed in hypotonic buffer, and lysates were centrifuged to separate cytosolic (soluble) and membrane (particulate) fractions. The ratio of PSD-95 in the soluble / particulate fractions (S/P ratio) was quantified by gel densitometry. As previously described the majority of PSD-95 in cultured hippocampal neurons is insoluble (S/P = 34±12); however, treatment with 2-bromopalmitate dramatically

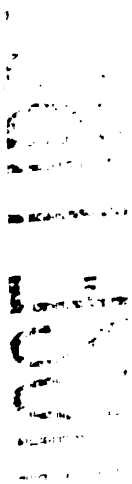

increased the soluble fraction of PSD-95 (S/P = 79±8; Fig. 1D). Interestingly, treatment with palmitate itself reduced the soluble fraction of PSD-95 (S/P = 19±9), suggesting it may not be fully palmitoylated in normal culture conditions.

Palmitate Cycling on PSD-95 is Regulated by Synaptic Activity

As palmitate turnover on the α-subunit of certain G-proteins is regulated by activation of their upstream receptors (Wedegaertner and Bourne, 1994), we asked whether palmitate turnover on PSD-95 might be regulated by glutamate receptor activity. Indeed, we found that blocking glutamate receptors with kynurenic acid, an ionotropic glutamate receptor antagonist, blocked the declustering of PSD-95 by 2-bromopalmitate (Fig. 4A, B). Similarly, we found that blocking glutamate receptors with a combination of CNQX, which blocks AMPARs and APV, which blocks NMDARs also partially prevented declustering of PSD-95 by 2-bromopalmitate (Fig. 4B). To determine if calcium is required for this process, we treated neurons with 2-Br palmitate in the absence of extracellular calcium and found that removing calcium protected clustering and palmitoylation of PSD-95 (Figs. 4A, B). These results indicate calcium entry associated with glutamate receptor activity is critical for depalmitoylation. In contrast, treatment with glutamate receptor antagonists or removing extracellular calcium alone did not detectably change PSD-95 clustering (Fig. 4B).

The activity-dependent loss of synaptic PSD-95 that occurs in the presence of 2-bromopalmitate has two possible explanations: 1) depalmitoylation of PSD-95 is

accelerated by glutamate receptor activity, or 2) diffusion of palmitate-free PSD-95 from the synapse requires glutamate receptor activity. To help to distinguish between these two possibilities, we quantitated the cycling of palmitate on PSD-95. Palmitate turnover on PSD-95 in neurons was monitored by metabolically labeling hippocampal cultures with [^{125}I]palmitate, which is a sensitive radioactive precursor that is incorporated faithfully into palmitoylated proteins (Berthiaume et al., 1995). We found that the half-life of palmitate on PSD-95 is approximately two hours, whereas the half-life of PSD-95 protein itself is much longer, approximately 36 hours (Fig. 3A; 5A, B). Importantly, the half-life of palmitate on PSD-95 was substantially increased in the presence of kynurenic acid (Fig. 5A, B). Conversely, glutamate treatment (10 μM) reduced the half-life of palmitate on PSD-95 (Fig. 5C). These data indicate that glutamate receptor activity stimulates palmitate turnover on PSD-95.

Palmitate Cycling on PSD-95 Regulates Synaptic AMPARs

NMDARs directly bind PSD-95 (Kornau et al., 1995) whereas AMPARs, which are indirectly associated (Chen et al., 2000), are recruited to synapses by PSD-95 overexpression (El-Husseini et al., 2000b). We therefore asked whether the 2-bromopalmitate induced loss of synaptic PSD-95 affects associated glutamate receptors. Immunohistochemical staining of hippocampal cultures treated with 2-bromopalmitate showed synaptic clustering of the AMPAR subunit GluR1 is diminished (Fig. 6A-C). The loss of GluR1 at synapses was quantitatively similar to that of PSD-95. On the other

hand, synaptic clustering of NMDARs as measured by NMDAR subunits 1 or 2B (NR1 or NR2B) was unaffected by 2-bromopalmitate (Fig. 6B, C).

We next asked whether disrupting PSD-95 clustering with 2-bromopalmitate causes specific changes in glutamatergic function. AMPA-mediated miniature excitatory post-synaptic currents (mEPSCs) were monitored with whole-cell recordings from cultured hippocampal neurons by an investigator blinded with regard to 2-bromopalmitate treatment. These experiments revealed a significant reduction in the amplitude and frequency of synaptic events in 2-bromopalmitate treated neurons (Fig. 7). These data suggest a decrease in the number of functional AMPARs at synaptic sites and are consistent with the reduction in punctate GluR1 immunostaining. The selective reduction in AMPAR immunostaining relative to NMDAR staining in 2-bromopalmitate treated cells predicts a reduction in the ratio of synaptic AMPARs to NMDARs at individual synapses. We therefore recorded dual component mEPSCs using conditions that allowed us to assay AMPA and NMDA currents simultaneously. We found that the ratio of AMPA-mediated currents to NMDA-mediated currents was significantly reduced in the 2-bromopalmitate treated cells (Fig. 8), demonstrating a selective effect of 2-bromopalmitate on synaptic AMPAR function.

This loss of synaptic GluR1 in 2-bromopalmitate treated cultures may result from changes in palmitoylation of PSD-95 or from loss of palmitate on other proteins. To help to assess this we employed a palmitoylation-deficient PSD-95 mutant (PSD-95-prenyl) that is isoprenylated at its C-terminus (Fig. 9) and recruited to synapses independent of

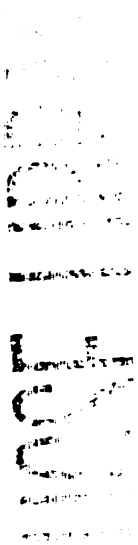

palmitoylation (El-Husseini et al., 2000a). We transfected neurons with constructs encoding GFP fused either to wild-type PSD-95 or to PSD-95-prenyl and assessed the effects of 2-bromopalmitate on synaptic clustering. As previously published (El-Husseini et al., 2000b), AMPAR clusters are enhanced in neurons transfected with PSD-95 (Fig. 9B, E), and these clusters are diminished following treatment with 2-bromopalmitate (Fig. 9C-E). PSD-95-prenyl also enhanced synaptic clustering of GluR1 in transfected cells (Fig. 6C, E). However, these synaptic AMPAR clusters as well as those of prenyl-PSD-95 were resistant to treatment with 2-bromopalmitate (Fig. 9C-E).

We used the PSD-95-prenyl mutant to assess a possible role for palmitate cycling on PSD-95 in activity dependent turnover of AMPARs. These experiments employed an "antibody feeding" immunofluorescence internalization assay to quantify AMPAR endocytosis. As previously reported (Beattie et al., 2000; Ehlers, 2000; Lin et al., 2000; Zhou et al., 2001), 15 min exposure to glutamate (100 μM) enhances internalization of AMPAR subunit GluR1 (Fig. 10). The internalized AMPAR vesicles accumulate in both the cell body and dendritic processes. This glutamate-mediated AMPAR internalization was enhanced in cells transfected with wild type PSD-95 (Fig. 10); this enhancement likely results from the increased synaptic expression of AMPARs in PSD-95 transfected neurons (El-Husseini et al., 2000b). Importantly, glutamate-mediated AMPAR internalization was abolished in cells transfected with PSD-95-prenyl (Fig. 10), indicating that palmitoylation is critical for this regulated AMPAR turnover. Neither wild type nor PSD-95-prenyl affected basal AMPAR internalization (Fig. 10B).

Regulation of AMPAR Clustering by Palmitate Turnover on PSD-95

To determine whether the role of palmitate cycling in clustering of PSD-95 and AMPARs can be reproduced in a model system that lacks the molecular complexity of neuronal synapses, we evaluated clustering in heterologous cells. In this model, co-transfection of COS cells with PSD-95, the glutamate receptor targeting protein stargazin, and the AMPAR subunit GluR4, yields clusters of the three proteins that appear as patches along the plasma membrane (Chen et al., 2000). Treating cultures with 2-bromopalmitate dispersed these pre-formed clusters and caused all three proteins to redistribute to perinuclear vesicles that suggest an intracellular accumulation (Fig. 11A). This vesicular distribution of PSD-95 and stargazin/GluR4 is also observed in transfections with a palmitoylation-deficient mutant of PSD-95 (Fig. 11A). This localization resembles the ER/golgi accumulations of palmitoylation-deficient PSD-95 co-transfected with Kv1.4 (Tiffany et al., 2000). To verify that the effects of 2-bromopalmitate on PSD-95/stargazin/GluR4 in heterologous cells are specific for palmitoylation of PSD-95, we used the prenylated mutant of PSD-95. When this construct was co-transfected with stargazin and GluR4, clusters of the three proteins are observed (Fig. 11B). Although these clusters are smaller than those observed with the palmitoylated version, they appear to be on the plasma membrane and otherwise resemble those found with palmitoylated PSD-95. Importantly, these clusters formed with PSD-95-prenyl are resistant to treatment with 2-bromopalmitate confirming the specificity of this drug for palmitoylated PSD-95 (Fig. 11B).

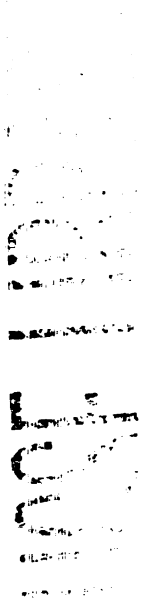

Discussion

This study identifies palmitate turnover on PSD-95 as a critical regulatory mechanism at the synapse. This cycling of palmitate is regulated by glutamate receptor activity and interrupting this cycle with 2-bromopalmitate disperses PSD-95 and AMPAR clusters. Disrupting palmitate cycling on PSD-95 blocks glutamate mediated AMPAR internalization. Regulated palmitoylation of PSD-95 therefore represents a novel physiological mechanism for activity-dependent changes in synaptic strength.

Regulation of the Dynamic Pool of AMPARs by PSD-95

Previous studies have shown that PSD-95 and related MAGUKs interact with glutamate receptors and other ion channels at the synapse (Craven and Bredt, 1998; Garner et al., 2000; Hayashi et al., 2000; Lee and Sheng, 2000; Tejedor et al., 1997). PDZ domains from PSD-95 directly bind the C-termini of NMDAR subunits and other proteins terminating with a tSXV motif (Kim et al., 1995; Kornau et al., 1997). This PDZ-binding sequence is also present on the AMPAR trafficking protein, stargazin (Chen et al., 2000). Stargazin is a tetraspanning transmembrane protein that interacts with AMPARs and is essential for their targeting to the plasma membrane (Chen et al., 2000; Tomita et al., 2001). By binding to the PDZ domain of PSD-95, stargazin indirectly links AMPARs to PSD-95. Through these PDZ interactions, PSD-95 can mediate clustering

of either NMDARs (Lee and Sheng, 2000) or stargazin/AMPARs (Chen et al., 2000) in heterologous cells.

The essential role for PSD-95 in glutamate receptor clustering at the synapse is less certain. Dislodging PSD-95 from synapses with peptides that block its binding to the cytoskeletal protein CRIPT does not disrupt synaptic NMDAR clusters (Passafaro et al., 1999). The converse strategy – overexpressing PSD-95 in neurons – causes a selective enhancement in synaptic AMPARs whereas NMDARs are unaltered (El-Husseini et al., 2000b). Furthermore, in mutant mice lacking PSD-95, there is no change in the distribution or activity of NMDARs though there are clear changes in synaptic plasticity (Migaud et al., 1998). Our studies show that disrupting palmitoylation of PSD-95 with 2-bromopalmitate decreases the number and frequency of miniature EPSCs consistent with the decreased immunohistochemical staining for AMPAR subunits. Additionally, 2-bromopalmitate selectively affects AMPARs but not NMDARs. Taken together, these studies suggest that PSD-95 is not essential for recruiting the constitutive pool of synaptic NMDARs, but that PSD-95 regulates a dynamic pool of AMPARs.

Palmitate Turnover Regulated by Synaptic Activity

Palmitoylation of residues of 3 and 5 plays an essential role in synaptic targeting of PSD-95 and in clustering of associated receptors (Craven et al., 1999; Topinka and Bredt, 1998). Palmitoylation of PSD-95 occurs first in the neuronal cell body and targets PSD-95 to a perinuclear endomembrane system (El-Husseini et al., 2000a). The pathway

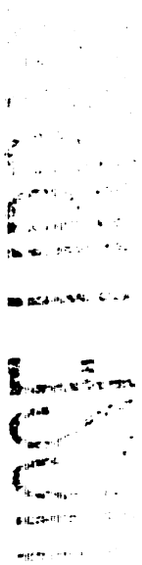

for trafficking PSD-95 from perinuclear endosomes to synaptic clusters is uncertain, but some insights have been gained from studies of receptor clustering with PSD-95 in heterologous cells. In COS cells co-transfected with PSD-95 and an interacting ion channel, clusters of both proteins form on the plasma membrane. Live cell-imaging shows that these surface patches are derived from dynamic vesiculotubular transport intermediates for PSD-95-GFP that fuse with the plasma membrane (El-Husseini et al., 2000a), suggesting that PSD-95 regulates vesicular trafficking of receptors. On the plasma membrane, these PSD-95 / ion channel clusters are immobile (Burke et al., 1999); however, studies here indicate that these are not static structures. Acutely blocking palmitoylation disperses these clusters and causes both PSD-95 and the interacting stargazin / AMPARs to redistribute to perinuclear endosomal structures, suggesting that de-palmitoylation enhances receptor endocytosis. These data are consistent with previous studies showing that the palmitoylation-deficient mutant PSD-95 (C3, 5S) enhances internalization of the associated ion channel, Kv 1.4 (Jugloff et al., 2000).

In neurons, blocking palmitoylation also disperses preformed synaptic clusters of PSD-95. This suggests that maintenance of PSD-95 synaptic clusters requires on-going palmitoylation. Importantly, palmitate turnover on PSD-95 is regulated by glutamate receptor activity, as glutamate receptor antagonists prolong the half-life of palmitate on PSD-95 and prevent declustering of PSD-95 by 2-bromopalmitate. This stimulation of palmitate turnover by activation of an upstream glutamate receptor is reminiscent of receptor-activated palmitate cycling on signaling proteins in non-neuronal cells. An elegant series of studies has shown that activation of β-adrenergic receptors stimulates

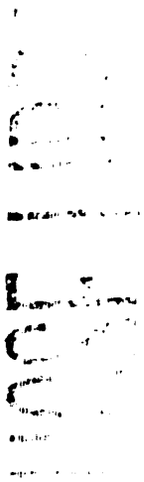

palmitate turnover on Gαs (Wedegaertner and Bourne, 1994). This depalmitoylation down regulates G-protein signaling by both a) removing Gα from the plasma membrane and b) enhancing deactivation of Gα by RGS proteins (Resh, 1996; Tu et al., 1997). Agonist stimulated depalmitoylation of endothelial nitric oxide synthase also disrupts its membrane localization and activity (Robinson et al., 1995). The cytosolic tails of some receptors are also palmitoylated, and this can regulate receptor-mediated endocytosis (Alvarez et al., 1990). By analogy, our studies show that activity-dependent depalmitoylation causes PSD-95 to diffuse from the PSD and down-regulates synaptic AMPARs. Taken together, these data suggest that agonist-stimulated palmitate turnover may represent a common mechanism for dampening receptor activated signaling.

Palmitate Turnover Regulating Synaptic Function

The enzymes that regulate palmitoylation of PSD-95 at the synapse remain unidentified. Our previous studies showed that the N-terminus of PSD-95 contains a five amino-acid consensus sequence that determines palmitoylation (El-Husseini et al., 2000a). However, the protein acyl-transferase that recognizes this sequence and mediates palmitoylation and the protein thioesterase that removes the palmitate remain uncertain. For this reason, it is unclear how glutamate receptor activity stimulates palmitate turnover. One possibility is that the protein thioesterase is a second messenger regulated enzyme whose activity is stimulated by calcium influx or protein phosphorylation at the postsynaptic density. Alternatively, synaptic activity may make the N-terminus of PSD-95 more accessible to the thioesterase in a mechanism akin to that proposed for receptor

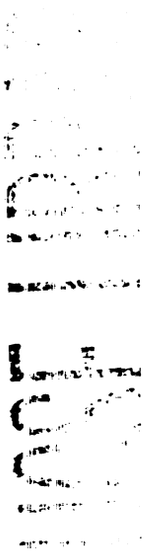

stimulated palmitate turnover on G-protein subunits. Isolation of the proteins that mediate addition and removal of palmitate will help address these issues.

PSD-93, a close homologue of PSD-95 is palmitoylated, expressed in hippocampal neurons, and can interact with stargazin. Furthermore, synaptic clusters of PSD-93 are dispersed by 2-bromopalmitate. This isoform redundancy may explain why basal synaptic transmission remains intact in PSD-95 mutant mice (Migaud et al., 1998). In addition to PSD-95 and PSD-93 (El-Husseini et al., 2000c), a variety of proteins associated with glutamatergic transmission are regulated by palmitoylation and inhibiting their palmitoylation could influence synaptic function. These include the metabotropic glutamate receptor mGluR4 (Alaluf et al., 1995), the kainate receptor subunit GluR6 (Pickering et al., 1995), and the glutamate receptor interacting protein GRIP (Yamazaki et al., 2001). Changes in palmitoylation of these proteins are unlikely to explain the affects observed here, as we found that expression of a palmitate-resistant mutant of PSD-95 (PSD-95-prenyl) blocked the effects of 2-bromopalmitate on AMPAR clustering and prevented glutamate-mediated AMPAR internalization. Nevertheless, palmitoylation of numerous proteins at the PSD suggests that this protein modification may play multiple important roles at the synapse. Our studies of activity regulated cycling of palmitate on PSD-95 should serve as a prototype for understanding how this mechanism can regulate synaptic structure and function.

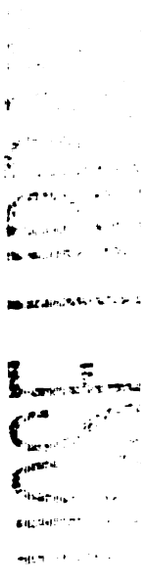

Figure 1. Blocking palmitoylation disperses synaptic clusters of PSD-95.

(A) Cultured hippocampal neurons (DIV 14) were treated for 8 hr with 10 μM 2-bromopalmitate (2-Br Palm), 2-bromo palmitoyl-CoA (2-Br Palm CoA), 10 μg/ml cycloheximide (CHX), 16-hydroxypalmitate (16-OH Palm), or 10 μm palmitate (Palm), or palmitate. Neurons were then fixed and stained for PSD-95 and synaptophysin. Treatment with agents that block protein palmitoylation results in declustering of PSD-95. In contrast, treatment with palmitate slightly enhanced clustering of PSD-95. Cycloheximide did not alter PSD-95 clustering, and none of the treatments changed synaptophysin staining. (B) Quantitative analysis of the intensity of PSD-95 clusters after these treatments. Treatment with 2-Br Palm or 2-Br Palm-CoA significantly reduced PSD-95 clustering ($p<0.001$), whereas treatment with palmitate significantly enhanced ($p<0.01$) PSD-95 clustering when compared to cells treated with vehicle. (C) 2-Bromopalmitate blocks palmitoylation of PSD-95. Neurons were treated with [^{125}I]palmitate and either vehicle or 10 μM 2-bromopalmitate for three hours. PSD-95 was purified by immunoprecipitation; [^{125}I] incorporation was visualized by autoradiography; and PSD-95 protein was visualized by western blotting (W.B.). (D) Blocking palmitoylation increases the solubility of PSD-95. After treatment with 2-bromopalmitate or palmitate, neurons were harvested and the lysate (L) was subjected to protein fractionation (see Experimental Procedures). Treatment with 2-bromopalmitate increased the amount of PSD-95 in the soluble fraction (S). In contrast, PSD-95 in untreated or palmitate-treated cultures was primarily in the pellet (P). Scale bar, 10 μm.

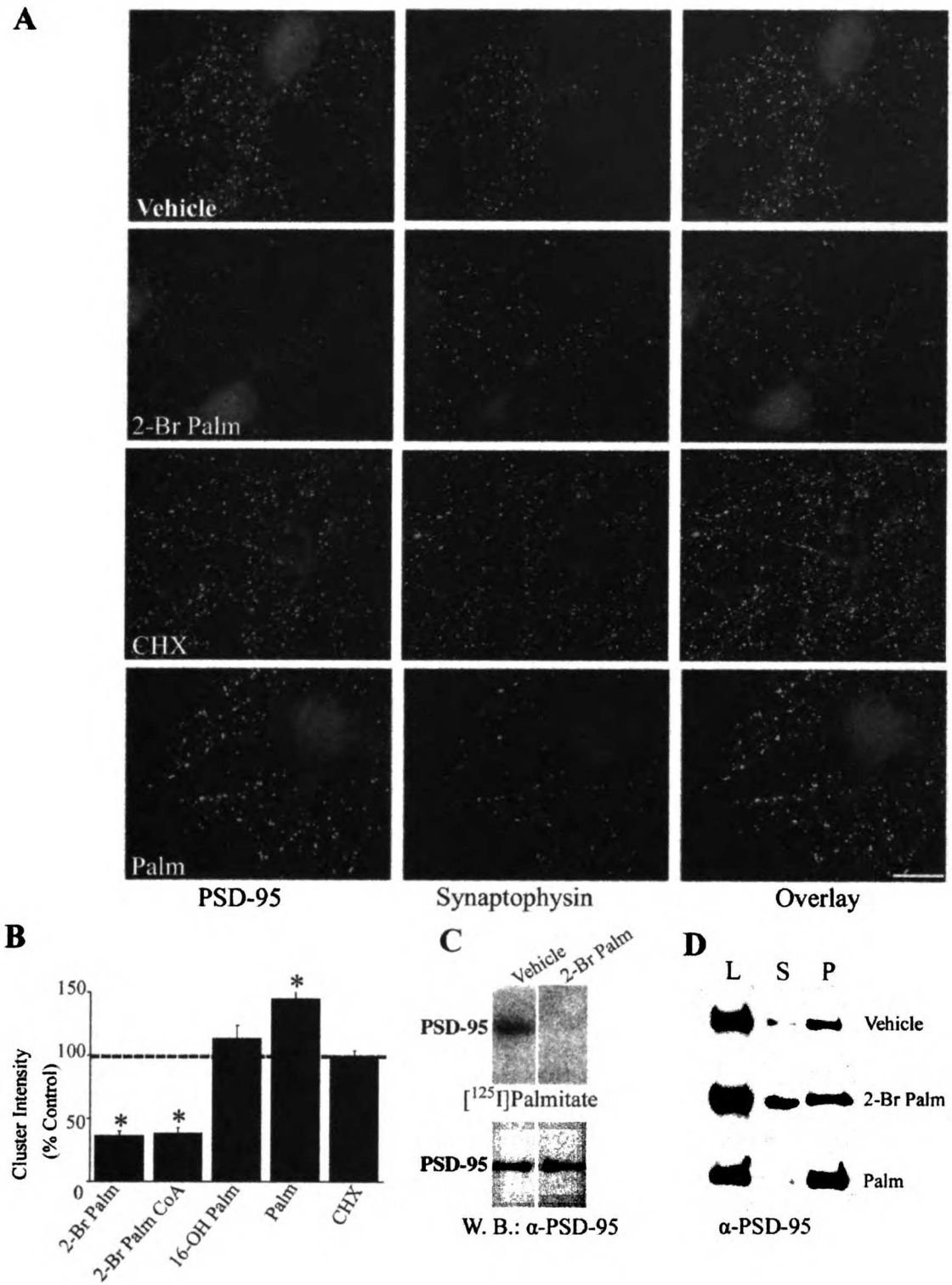
A
Vehicle
2-Br Palm
CHX
Palm
PSD-95
Synaptophysin
Overlay
B
Cluster Intensity (% Control)
150
100
50
0
2-Br Palm
2-Br Palm CoA
16-OH Palm
Palm
CHX
C
Vehicle
2-Br Palm
PSD-95
[125I]Palmitate
PSD-95
W. B.: α-PSD-95
D
L
S
P
Vehicle
2-Br Palm
Palm
α-PSD-95

Figure 2. Blocking palmitoylation disperses synaptic clusters of PSD-93.

Cultured hippocampal neurons (DIV 14) were treated for 8 hours with 10 μM 2-bromopalmitate (2-Br palm) and neurons were then fixed and stained for PSD-93 and synaptophysin. Treatment with 2-Br palmitate disperses synaptic clusters of PSD-93.

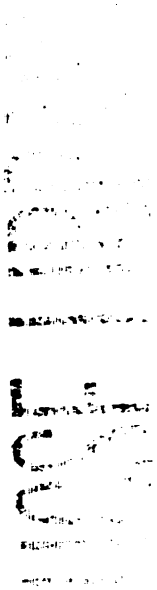

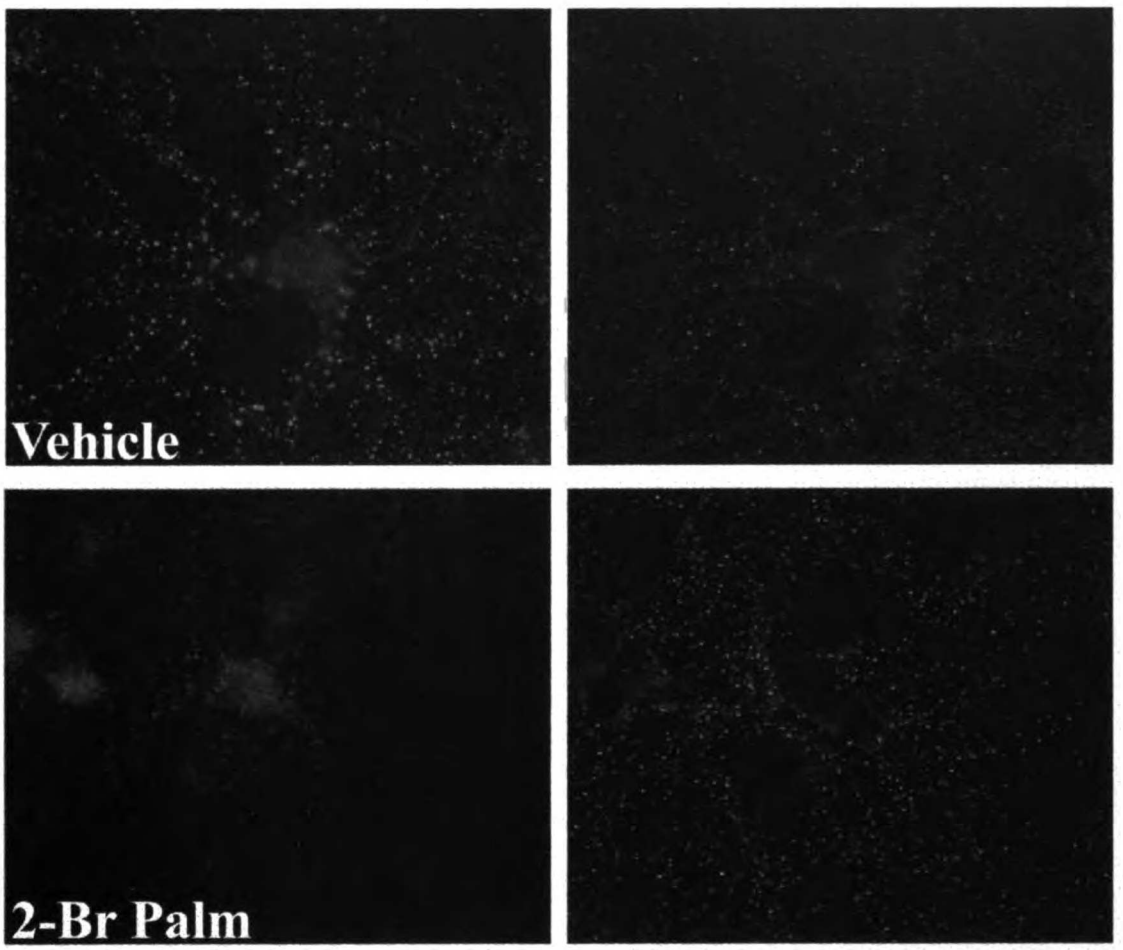
Vehicle
2-Br Palm
PSD-93
Synaptophysin

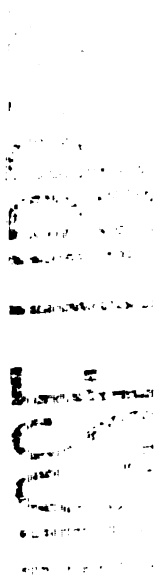

Figure 3. Slow turnover of PSD-95 protein in cultured neurons.

(A) Hippocampal neurons were labeled with [^{35}S]methionine for 1 hr. Cultures were then chased with 2 mM unlabelled methionine for 0, 1, 2, 4, 8 16 or 24 hr; cells were lysed; and PSD-95 was immunoprecipitated from the solubilized material. Immunoprecipitates were loaded onto gels that were analyzed by fluorography for [^{35}S]methionine (top gel) or were immunoblotted for PSD-95 (WB; lower gel). (B) Immunoprecipitation of PSD-95 is quantitative. Cultured cells were lysed and PSD-95 was immunoprecipitated from the solubilized material using sheep anti-PSD-95 antibodies. After IP supernatant (sup) material was collected. Immunoprecipitated products and equal volumes of load and sup were immunoblotted for PSD-95 using mouse anti-PSD-95 antibodies. (C) Cycloheximide treatment blocks protein synthesis in neurons. Hippocampal neurons were labeled for 1 hr with [^{35}S]methionine in the presence or absence of 10 μM cycloheximide (CHX). (D) Treating neurons with cycloheximide (10 μM) for 7 hrs. does not significantly reduce the total amount of PSD-95, consistent with the long half-life of PSD-95 protein.

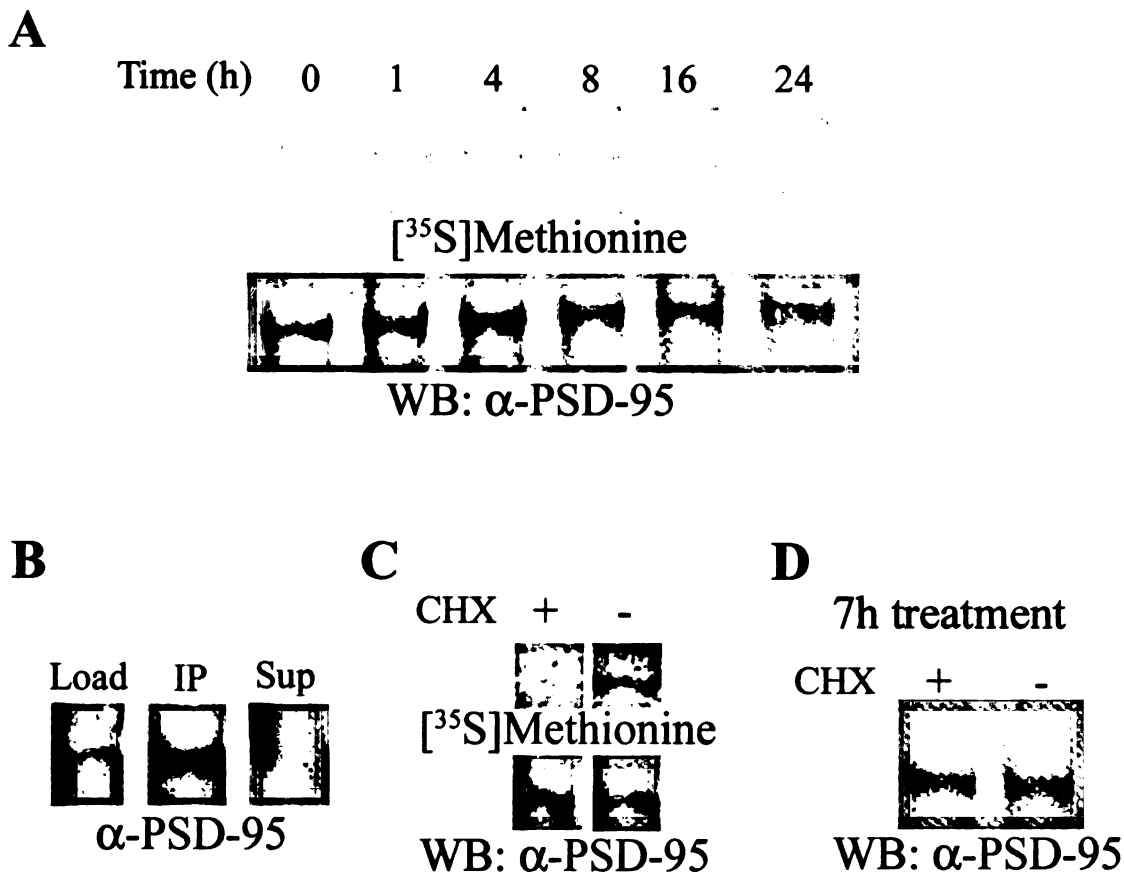
A
Time (h) 0 1 4 8 16 24
[35S]Methionine
WB: α-PSD-95
B
Load IP Sup
α-PSD-95
C
CHX + -
[35S]Methionine
WB: α-PSD-95
D
7h treatment
CHX + -
WB: α-PSD-95

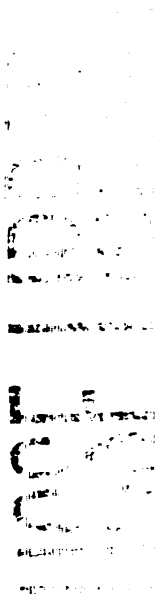

Figure 4. Synaptic clustering of PSD-95 is regulated by glutamate receptor activity. Declustering of PSD-95 by 2-bromopalmitate (2-Br Palm) requires glutamate receptor activity. Cultures were treated with vehicle or with 2-bromopalmitate in the absence or presence of 10 mM kynurenate (Kyn), 100 μM CNQX, 100 μM APV, or low extracellular calcium (-Ca^{2+}). (A) Blocking glutamate receptors or eliminating extracellular calcium blocks the effect of 2-bromopalmitate on declustering of synaptic PSD-95 (red) but had no effect on the presynaptic marker, synaptophysin (green). (B) A graph summarizes the quantitative changes in the intensity of PSD-95 clusters after these treatments. In all treatments with glutamate receptor antagonists, PSD-95 clustering was significantly higher than in cells treated with 2Br-palmitate alone ($p>0.001$). Scale bar, 10 μm.

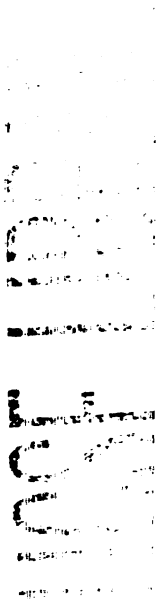

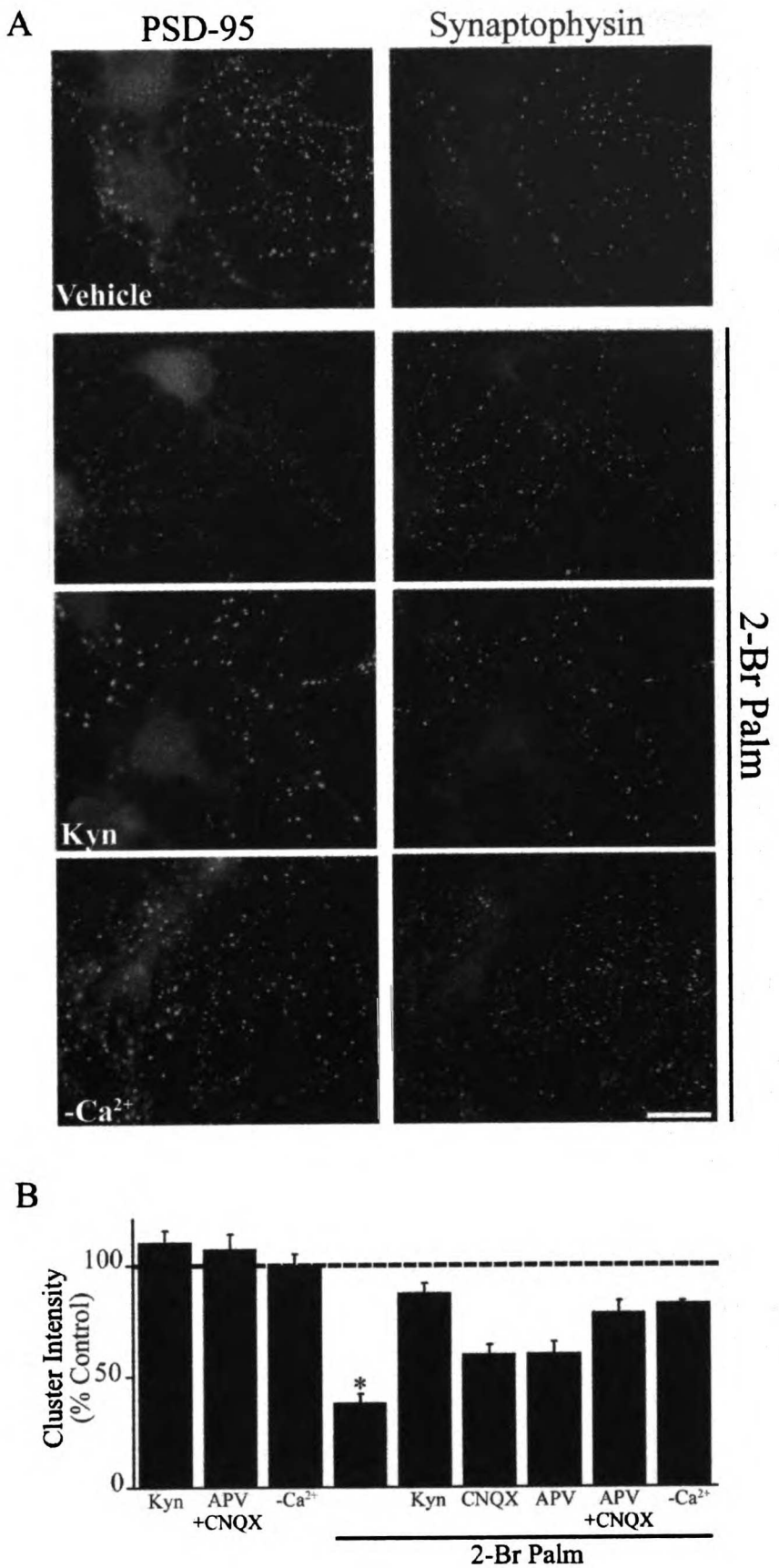
A
PSD-95
Synaptophysin
Vehicle
Kyn
-Ca2+
2-Br Palm
B
Cluster Intensity (% Control)
100
50
0
*
Kyn
APV +CNQX
-Ca2+
Kyn
CNQX
APV
APV +CNQX
-Ca2+
2-Br Palm

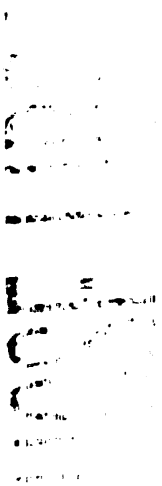

Figure 5. Regulation of palmitate turnover on PSD-95 by glutamate receptor activity.

(A) Turnover of palmitate on PSD-95 is regulated by glutamate receptor activity. Hippocampal neurons were labeled with [^{125}I]palmitate for 3 hr or with [^{35}S]methionine for 1 hr. Cultures were treated with vehicle (Veh) or with 10 mM kynurenate for 0, 1, 3, and 6 hr; cells were lysed; and PSD-95 was immunoprecipitated from the solubilized material. Immunoprecipitates were loaded onto gels that were analyzed by fluorography for [^{125}I]palmitate (upper gel), [^{35}S]methionine (middle gel) or were immunoblotted for PSD-95 (lower gel). (B) A graph showing that the half-life ($t_{1/2}$) of palmitoylated PSD-95 is prolonged by blocking glutamate receptors with kynurenate. (C) Treating neurons with glutamate (10 μM) significantly accelerates ($p<0.001$) the turnover of [^{125}I]palmitate on PSD-95. Metabolic pulse-chase labeling of cultures and analysis of PSD-95 was done as described in A.

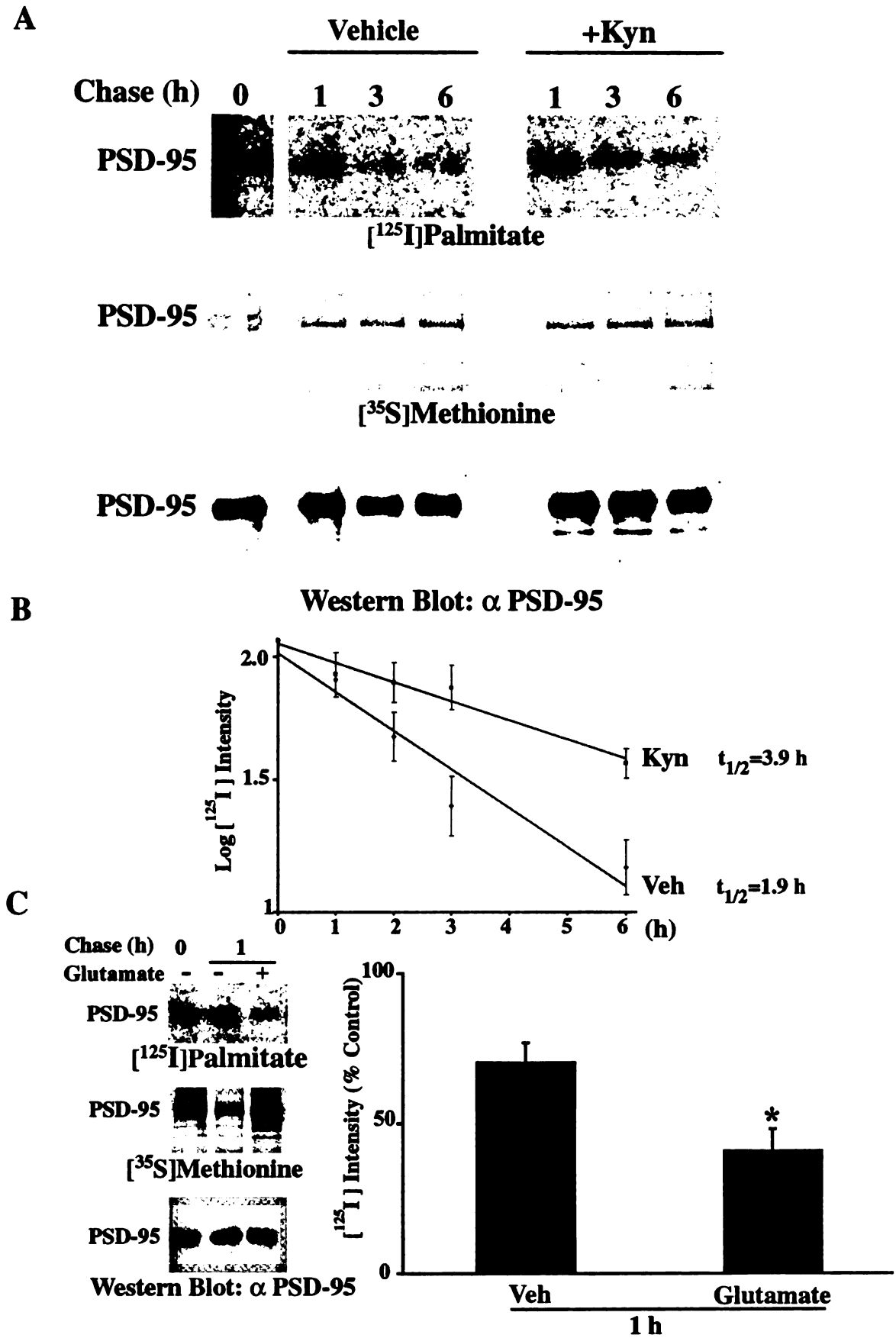
A
Vehicle
+Kyn
Chase (h) 0 1 3 6 1 3 6
PSD-95
[125I]Palmitate
PSD-95
[35S]Methionine
PSD-95
B
Western Blot: α PSD-95
2.0
1.5
1
Log [125I] Intensity
Kyn t1/2=3.9 h
Veh t1/2=1.9 h
0 1 2 3 4 5 6 (h)
C
Chase (h) 0 1
Glutamate - - +
PSD-95
[125I]Palmitate
PSD-95
[35S]Methionine
PSD-95
Western Blot: α PSD-95
100
50
0
[125I] Intensity (% Control)
*
Veh
Glutamate
1 h

Figure 6. Blocking protein palmitoylation declusters synaptic AMPARs but not NMDARs.

(A) Treatment of neurons with 2-bromopalmitate (2-Br Palm) yields a reduction of synaptic GluR1 clustering that correlates with the depalmitoylation-induced loss of synaptic PSD-95. Hippocampal neurons were treated with 10 μM 2-bromopalmitate for 8 hrs, then fixed and stained for PSD-95 (green) and GluR1 (red). (B) 2-Bromopalmitate disperses synaptic clusters of GluR1 but not NR1. Hippocampal neurons treated with 2-bromopalmitate were fixed and stained for NR1 (green) and GluR1 (red). (C) A graph summarizes the quantitative changes in the intensity of GluR1, NR1 and NR2B after treatment with 2-bromopalmitate. Treatment with 2-bromopalmitate significantly reduced GluR1 clustering ($p<0.001$) but not NR1 ($p>0.1$) or NR2B ($p>0.2$). Scale bar, 10 μm.

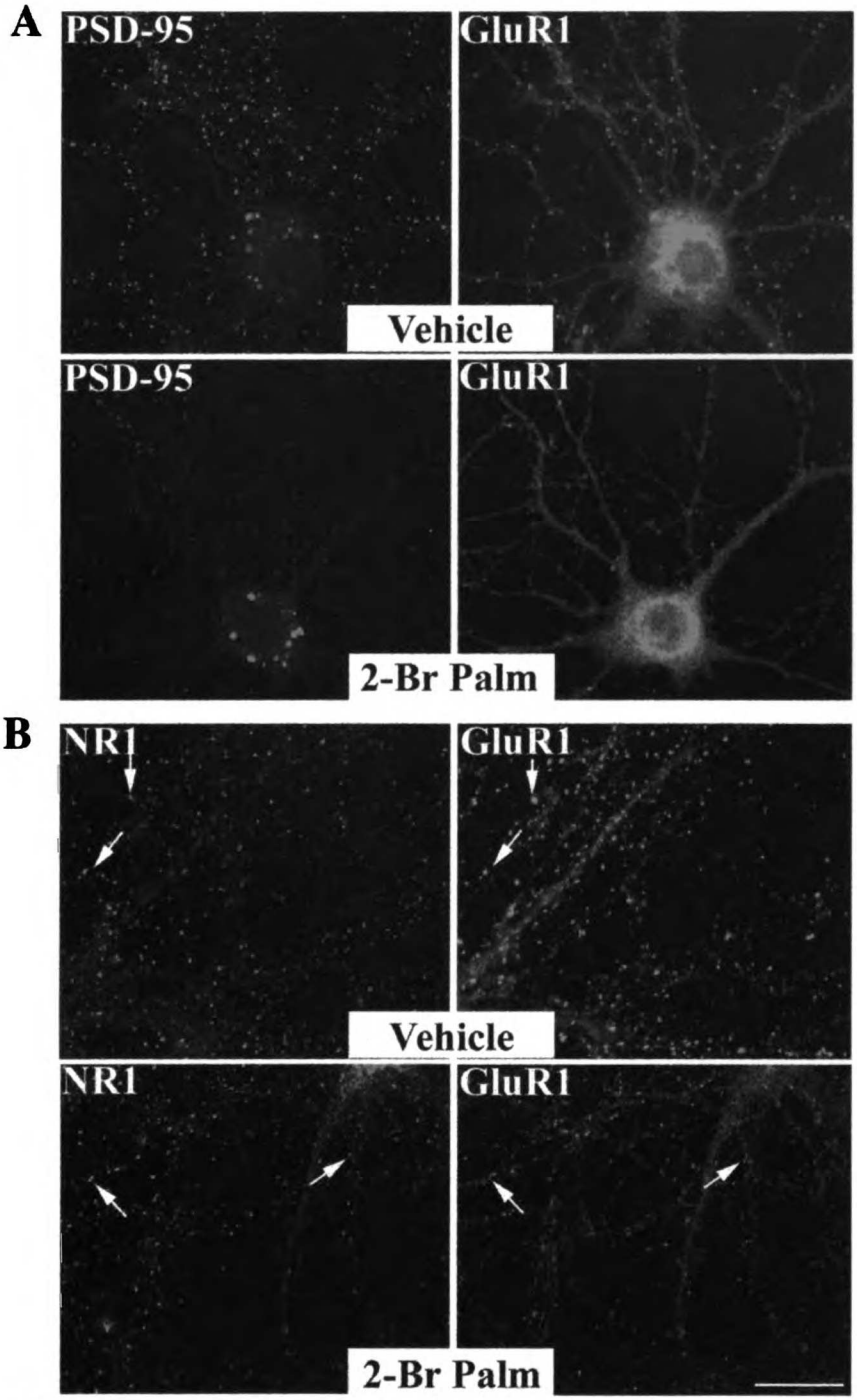
A
PSD-95
GluR1
Vehicle
PSD-95
GluR1
2-Br Palm
B
NR1
GluR1
Vehicle
NR1
GluR1
2-Br Palm
C
Cluster Intensity
(% Control)
100
50
0
*
GluR1
NR1
NR2B
2-Br Palm

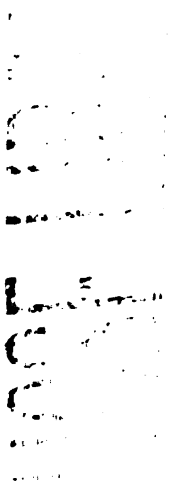

Figure 7. Alteration of glutamate-receptor mediated activity by inhibition of palmitoylation.

(A) 2-Bromopalmitate (2-Br Palm) treatment reduces the amplitude and frequency of AMPA-receptor mediated miniature excitatory synaptic currents (mEPSCs). Hippocampal neurons treated with vehicle (control) or with 20μM 2-Br Palm for 8 hours and whole cell voltage clamp recordings were made in the presence of picrotoxin and TTX to isolate AMPA-mediated spontaneous synaptic responses. Sample traces from representative neurons are shown. Scale bars 10pA, 50msec. (B) Mean mEPSC amplitude is reduced in 2-Br Palm treated cells ($p < 0.005$). (C) Mean mEPSC frequency is also reduced by 2-Br Palm treatment ($p < 0.05$).

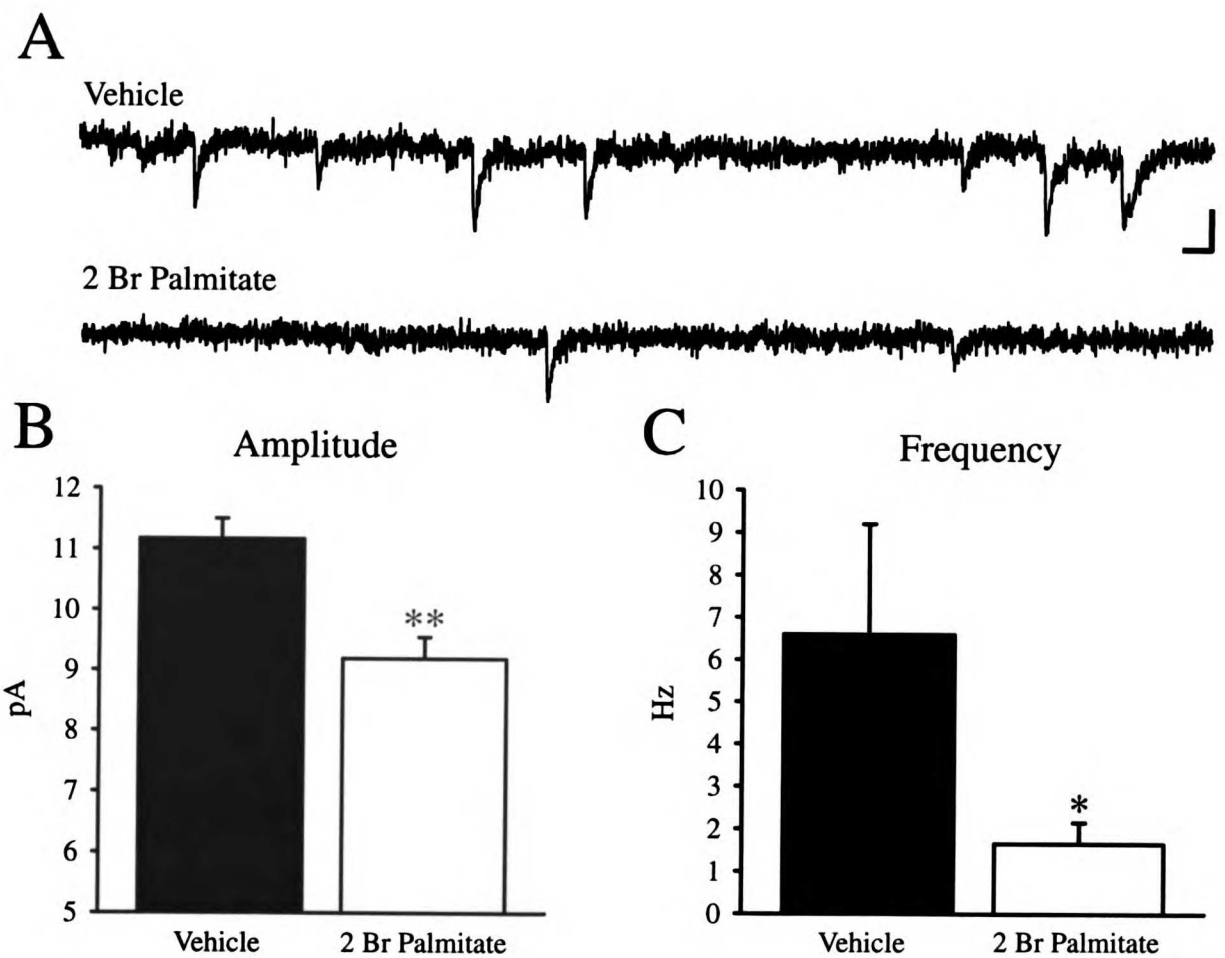
A
Vehicle
2 Br Palmitate
B
Amplitude
pA
12
11
10
9
8
7
6
5
**
Vehicle
2 Br Palmitate
C
Frequency
Hz
10
9
8
7
6
5
4
3
2
1
0
*
Vehicle
2 Br Palmitate

Figure 8. Inhibiting palmitoylation selectively affects AMPAR-mediated synaptic transmission.

(A) Cultured hippocampal neurons were recorded in the presence of 20μM glycine and 0 mM magnesium to evoke dual component (AMPA + NMDA) responses at –70 mV. Representative averaged mEPSCs from control and 2-Br Palm treated neurons are shown, demonstrating a reduction in the AMPA-mediated (fast) component of the response and preservation of the NMDA-mediated (slow) component. Scale bars 10 pA, 10 msec. (B) The ratio of the AMPA-receptor mediated amplitude to that of the NMDA-receptor mediated component is significantly reduced in 2-Br palmitate treated cells ($p < 0.05$).

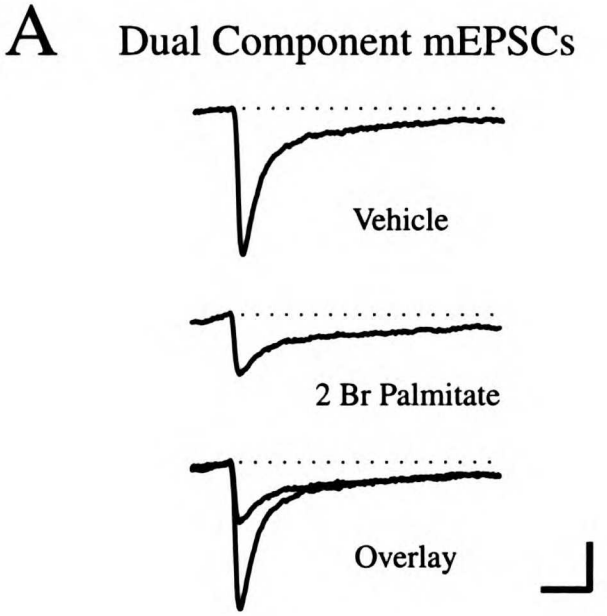
A
Dual Component mEPSCs
Vehicle
2 Br Palmitate
Overlay

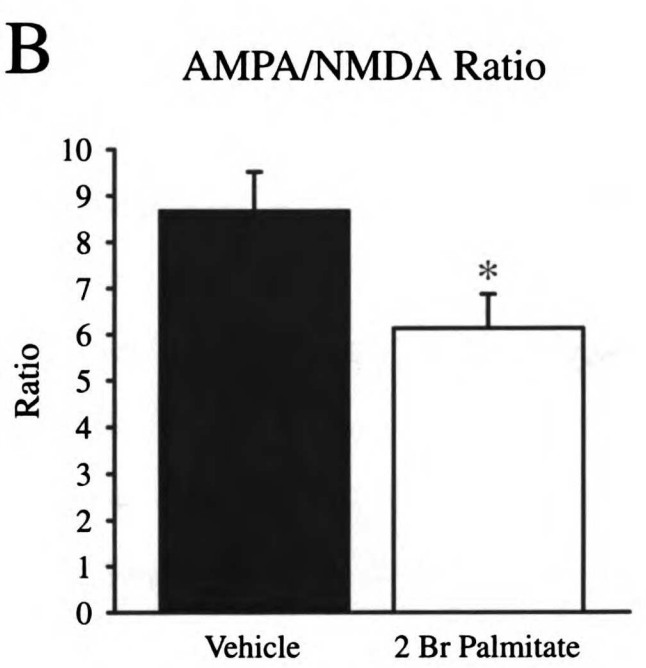
B
AMPA/NMDA Ratio
Ratio
10
9
8
7
6
5
4
3
2
1
0
*
Vehicle
2 Br Palmitate

Figure 9. Palmitoylation-dependent clustering of AMPARs specifically involves PSD-95.

(A) Schematic diagrams of palmitoylated PSD-95 GFP and palmitoylation-deficient PSD-95 GFP containing a C-terminal prenylation motif (PSD-95-Prenyl). (B, C) Hippocampal neurons were transfected with either PSD-95 GFP (PSD-95) or with PSD-95-GFP-Prenyl (PSD-95 Prenyl) and were treated with vehicle or with 10μM 2-bromopalmitate (2-Br Palm) for 8 hr. Neurons were then fixed and stained for GluR1 (red) and the PSD-95 was visualized on the green channel. (B) GluR1 clusters in neurons transfected with PSD-95 GFP (arrowheads) were enhanced relative to untransfected neurons (arrows). (C) Treatment with 2-bromopalmitate diminished clustering of PSD-95 GFP and GluR1. However, the prenylated PSD-95 GFP and associated GluR1 clusters were resistant to 2-bromopalmitate treatment. Note in (C) that the neuron transfected with PSD-95-GFP-prenyl shows strong GluR1 clusters (arrowheads) that are resistant to 2-bromopalmitate whereas the untransfected neighbors show minimal GluR1 clusters (arrows). (D) Quantitative analysis shows that 2-bromopalmitate significantly reduces synaptic clusters of transfected PSD-95-GFP ($p<0.001$) but has no significant effect on synaptic clustering of PSD-95-GFP-prenyl. (E) Quantitative analysis shows that synaptic clusters of GluR1 in cells transfected with PSD-95-GFP are reduced by 2-bromopalmitate ($p<0.001$). By contrast, GluR1 clusters in cells transfected with PSD-95-GFP-prenyl are resistant to 2-bromopalmitate. Scale bar, 10 μm.

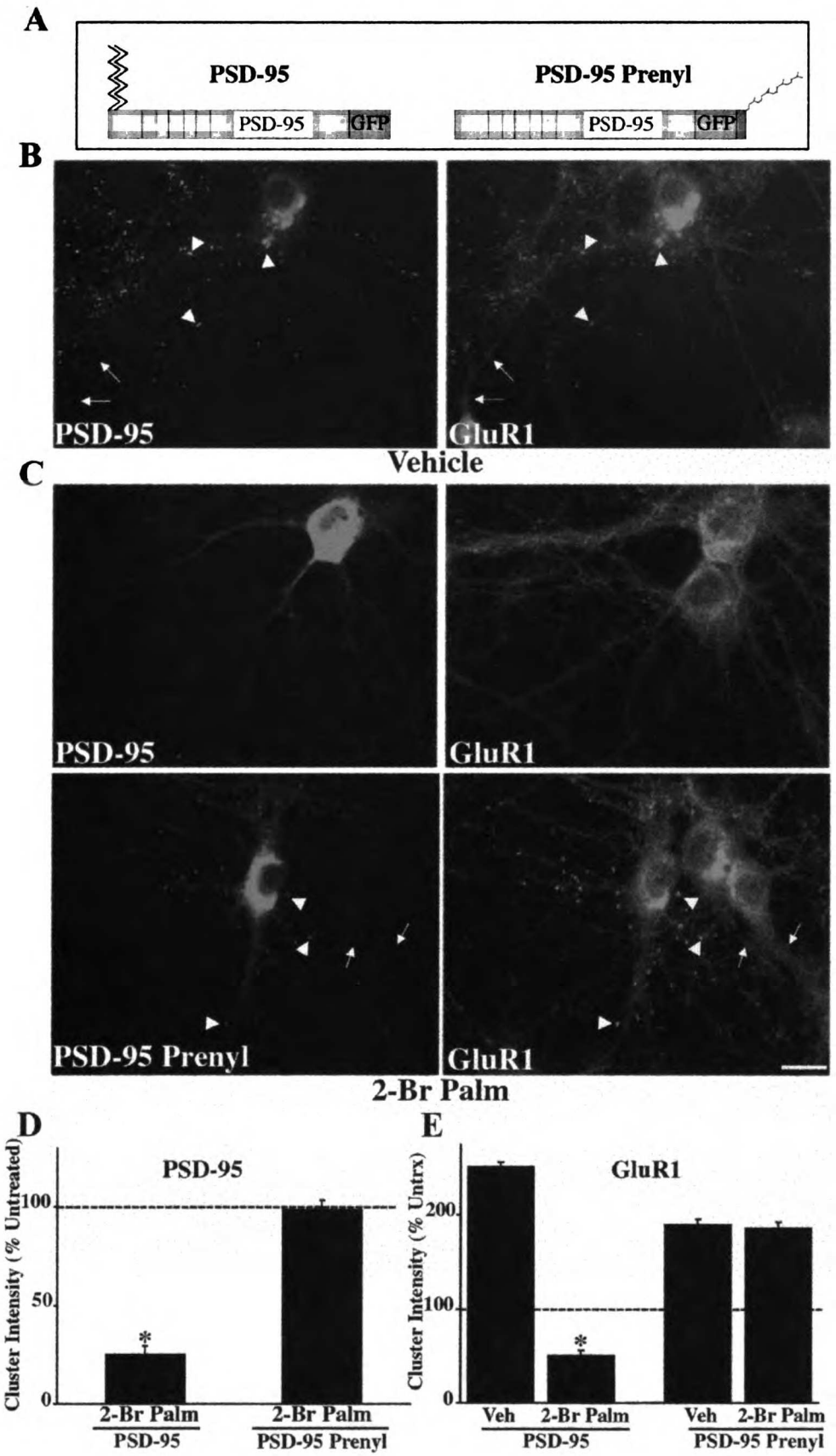
A
PSD-95
PSD-95
GFP
PSD-95 Prenyl
PSD-95
GFP
B
PSD-95
GluR1
Vehicle
C
PSD-95
GluR1
PSD-95 Prenyl
GluR1
2-Br Palm
D
PSD-95
Cluster Intensity (% Untreated)
100
50
0
*
2-Br Palm
PSD-95
2-Br Palm
PSD-95 Prenyl
E
GluR1
Cluster Intensity (% Untrx)
200
100
0
*
Veh
2-Br Palm
PSD-95
Veh
2-Br Palm
PSD-95 Prenyl

Figure 10. Palmitoylation-regulated internalization of AMPARs mediated by PSD-95.

Endocytosis of AMPARs (GluR1) was analyzed by an immunofluorescence internalization assay. Hippocampal neurons were transfected with either PSD-95 GFP (PSD-95) or with PSD-95-GFP-prenyl (PSD-95 Prenyl), and following glutamate treatment (15 min, 100 μM), neurons were fixed and stained for internalized AMPARs (GluR1; red). (A) Glutamate enhances internalization of GluR1 in untransfected cells (top panels). PSD-95-GFP overexpression (arrows) enhances internalization of GluR1 as compared to untransfected cells (arrowheads; middle panels). In contrast, the prenylated PSD-95-GFP (arrows) prevents glutamate-induced GluR1 internalization as compared to neighboring untransfected cells (lower panels). (B) Quantitative analysis shows that glutamate increases GluR1 internalization relative to untreated cells ($p<0.01$), that overexpression of PSD-95-GFP significantly enhances this internalization ($p<0.01$) and that PSD-95GFP-prenyl abolishes the glutamate stimulated internalization ($p<0.01$). Scale bar, 10 μm.

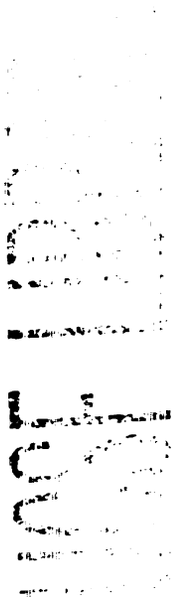

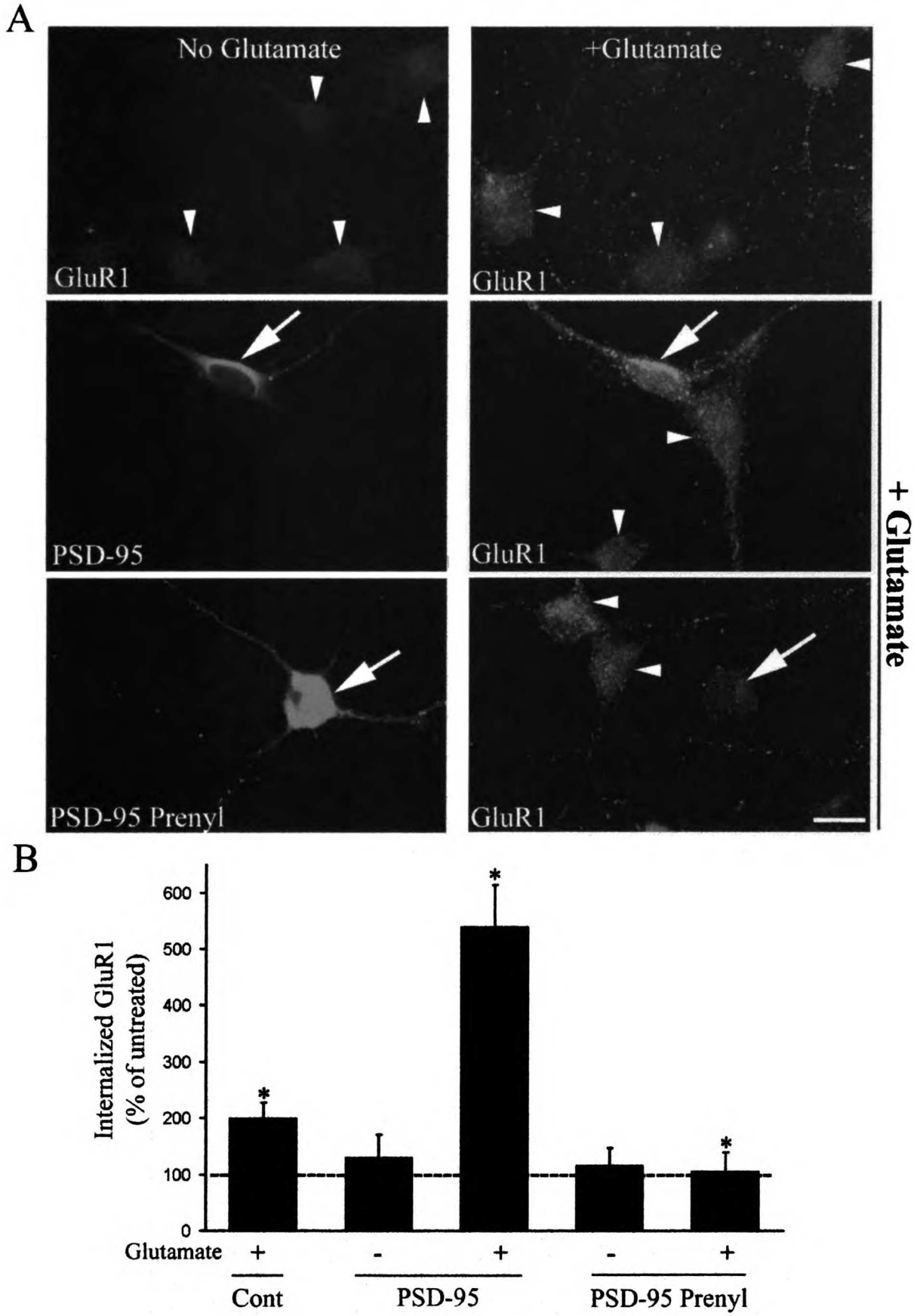
A
No Glutamate
+Glutamate
GluR1
GluR1
PSD-95
GluR1
PSD-95 Prenyl
GluR1
+ Glutamate
B
Internalized GluR1
(% of untreated)
600
500
400
300
200
100
0
*
*
*
Glutamate + - + - +
Cont
PSD-95
PSD-95 Prenyl

Figure 11. Assembly of the stargazin-glutamate receptor complex by PSD-95 is modulated by palmitoylation.

(A) Depalmitoylation of PSD-95 inhibits clustering of stargazin and GluR4. COS cells were co-transfected with GluR4, stargazin-GFP (Stg GFP) and wild type PSD-95. Twelve hours post-transfection, cells were treated with vehicle or 10μM 2-bromopalmitate (2-Br Palm) for 8 hr then were stained with antibodies to PSD-95 (blue) and GluR4 (red); stargazin was visualized on the green channel. Treatment with 2-bromopalmitate blocks clustering of PSD-95, stargazin and GluR4 and causes all three proteins to accumulate in a perinuclear pattern that resembles the distribution of the proteins in cells co-transfected with the palmitoylation-deficient mutant of PSD-95 (PSD-95:C3,5S). (B) Stargazin and GluR4 are also clustered by a prenylated PSD-95 mutant (GFP-PSD-95-prenyl) though the clusters are somewhat smaller and more punctate than with wild type PSD-95. Importantly, the stargazin / AMPAR clusters with GFP-PSD-95-prenyl are resistant to 2-bromopalmitate. (C) Schematic diagram of activity-dependent palmitate cycling on PSD-95 at the synapse. 2-bromopalmitate causes accumulation of depalmitoylated PSD-95 and decreases synaptic AMPARs.

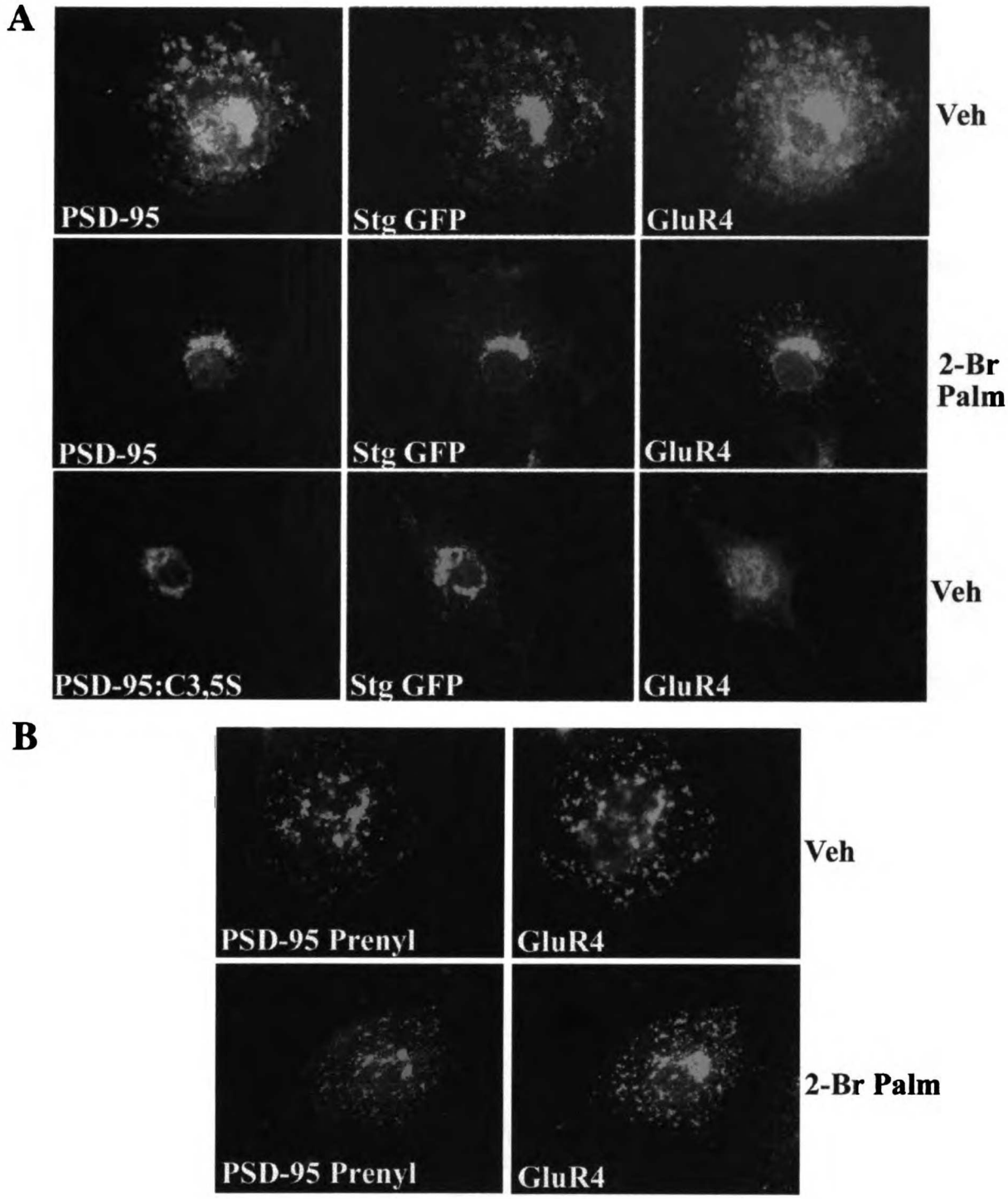
A
PSD-95
Stg GFP
GluR4
Veh
PSD-95
Stg GFP
GluR4
2-Br Palm
PSD-95:C3,5S
Stg GFP
GluR4
Veh
B
PSD-95 Prenyl
GluR4
Veh
PSD-95 Prenyl
GluR4
2-Br Palm

CHAPTER 7:

General Conclusions

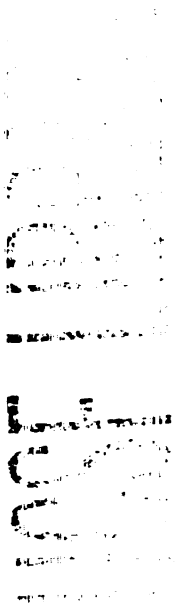

Application of molecular biological techniques to neurobiology has permitted a rapid expansion of our knowledge of nervous system structure and function in an extremely short time. In the series of studies presented here, we combined techniques from recently diverse disciplines to answer a fundamental question in neurobiology. Perhaps our most significant finding demonstrates the molecular mechanism for AMPAR localization at glutamatergic synapses. We also demonstrate that this localization is dynamic and that PSD-95 might not only be involved in anchoring AMPARs but might also be a point of regulation for plasticity. Future studies will undoubtedly further elucidate these mechanisms.

MAGUK Proteins Cluster AMPARs at Synapses

The study of mammalian MAGUK proteins has rapidly expanded to many laboratories since their cloning approximately 10 years ago (Cho et al., 1992; Kistner et al., 1993). This intensive study has yielded many insights into the functions of these proteins, most notably their putative identification as receptor clustering and trafficking proteins (El-Husseini et al., 2000c; Kim et al., 1996; Kim et al., 1995; Tejedor et al., 1997; Tiffany et al., 2000; Zito et al., 1997). However, previous attempts to firmly identify roles for these proteins in mammalian neurons have been teechnically limited by the use of heterologous cell systems. In this study, we have identified that PSD-95 is able to cluster a specific transmembrane protein, stargazin, at synapses in mammalian neurons, and by doing so controls synaptic localization of AMPARs.

Based on our experiments, we propose the following model (Fig. 1a): through an association with stargazin, AMPARs that are localized to intracellular compartments are brought to the surface. These surface AMPAR/stargazin complexes are retained at the synapse when stargazin binds a synaptic MAGUK PDZ domain, and otherwise

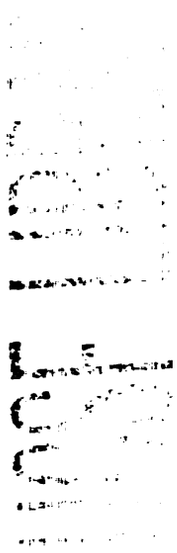

potentially serve as a reserve pool of receptors. Thus, the number of PSD-95/MAGUK molecules present at an excitatory synapse determines the number of synaptic AMPARs. Such a model relies heavily on the central role of PSD-95 or other MAGUKs in controlling the number of synaptic AMPARs. That synaptic AMPARs appear to be unaltered in PSD-95 mutant mice (Migaud et al., 1998) suggests that other MAGUKs, such as SAP102, which we show are functionally similar to PSD-95, can also mediate synaptic AMPAR targeting. Similarly, hippocampal AMPARs appear normally localized in the stargazer mutant mouse (Hashimoto et al., 1999), presumably because other stargazin isoforms (such as γ-3 or γ-4) are present. It will be important to elucidate the mechanisms that might regulate the amount of synaptic MAGUK protein, as well as those that potentially modulate the binding of stargazin to both AMPARs and PDZ domains, as they could have profound effects on surface and synaptic AMPAR trafficking.

An alternative model is that the PSD-95/stargazin interaction is responsible for delivering AMPARs to the synapse, at which point AMPARs are transferred to other clustering proteins, such as GRIP/ABP or PICK1 (Fig. 1b). This would be consistent with data suggesting that GluR1 and GluR2 constructs lacking C-terminal PDZ-binding motifs are delivered to synapses, but not retained (Hayashi et al., 2000; Osten et al., 2000). However, as the AMPAR EPSC correlates with the amount of synaptic MAGUK protein, another mechanism would have to regulate the binding or number of these secondary AMPAR binding proteins. Also, the localizations of the various stargazin GFP constructs at synapses, and their correlation with AMPAR-mediated transmission, suggests stargazin remains associated with AMPARs at the synapse. Regardless of the exact model, our results demonstrate the critical role played by the stargazin/PSD-95 interaction in controlling the number of synaptic AMPARs.

MAGUK Protein Involvement in Synaptic Plasticity

Our results also suggest important roles for MAGUK proteins in synaptic plasticity. Specifically, we show that PSD-95 is continually cycling into and out of the synapse as a result of changes in its palmitoylation state. As a consequence of this cycling, AMPARs are moving into and out of synapses. A prolonged change in the steady-state localization of PSD-95 would lead to long-term changes in synaptic strength. Changes in the activities of the PSD-95 palmitate acyl-transferase and thioesterase could thus control AMPAR localization. Hopefully future work will be able to identify these enzymes and elucidate their regulation, which may yield novel insights into the mechanisms of synaptic plasticity.

Our study suggests that the removal of synaptic AMPARs that is manifest in long-term depression might be mediated by the de-palmitoylation of synaptic PSD-95. Conversely, long-term potentiation, which involves addition of AMPARs to the synapse (Hayashi et al., 2000; Shi et al., 1999), might be mediated by an increase in the level of synaptic PSD-95. The increased PSD-95 level at the synapse would either recruit more AMPARs to the synapse from an extrasynaptic reserve pool or deliver new receptors to the synapse from intracellular stores.

The immediate source of the new synaptic AMPARs that mediates LTP is uncertain. In one model, LTP could involve the palmitoylation of soluble PSD-95, causing its insertion at the synapse and the consequent shuttling of reserve surface AMPARs to the synapse. This model would be consistent with an insight derived from the GluR1 knockout mouse, which both lacks LTP and does not have any extrasynaptic

AMPA receptors (Zamanillo et al., 1999). A two-step model of synaptic AMPA receptor trafficking has already been demonstrated (Chen et al., 2000; Osten et al., 2000; Passafaro et al., 2001).

Alternatively, LTP could involve the insertion of additional AMPARs directly from intracellular pools. Such a model is tentatively supported by data suggesting that patterns of stimulation that induce LTP cause a dendritic exocytosis (Maletic-Savatic et al., 1998; Maletic-Savatic and Malinow, 1998), and that LTP is blocked by inhibitors of exocytosis (Lledo et al., 1998). At the same time, however, PSD-95 associates with early endosomes, and is trafficked to the cell surface along tubulovesicular structures (El-Husseini et al., 2000c). It is conceivable that the membrane trafficking events putatively related to LTP are actually delivering membrane-bound PSD-95 to the synapse. Whether stargazin and AMPARs are already associated with the PSD-95 at this stage would then still remain to be determined.

Regardless, it does seem quite clear that PSD-95 does have some role in the phenomenon of LTP, as the PSD-95 mutant mouse has dramatically enhanced LTP (Migaud et al., 1998). Unfortunately, an understanding of this phenotype is obscured for two reasons. First of all, this mutant is not a true PSD-95 knockout. It expresses a truncated from of PSD-95, which incorporates both the palmitoylation motif and the first two PDZ domains (Migaud et al., 1998). Our experiments show that a similar protein retains the AMPAR-enhancing property of wild-type PSD-95 (Chap. 5, Fig. 4C-D), so the phenotype resulting from a complete absence of PSD-95 remains to be determined. Second, other MAGUK proteins might have similar roles to PSD-95 in the synaptic

targeting of AMPARs in neurons. This redundancy continues to be a major obstacle in understanding the roles for these proteins in synaptic function.

Future studies will undoubtedly focus more closely on some of the differences between the various MAGUK isoforms, including an analysis of their splice variants. While two mammalian MAGUKs, PSD-95 and PSD-93 are very highly homologous, SAP97 and SAP102 are a bit more distinct, particularly in their N-terminus. Given the importance of this region in the synaptic targeting of MAGUKs, the differences between the various MAGUKs might have important functional implications. Different MAGUK isoforms might have specialized roles in synaptic plasticity. For instance, the unique N-terminus of SAP102 might allow for its regulation by various signals, such as phosphorylation, and it specifically could be delivered to synapses during LTP. If PSD-95 were mainly involved in steady-state AMPAR trafficking, this could also account for some of the observed PSD-95 mutant phenotype. Additionally, identification of alternative splice variants of both rat (Bunn et al., submitted) and human (Bredt et al., in preparation) PSD-95, which either lack or contain the palmitoylation motif, suggests a novel point of regulation for PSD-95 localization. Further understanding of PSD-95 may result from a study of the functions of its SH3 and GK domains, as they are likely to play a modulatory role in MAGUK function (McGee et al., 2001).

Future Directions

Our models predict that PSD-95 localization directly determines AMPAR localization, and thus synaptic strength. If correct, the highest priority for future studies would be to obtain an understanding of mechanisms regulating PSD-95 trafficking, as

these mechanisms would likely be central to changes in synaptic strength. One mechanism that we address in this study involves regulated changes in the palmitoylation state of PSD-95. Thus, an identification of the enzymes involved in regulating palmitate addition and removal from PSD-95 would vastly improve our understanding of how palmitoylation is regulated. Perhaps the N-terminal palmitoylation motifs of PSD-95 and PSD-93 could be used in a yeast two-hybrid assay to identify these enzymes. Once cloned, biochemical analyses could be performed with purified enzymes and substrates in order to determine how various kinases and second messengers regulate palmitoylation. This would allow for a comparison of how the palmitoylation state of PSD-95 is regulated by specific stimuli with what is known about the regulation of synaptic strength.

We also suggest that the regulated trafficking of PSD-95 might underlie the changes in AMPAR number observed during synaptic plasticity. Movement of PSD-95 GFP has been observed in transfected neurons, and was found to be influenced by activity (Okabe et al., 1999). However, our data suggest that overexpressed PSD-95 has effects on its own. Thus, it would be desirable to image the movement of endogenous PSD-95. A knock-in mouse expressing PSD-95 GFP instead of wild-type PSD-95 would allow for direct visualization of "endogenous" PSD-95 in live cells, and determination of any activity-dependence to its movement. Alternatively, as a first attempt, one could image slice cultured pyramidal cells (which, unlike dissociated cultures, retain the capacity for LTP) expressing PSD-95 GFP to see if any changes in localization are induced during LTP. According to our model, PSD-95 should move into spines coincident with the induction of LTP, and move out of spines during LTD.

One specific regulator of synaptic strength that has been studied in great detail is post-synaptic calcium. Increases in intracellular calcium, via CaMKII activation, might cause an increase in the synaptic localization of PSD-95, thus recruiting more AMPARs to the synapse. Neurons transfected with truncated, active CaMKII could be stained for PSD-95, allowing for the assessment of possible increases in its synaptic localization.

According to our model, calcium could regulate AMPAR localization in several distinct ways via PSD-95. First of all, calcium could regulate the palmitoylation of PSD-95. Our data (Chapter 6) show that decreases in extracellular calcium slow the turnover of palmitate on PSD-95. The converse experiment, showing an increase in PSD-95 palmitoylation when calcium is elevated, would be consistent with the concept that the increased synaptic localization of PSD-95 might cause the increase in synaptic strength observed during LTP. This could be simply accomplished by adding a calcium ionophore during the pulse labeling of neurons with ^{125}I-palmitate.

However, as membrane fusion events are required for LTP (Lledo et al., 1998), LTP could involve simply involve the regulated surface insertion of palmitoylated, membrane-bound PSD-95 from intracellular compartments. This would be consistent with data showing that PSD-95 is trafficked in tubulovesicluar compartments from an early endosomal stage (El-Husseini et al., 2000a). Membrane insertion of PSD-95 would thus result in the increased synaptic localization of AMPARs. Studies of the regulation of palmitate transfer to PSD-95 as well as live imaging of endogenous PSD-95 would be able to address this issue.

Calcium could also potentially regulate the localization of PSD-95 by CaMKII-mediated phosphorylation. CaMKII phosphorylates Drosophila *discs-large*, leading to a

massive change in its localization (Koh et al., 1999). The identified phosphorylation site resides in PDZ1, and is highly conserved between *discs-large* and mammalian MAGUKs (unpublished observation). PSD-95 localization in mammalian neurons could be regulated directly via CaMKII-mediated phosphorylation in a similar manner. An analysis of the trafficking of PSD-95 constructs bearing mutations at this site would allow for an assessment of this hypothesis. A broader approach could involve an analysis of phosphorylation of PSD-95 by CaMKII and an identification of alternative phosphorylation sites. These could then be subjected to the same mutational analysis as above.

Figure 1. Two alternative models for the synaptic interactions of PSD-95 and stargazin.

(A) Association with stargazin brings intracellular AMPARs to the cell surface (step1). For synaptic clustering, these receptors must be retained by a synaptic MAGUK protein, such as PSD-95, binding directly to the C-terminus of stargazin (step 2). The amount of PSD-95 therefore determines the number of synaptic AMPARs and stargazin serves as an adaptor protein. (B) **In an alternative model,** stargazin traffics AMPARs to the surface (step1), and a direct association between stargazin and PSD-95 (step 2) results in the synaptic delivery of AMPARs. After synaptic delivery, a separate protein retains AMPARs through a direct interaction (step 3).

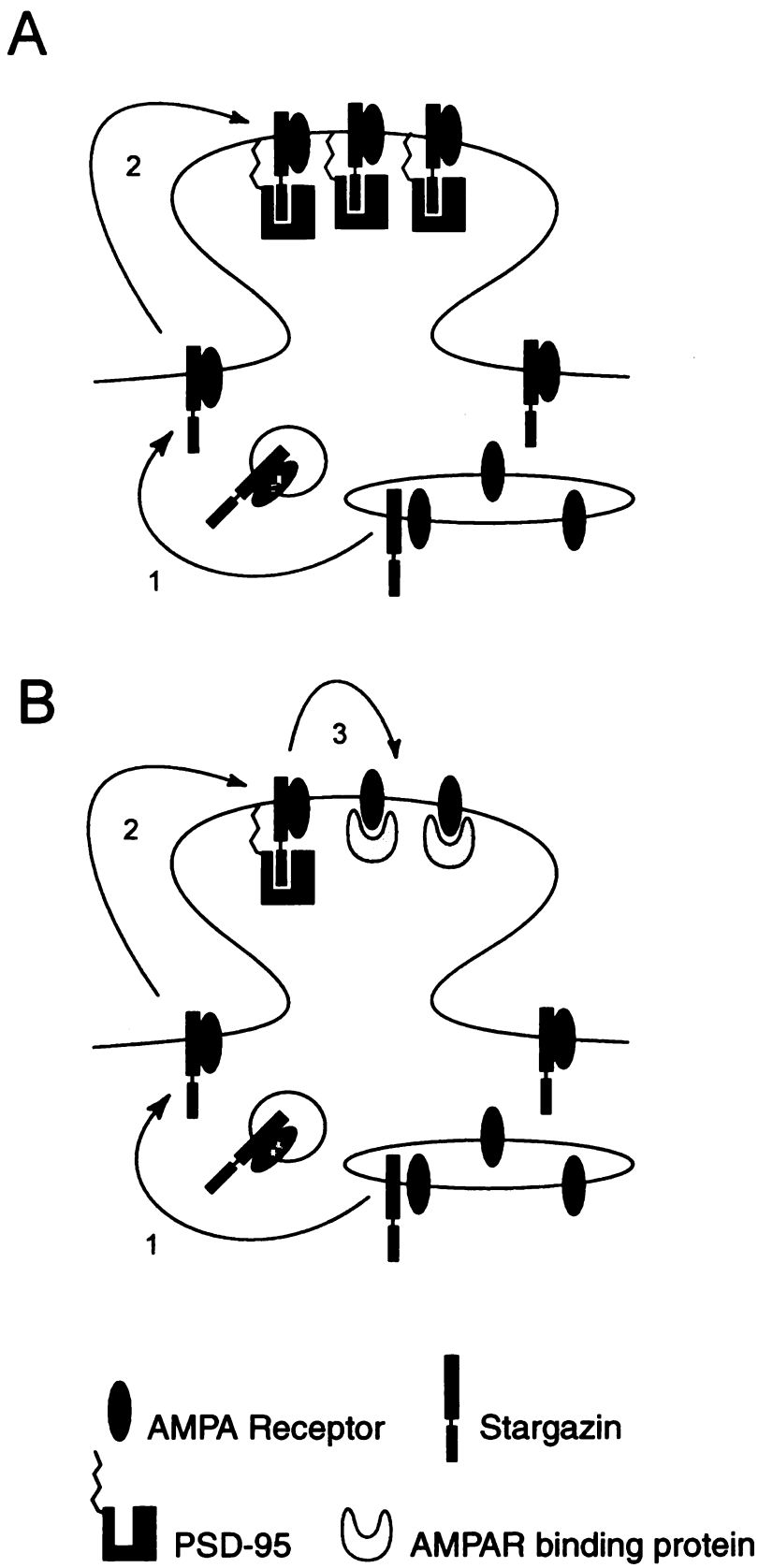
A
2
1
B
3
2
1
AMPA Receptor
Stargazin
PSD-95
AMPAR binding protein

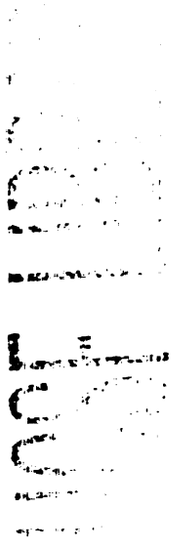

CHAPTER 8:

References

Ahmari, S. E., Buchanan, J., and Smith, S. J. (2000). Assembly of presynaptic active zones from cytoplasmic transport packets. Nat Neurosci *3*, 445-451.

Alaluf, S., Mulvihill, E. R., and McIlhinney, R. A. (1995). The metabotropic glutamate receptor mGluR4, but not mGluR1 alpha, is palmitoylated when expressed in BHK cells. Journal of Neurochemistry *64*, 1548-1555.

Alvarez, E., Gironès, N., and Davis, R. J. (1990). Inhibition of the receptor-mediated endocytosis of diferric transferrin is associated with the covalent modification of the transferrin receptor with palmitic acid. Journal of Biological Chemistry *265*, 16644-16655.

Aoki, C., Bredt, D. S., Fenstemaker, S., and Lubin, M. (1998). The subcellular distribution of nitric oxide synthase relative to the NR1 subunit of NMDA receptors in the cerebral cortex. Progress in Brain Research *118*, 83-97.

Aoki, C., Oviedo, H., Alexandre, L., and Bredt, D. S. (1999a). Synaptic membranous and cytoplasmic localization of PSD-95: EM-immunocytochemical detection with intact developing cortical neuropil. Society for Neuroscience Abstracts *510.8*, 1277.

Aoki, C., Rodrigues, S., and Kurose, H. (1999b). Use of electron microscopy in the detection of adrenergic receptors. In Methods in Molecular Biology: Adrenergic Receptor Protocols, C. M. Machinda, ed. (Humana Press), pp. 535-563.

Arnold, D. B., and Clapham, D. E. (1999). Molecular determinants for subcellular localization of PSD-95 with an interacting K+ channel. Neuron *23*, 149-157.

Beattie, E. C., Carroll, R. C., Yu, X., Morishita, W., Yasuda, H., von Zastrow, M., and Malenka, R. C. (2000). Regulation of AMPA receptor endocytosis by a signaling mechanism shared with LTD. Nature Neuroscience *3*, 1291-1300.

Berthiaume, L., Peseckis, S. M., and Resh, M. D. (1995). Synthesis and use of iodo-fatty acid analogs. Methods in Enzymology *250*, 454-466.

Brenman, J. E., Chao, D. S., Gee, S. H., McGee, A. W., Craven, S. E., Santillano, D. R., Huang, F., Xia, H., Peters, M. F., Froehner, S. C., and Bredt, D. S. (1996a). Interaction of nitric oxide synthase with the postsynaptic density protein PSD-95 and α-1 syntrophin mediated by PDZ motifs. Cell *84*, 757-767.

Brenman, J. E., Chao, D. S., Xia, H., Aldape, K., and Bredt, D. S. (1995). Nitric oxide synthase complexed with dystrophin and absent from skeletal muscle sarcolemma in Duchenne muscular dystrophy. Cell *82*, 743-752.

Brenman, J. E., Christopherson, K. S., Craven, S. E., McGee, A. W., and Bredt, D. S. (1996b). Cloning and characterization of postsynaptic density 93 (PSD-93), a nitric oxide synthase interacting protein. Journal of Neuroscience *16*, 7407-7415.

Bresler, T., Ramati, Y., Zamorano, P. L., Zhai, R., Garner, C. C., and Ziv, N. E. (2001). The dynamics of SAP90/PSD-95 recruitment to new synaptic junctions. Mol Cell Neurosci *18*, 149-167.

Burke, N. A., Takimoto, K., Li, D., Han, W., Watkins, S. C., and Levitan, E. S. (1999). Distinct structural requirements for clustering and immobilization of K+ channels by PSD-95. Journal of General Physiology *113*, 71-80.

Carroll, R. C., Beattie, E. C., Xia, H., Luscher, C., Altschuler, Y., Nicoll, R. A., Malenka, R. C., and von Zastrow, M. (1999a). Dynamin-dependent endocytosis of ionotropic glutamate receptors. Proceedings of the National Academy of Sciences of the United States of America *96*, 14112-14117.

Carroll, R. C., Lissin, D. V., von Zastrow, M., Nicoll, R. A., and Malenka, R. C. (1999b). Rapid redistribution of glutamate receptors contributes to long-term depression in hippocampal cultures. Nature Neuroscience *2*, 454-460.

Chan, J., Aoki, C., and Pickel, V. M. (1990). Optimization of differential immunogold-silver and peroxidase labeling with maintenance of ultrastructure in brain sections before plastic embedding. Journal of Neuroscience Methods *33*, 113-127.

Chen, L., Bao, S., Qiao, X., and Thompson, R. F. (1999). Impaired cerebellar synapse maturation in waggler, a mutant mouse with a disrupted neuronal calcium channel gamma subunit. Proceedings of the National Academy of Sciences of the United States of America *96*, 12132-12137.

Chen, L., Chetkovich, D. M., Petrailia, R., Sweeney, N., Kawaski, Y., Wenthold, R., Bredt, D. S., and Nicoll, R. A. (2000). Stargazin mediates synaptic targeting of AMPA receptors by two distinct mechanisms. Nature *408*, 936-943.

Cho, K. O., Hunt, C. A., and Kennedy, M. B. (1992). The rat brain postsynaptic density fraction contains a homolog of the Drosophila discs-large tumor suppressor protein. Neuron *9*, 929-942.

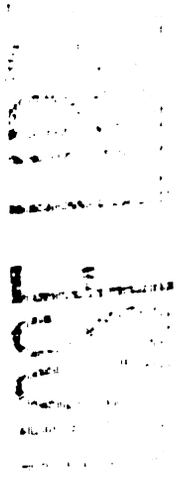

Cochilla, A. J., Angleson, J. K., and Betz, W. J. (1999). Monitoring secretory membrane with FM1-43 fluorescence. Annual Review of Neuroscience *22*, 1-10.

Cole, N. B., Sciaky, N., Marotta, A., Song, J., and Lippincott-Schwartz, J. (1996). Golgi dispersal during microtubule disruption: regeneration of Golgi stacks at peripheral endoplasmic reticulum exit sites. Molecular Biology of the Cell *7*, 631-650.

Craven, S. E., and Bredt, D. S. (1998). PDZ proteins organize synaptic signaling pathways. Cell *93*, 495-498.

Craven, S. E., El-Husseini, A. E., and Bredt, D. S. (1999). Synaptic targeting of the postsynaptic density protein PSD-95 mediated by lipid and protein motifs. Neuron *22*, 497-509.

Daniels, D. L., Cohen, A. R., Anderson, J. M., and Brunger, A. T. (1998). Crystal structure of the hCASK PDZ domain reveals the structural basis of class II PDZ domain target recognition. Nature Structural Biology *5*, 317-325.

Daw, M. I., Chittajallu, R., Bortolotto, Z. A., Dev, K. K., Duprat, F., Henley, J. M., Collingridge, G. L., and Isaac, J. T. (2000). PDZ proteins interacting with C-terminal GluR2/3 are involved in a PKC- dependent regulation of AMPA receptors at hippocampal synapses. Neuron *28*, 873-886.

Dev, K. K., Nishimune, A., Henley, J. M., and Nakanishi, S. (1999). The protein kinase C alpha binding protein PICK1 interacts with short but not long form alternative splice variants of AMPA receptor subunits. Neuropharmacology *38*, 635-644.

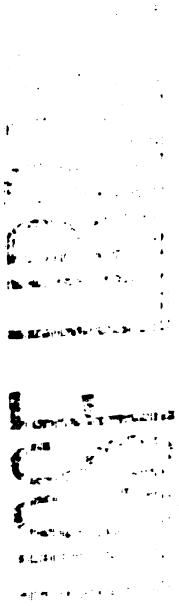

Dong, H., O'Brien, R. J., Fung, E. T., Lanahan, A. A., Worley, P. F., and Huganir, R. L. (1997). GRIP: a synaptic PDZ domain-containing protein that interacts with AMPA receptors. Nature *386*, 279-284.

Dotti, C. G., and Simons, K. (1990). Polarized sorting of viral glycoproteins to the axon and dendrites of hippocampal neurons in culture. Cell *62*, 63-72.

Doyle, D. A., Lee, A., Lewis, J., Kim, E., Sheng, M., and MacKinnon, R. (1996). Crystal structures of a complexed and peptide-free membrane protein- binding domain: molecular basis of peptide recognition by PDZ. Cell *85*, 1067-1076.

Dunphy, J. T., and Linder, M. E. (1998). Signalling functions of protein palmitoylation. Biochimica et Biophysica Acta *1436*, 245-261.

Ehlers, M. D. (2000). Reinsertion or degradation of AMPA receptors determined by activity- dependent endocytic sorting. Neuron *28*, 511-525.

El-Husseini, A. E., Craven, S. E., Chetkovich, D. M., Firestein, B. L., Schnell, E., Aoki, C., and Bredt, D. S. (2000a). Dual palmitoylation of PSD-95 mediates its vesiculotubular sorting, postsynaptic targeting, and ion channel clustering. Journal of Cell Biology *148*, 159-172.

El-Husseini, A. E., Schnell, E., Chetkovich, D. M., Nicoll, R. A., and Bredt, D. S. (2000b). PSD-95 involvement in maturation of excitatory synapses. Science *290*, 1364-1368.

El-Husseini, A. E., Schnell, E., Dakoji, S., Sweeney, N. T., Zhou, Q., Prange, O., Gauthier-Campbell, C., Aguilera-Moreno, A., Nicoll, R. A., and Bredt, D. S. (2002). Synaptic strength regulated by palmitate cycling on PSD-95. Cell *108*, 849-863.

El-Husseini, A. E., Topinka, J. R., Lehrer-Graiwer, J. E., Firestein, B. L., Craven, S. E., Aoki, C., and Bredt, D. S. (2000c). Ion channel clustering by membrane-associated guanylate kinases. Differential regulation by N-terminal lipid and metal binding motifs. Journal of Biological Chemistry *275*, 23904-23910.

Fischer, M., Kaech, S., Wagner, U., Brinkhaus, H., and Matus, A. (2000). Glutamate receptors regulate actin-based plasticity in dendritic spines. Nat Neurosci *3*, 887-894.

Friedman, H. V., Bresler, T., Garner, C. C., and Ziv, N. E. (2000). Assembly of new individual excitatory synapses: time course and temporal order of synaptic molecule recruitment. Neuron *27*, 57-69.

Garner, C. C., Nash, J., and Huganir, R. L. (2000). PDZ domains in synapse assembly and signalling. Trends in Cell Biology *10*, 274-280.

Gautam, M., Noakes, P. G., Mudd, J., Nichol, M., Chu, G. C., Sanes, J. R., and Merlie, J. P. (1995). Failure of postsynaptic specialization to develop at neuromuscular junctions of rapsyn-deficient mice. Nature *377*, 232-236.

Gomperts, S. N., Carroll, R., Malenka, R. C., and Nicoll, R. A. (2000). Distinct roles for ionotropic and metabotropic glutamate receptors in the maturation of excitatory synapses. Journal of Neuroscience *20*, 2229-2237.

Gomperts, S. N., Rao, A., Craig, A. M., Malenka, R. C., and Nicoll, R. A. (1998). Postsynaptically silent synapses in single neuron cultures. Neuron *21*, 1443-1451.

Gray, E. G. (1959). Axo-somatic and axo-dendritic synapses of the cerebral cortex: an electron microscope study. Journal of Anatomy *93*, 420-433.

Griffiths, G., Hoflack, B., Simons, K., Mellman, I., and Kornfeld, S. (1988). The mannose 6-phosphate receptor and the biogenesis of lysosomes. Cell *52*, 329-341.

Harris, B. Z., and Lim, W. A. (2001). Mechanism and role of PDZ domains in signaling complex assembly. Journal of Cell Science *114*, 3219-3231.

Hashimoto, K., Fukaya, M., Qiao, X., Sakimura, K., Watanabe, M., and Kano, M. (1999). Impairment of AMPA receptor function in cerebellar granule cells of ataxic mutant mouse stargazer. Journal of Neuroscience *19*, 6027-6036.

Hayashi, Y., Shi, S. H., Esteban, J. A., Piccini, A., Poncer, J. C., and Malinow, R. (2000). Driving AMPA receptors into synapses by LTP and CaMKII: requirement for GluR1 and PDZ domain interaction. Science *287*, 2262-2267.

Hsueh, Y. P., Kim, E., and Sheng, M. (1997). Disulfide-linked head-to-head multimerization in the mechanism of ion channel clustering by PSD-95. Neuron *18*, 803-814.

Hunt, A. C., Schenker, L. J., and Kennedy, M. B. (1996). PSD-95 is associated with the postsynaptic density and not with the presynaptic membrane at forebrain synapses. Journal of Neuroscience *16*, 1380-1388.

Husi, H., Ward, M. A., Choudhary, J. S., Blackstock, W. P., and Grant, S. G. (2000). Proteomic analysis of NMDA receptor-adhesion protein signaling complexes. Nature Neuroscience *3*, 661-669.

Ichtchenko, K., Hata, Y., Nguyen, T., Ullrich, B., Missler, M., Moomaw, C., and Südhof, T. C. (1995). Neuroligin 1: a splice site-specific ligand for beta-neurexins. Cell *81*, 435-443.

Irie, M., Hata, Y., Takeuchi, M., Ichtchenko, K., Toyoda, A., Hirao, K., Takai, Y., Rosahl, T. W., and Sudhof, T. C. (1997). Binding of neuroligins to PSD-95. Science *277*, 1511-1515.

Isaac, J. T., Nicoll, R. A., and Malenka, R. C. (1995). Evidence for silent synapses: implications for the expression of LTP. Neuron *15*, 427-434.

Itoh, M., Nagafuchi, A., Yonemura, S., Kitani-Yasuda, T., and Tsukita, S. (1993). The 220-kD protein colocalizing with cadherins in non-epithelial cells is identical to ZO-1, a tight junction-associated protein in epithelial cells: cDNA cloning and immunoelectron microscopy. Journal of Cell Biology *121*, 491-502.

Jareb, M., and Banker, G. (1998). The polarized sorting of membrane proteins expressed in cultured hippocampal neurons using viral vectors. Neuron *20*, 855-867.

Jugloff, D. G., Khanna, R., Schlichter, L. C., and Jones, O. T. (2000). Internalization of the Kv1.4 potassium channel is suppressed by clustering interactions with PSD-95. Journal of Biological Chemistry *275*, 1357-1364.

Kaech, S. M., Whitfield, C. W., and Kim, S. K. (1998). The LIN-2/LIN-7/LIN-10 complex mediates basolateral membrane localization of the C. elegans EGF receptor LET-23 in vulval epithelial cells. Cell *94*, 761-771.

Kennedy, M. B. (1997). The postsynaptic density at glutamatergic synapses. Trends in Neurosciences *20*, 264-268.

Kennedy, M. B. (1998). Signal transduction molecules at the glutamatergic postsynaptic membrane. Brain Research Brain Research Reviews *26*, 243-257.

Kennedy, M. B. (2000). Signal-processing machines at the postsynaptic density. Science *290*, 750-754.

Kim, E., Cho, K. O., Rothschild, A., and Sheng, M. (1996). Heteromultimerization and NMDA receptor-clustering activity of Chapsyn-110, a member of the PSD-95 family of proteins. Neuron *17*, 103-113.

Kim, E., Naisbitt, S., Hsueh, Y. P., Rao, A., Rothschild, A., Craig, A. M., and Sheng, M. (1997). GKAP, a novel synaptic protein that interacts with the guanylate kinase-like domain of the PSD-95/SAP90 family of channel clustering molecules. Journal of Cell Biology *136*, 669-678.

Kim, E., Niethammer, M., Rothschild, A., N., J. Y., and Sheng, M. (1995). Clustering of Shaker-type K+ channels by direct interaction with the PSD-95/SAP90 family of membrane-associated guanylate kinases. Nature *378*, 85-88.

Kistner, U., Wenzel, B. M., Veh, R. W., Cases-Langhoff, C., Garner, A. M., Appeltauer, U., Voss, B., Gundelfinger, E. D., and Garner, C. C. (1993). SAP90, a rat presynaptic protein related to the product of the Drosophila tumor suppressor gene dlg-A. Journal of Biological Chemistry *268*, 4580-4583.

Koh, Y. H., Popova, E., Thomas, U., Griffith, L. C., and Budnik, V. (1999). Regulation of DLG localization at synapses by CaMKII-dependent phosphorylation. Cell *98*, 353-363.

Kornau, H. C., Schenker, L. T., Kennedy, M. B., and Seeburg, P. H. (1995). Domain interaction between NMDA receptor subunits and the postsynaptic density protein PSD-95. Science *269*, 1737-1740.

Kornau, H.-C., Seeburg, P. H., and Kennedy, M. B. (1997). Interaction of ion channels and receptors with PDZ domains. Current Opinions in Neurobiology *7*, 368-373.

Kutzleb, C., Sanders, G., Yamamoto, R., Wang, X., Lichte, B., Petrasch-Parwez, E., and Kilimann, M. W. (1998). Paralemmin, a prenyl-palmitoyl-anchored phosphoprotein abundant in neurons and implicated in plasma membrane dynamics and cell process formation. Journal of Cell Biology *143*, 795-813.

Lahey, T., Gorczyca, M., Jia, X. X., and Budnik, V. (1994). The Drosophila tumor suppressor gene dlg is required for normal synaptic bouton structure. Neuron *13*, 823-835.

Lee, S. H., and Sheng, M. (2000). Development of neuron-neuron synapses. Current Opinion in Neurobiology *10*, 125-131.

Leonard, A. S., Davare, M. A., Horne, M. C., Garner, C. C., and Hell, J. W. (1998). SAP97 is associated with the alpha-amino-3-hydroxy-5-methylisoxazole-4- propionic acid receptor GluR1 subunit. Journal of Biological Chemistry *273*, 19518-19524.

Liao, D., Hessler, N. A., and Malinow, R. (1995). Activation of postsynaptically silent synapses during pairing-induced LTP in CA1 region of hippocampal slice. Nature *375*, 400-404.

Lin, J. W., Ju, W., Foster, K., Lee, S. H., Ahmadian, G., Wyszynski, M., Wang, Y. T., and Sheng, M. (2000). Distinct molecular mechanisms and divergent endocytotic pathways of AMPA receptor internalization. Nature Neuroscience *3*, 1282-1290.

Lippincott-Schwartz, J., Yuan, L., Tipper, C., Amherdt, M., Orci, L., and Klausner, R. D. (1991). Brefeldin A's effects on endosomes, lysosomes, and the TGN suggest a general mechanism for regulating organelle structure and membrane traffic. Cell *67*, 601-616.

Lledo, P. M., Zhang, X., Sudhof, T. C., Malenka, R. C., and Nicoll, R. A. (1998). Postsynaptic membrane fusion and long-term potentiation. Science *279*, 399-403.

Lu, W., Man, H., Ju, W., Trimble, W. S., MacDonald, J. F., and Wang, Y. T. (2001). Activation of synaptic NMDA receptors induces membrane insertion of new AMPA receptors and LTP in cultured hippocampal neurons. Neuron *29*, 243-254.

Lüscher, C., Xia, H., Beattie, E. C., Carroll, R. C., von Zastrow, M., Malenka, R. C., and Nicoll, R. A. (1999). Role of AMPA receptor cycling in synaptic transmission and plasticity. Neuron *24*, 649-658.

Lüscher, C., Nicoll, R. A., Malenka, R. C., and Muller, D. (2000). Synaptic plasticity and dynamic modulation of the postsynaptic membrane. Nat Neurosci *3*, 545-550.

Malenka, R. C., and Nicoll, R. A. (1999). Long-term potentiation--a decade of progress? Science *285*, 1870-1874.

Maletic-Savatic, M., and Malinow, R. (1998). Calcium-evoked dendritic exocytosis in cultured hippocampal neurons. Part I: trans-Golgi network-derived organelles undergo regulated exocytosis. Journal of Neuroscience *18*, 6803-6813.

Maletic-Savatic, M., Koothan, T., and Malinow, R. (1998). Calcium-evoked dendritic exocytosis in cultured hippocampal neurons. Part II: mediation by calcium/calmodulin-dependent protein kinase II. Journal of Neuroscience *18*, 6814-6821.

Maletic-Savatic, M., Malinow, R., and Svoboda, K. (1999). Rapid dendritic morphogenesis in CA1 hippocampal dendrites induced by synaptic activity. Science *283*, 1923-1927.

Malinow, R., Mainen, Z. F., and Hayashi, Y. (2000). LTP mechanisms: from silence to four-lane traffic. Current Opinion in Neurobiology *10*, 352-357.

Man, H. Y., Lin, J. W., Ju, W. H., Ahmadian, G., Liu, L., Becker, L. E., Sheng, M., and Wang, Y. T. (2000). Regulation of AMPA receptor-mediated synaptic transmission by clathrin- dependent receptor internalization. Neuron *25*, 649-662.

Matus, A., Brinkhaus, H., and Wagner, U. (2000). Actin dynamics in dendritic spines: a form of regulated plasticity at excitatory synapses. Hippocampus *10*, 555-560.

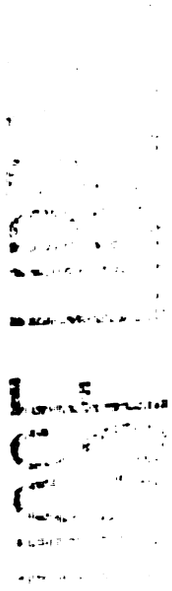

McGee, A. W., and Bredt, D. S. (1999). Identification of an intramolecular interaction between the SH3 and guanylate kinase domains of PSD-95. Journal of Biological Chemistry *274*, 17431-17436.

McGee, A. W., Dakoji, S. R., Olsen, O., Bredt, D. S., Lim, W. A., and Prehoda, K. E. (2001). Structure of the SH3-guanylate kinase module from PSD-95 suggests a mechanism for regulated assembly of MAGUK scaffolding proteins. Molecular Cell *8*, 1291-1301.

McKinney, R. A., Capogna, M., Dürr, R., Gähwiler, B. H., and Thompson, S. M. (1999). Miniature synaptic events maintain dendritic spines via AMPA receptor activation. Nature Neuroscience *2*, 44-49.

Migaud, M., Charlesworth, P., Dempster, M., Webster, L. C., Watabe, A. M., Makhinson, M., He, Y., Ramsay, M. F., Morris, R. G., Morrison, J. H., *et al.* (1998). Enhanced long-term potentiation and impaired learning in mice with mutant postsynaptic density-95 protein. Nature *396*, 433-439.

Milligan, G., Parenti, M., and Magee, A. I. (1995). The dynamic role of palmitoylation in signal transduction. Trends in Biochemical Sciences *20*, 181-187.

Moon, I. S., Apperson, M. L., and Kennedy, M. B. (1994). The major tyrosine-phosphorylated protein in the postsynaptic density fraction is N-methyl-D-aspartate receptor subunit 2B. Proceedings of the National Academy of Sciences of the United States of America *91*, 3954-3958.

Muller, B. M., Kistner, U., Kindler, S., Chung, W. K., Kuhlendahl, S., Fenster, S. D., Lau, L.-F., Veh, R. W., Huganir, R. L., Gundelfinger, E. D., and Garner, C. C. (1996). SAP102, a novel postsynaptic protein that interacts with NMDA receptor complexes in vivo. Neuron *17*, 255-265.

Mumby, S. M. (1997). Reversible palmitoylation of signaling proteins. Current Opinion in Cell Biology *9*, 148-154.

Murthy, V. N., Sejnowski, T. J., and Stevens, C. F. (1997). Heterogeneous release properties of visualized individual hippocampal synapses. Neuron *18*, 599-612.

Naisbitt, S., Kim, E., Tu, J. C., Xiao, B., Sala, C., Valtschanoff, J., Weinberg, R. J., Worley, P. F., and Sheng, M. (1999). Shank, a novel family of postsynaptic density proteins that binds to the NMDA receptor/PSD-95/GKAP complex and cortactin. Neuron *23*, 569-582.

Niethammer, M., Kim, E., and Sheng, M. (1996). Interaction between the C terminus of NMDA receptor subunits and multiple members of the PSD-95 family of membrane-associated guanylate kinases. Journal of Neuroscience *16*, 2157-2163.

Nishimune, A., Isaac, J. T., Molnar, E., Noel, J., Nash, S. R., Tagaya, M., Collingridge, G. L., Nakanishi, S., and Henley, J. M. (1998). NSF binding to GluR2 regulates synaptic transmission. Neuron *21*, 87-97.

Nusser, Z., Lujan, R., Laube, G., Roberts, J. D., Molnar, E., and Somogyi, P. (1998). Cell type and pathway dependence of synaptic AMPA receptor number and variability in the hippocampus. Neuron *21*, 545-559.

O'Brien, R. J., Xu, D., Petralia, R. S., Steward, O., Huganir, R. L., and Worley, P. (1999). Synaptic clustering of AMPA receptors by the extracellular immediate-early gene product Narp. Neuron *23*, 309-323.

Okabe, S., Kim, H. D., Miwa, A., Kuriu, T., and Okado, H. (1999). Continual remodeling of postsynaptic density and its regulation by synaptic activity. Nature Neuroscience 2, 804-811.

Osten, P., Khatri, L., Perez, J. L., Kohr, G., Giese, G., Daly, C., Schulz, T. W., Wensky, A., Lee, L. M., and Ziff, E. B. (2000). Mutagenesis reveals a role for ABP/GRIP binding to GluR2 in synaptic surface accumulation of the AMPA receptor. Neuron *27*, 313-325.

Palay, S. L. (1958). The morphology of synapses in the central nervous system. Experimental Cell Research, Supplement *5*, 275-293.

Passafaro, M., Piech, V., and Sheng, M. (2001). Subunit-specific temporal and spatial patterns of AMPA receptor exocytosis in hippocampal neurons. Nature Neuroscience *4*, 917-926.

Passafaro, M., Sala, C., Niethammer, M., and Sheng, M. (1999). Microtubule binding by CRIPT and its potential role in the synaptic clustering of PSD-95. Nature Neuroscience *2*, 1063-1069.

Perez, J. L., Khatri, L., Chang, C., Srivastava, S., Osten, P., and Ziff, E. B. (2001). PICK1 targets activated protein kinase Calpha to AMPA receptor clusters in spines of hippocampal neurons and reduces surface levels of the AMPA- type glutamate receptor subunit 2. Journal of Neuroscience *21*, 5417-5428.

Petralia, R. S., Esteban, J. A., Wang, Y. X., Partridge, J. G., Zhao, H. M., Wenthold, R. J., and Malinow, R. (1999). Selective acquisition of AMPA receptors over postnatal development suggests a molecular basis for silent synapses. Nature Neuroscience *2*, 31-36.

Pickering, D. S., Taverna, F. A., Salter, M. W., and Hampson, D. R. (1995). Palmitoylation of the GluR6 kainate receptor. Proceedings of the National Academy of Sciences of the United States of America *92*, 12090-12094.

Piserchio, A., Pellegrini, M., Mehta, S., Blackman, S. M., Garcia, E. P., Marshall, J., and Mierke, D. F. (2002). The PDZ1 Domain of SAP90. Characterization of Structure and Binding. Journal of Biological Chemistry *277*, 6967-6973.

Rao, A., and Craig, A. M. (1997). Activity regulates the synaptic localization of the NMDA receptor in hippocampal neurons. Neuron *19*, 801-812.

Rao, A., Kim, E., Sheng, M., and Craig, A. M. (1998). Heterogeneity in the molecular composition of excitatory postsynaptic sites during development of hippocampal neurons in culture. Journal of Neuroscience *18*, 1217-1229.

Resh, M. D. (1996). Regulation of cellular signalling by fatty acid acylation and prenylation of signal transduction proteins. Cellular Signalling *8*, 403-412.

Resh, M. D. (1999). Fatty acylation of proteins: new insights into membrane targeting of myristoylated and palmitoylated proteins. Biochimica et Biophysica Acta *1451*, 1-16.

Robinson, L. J., Busconi, L., and Michel, T. (1995). Agonist-modulated palmitoylation of endothelial nitric oxide synthase. Journal of Biological Chemistry *270*, 995-998.

Rongo, C., Whitfield, C. W., Rodal, A., Kim, S. K., and Kaplan, J. M. (1998). LIN-10 is a shared component of the polarized protein localization pathways in neurons and epithelia. Cell *94*, 751-759.

Sans, N., Racca, C., Petralia, R. S., Wang, Y. X., McCallum, J., and Wenthold, R. J. (2001). Synapse-associated protein 97 selectively associates with a subset of AMPA receptors early in their biosynthetic pathway. Journal of Neuroscience *21*, 7506-7516.

Sattler, R., Xiong, Z., Lu, W. Y., Hafner, M., MacDonald, J. F., and Tymianski, M. (1999). Specific coupling of NMDA receptor activation to nitric oxide neurotoxicity by PSD-95 protein. Science *284*, 1845-1848.

Scheiffele, P., Fan, J., Chioh, J., Fetter, R., and Serafini, T. (2000). Neuroligin expressed in nonneuronal cells triggers presynaptic development of contacting axons. Cell *101*, 657-669.

Sheng, M., and Sala, C. (2001). PDZ domains and the organization of supramolecular complexes. Annual Reviews in Neuroscience *24*, 1-29.

Sheng, M., and Wyszynski, M. (1997). Ion channel targeting in neurons. Bioessays *19*, 847-853.

Shi, S. H., Hayashi, Y., Petralia, R. S., Zaman, S. H., Wenthold, R. J., Svoboda, K., and Malinow, R. (1999). Rapid spine delivery and redistribution of AMPA receptors after synaptic NMDA receptor activation. Science *284*, 1811-1816.

Shin, H., Hsueh, Y. P., Yang, F. C., Kim, E., and Sheng, M. (2000). An intramolecular interaction between Src homology 3 domain and guanylate kinase-like domain required for channel clustering by postsynaptic density-95/SAP90. Journal of Neuroscience *20*, 3580-3587.

Songyang, Z., Fanning, A. S., Fu, C., Xu, J., Marfatia, S. M., Chishti, A. H., Crompton, A., Chan, A. C., Anderson, J. M., and Cantley, L. C. (1997). Recognition of unique carboxyl-terminal motifs by distinct PDZ domains. Science *275*, 73-77.

Srivastava, S., Osten, P., Vilim, F. S., Khatri, L., Inman, G., States, B., Daly, C., DeSouza, S., Abagyan, R., Valtschanoff, J. G., *et al.* (1998). Novel anchorage of GluR2/3 to the postsynaptic density by the AMPA receptor-binding protein ABP. Neuron *21*, 581-591.

Stewart, M., Murphy, C., and Fristrom, J. W. (1972). The recovery and preliminary characterization of X chromosome mutants affecting imaginal discs of Drosophila melanogaster. Devopmental Biology *27*, 71-83.

Stoppini, L., Buchs, P. A., and Muller, D. (1991). A simple method for organotypic cultures of nervous tissue. Journal of Neuroscience Methods *37*, 173-182.

Takumi, Y., Ramirez-Leon, V., Laake, P., Rinvik, E., and Ottersen, O. P. (1999). Different modes of expression of AMPA and NMDA receptors in hippocampal synapses. Nature Neuroscience *2*, 618-624.

Tejedor, F. J., Bokhari, A., Rogero, O., Gorczyca, M., Zhang, J., Kim, E., Sheng, M., and Budnik, V. (1997). Essential role for dlg in synaptic clustering of Shaker K+ channels in vivo. Journal of Neuroscience *17*, 152-159.

Thomas, U., Kim, E., Kuhlendahl, S., Koh, Y. H., Gundelfinger, E. D., Sheng, M., Garner, C. C., and Budnik, V. (1997). Synaptic clustering of the cell adhesion molecule fasciclin II by discs-large and its role in the regulation of presynaptic structure. Neuron *19*, 787-799.

Tiffany, A. M., Manganas, L. N., Kim, E., Hsueh, Y. P., Sheng, M., and Trimmer, J. S. (2000). PSD-95 and SAP97 exhibit distinct mechanisms for regulating K(+) channel surface expression and clustering. Journal of Cell Biology *148*, 147-158.

Tochio, H., Hung, F., Li, M., Bredt, D. S., and Zhang, M. (2000). Solution structure and backbone dynamics of the second PDZ domain of postsynaptic density-95. Journal of Molecular Biology *295*, 225-237.

Tomita, S., Nicoll, R. A., and Bredt, D. S. (2001). PDZ protein interactions regulating glutamate receptor function and plasticity. Journal of Cell Biology *153*, F19-24.

Topinka, J. R., and Bredt, D. S. (1998). N-terminal palmitoylation of PSD-95 regulates association with cell membranes and interaction with K+ channel, Kv1.4. Neuron *20*, 125-134.

Tovar, K. R., and Westbrook, G. L. (2002). Mobile NMDA Receptors at Hippocampal Synapses. Neuron *34*, 255-264.

Trowbridge, I. S., Collawn, J. F., and Hopkins, C. R. (1993). Signal-dependent membrane protein trafficking in the endocytic pathway. Annual Review of Cell Biology *9*, 129-161.

Tu, Y. P., Wang, J., and Ross, E. M. (1997). Inhibition of brain G(z) GAP and other RGS proteins by palmitoylation of G protein alpha subunits. Science *278*, 1132-1135.

Valtschanoff, J. G., Burette, A., Wenthold, R. J., and Weinberg, R. J. (1999). Expression of NR2 receptor subunit in rat somatic sensory cortex: synaptic distribution and colocalization with NR1 and PSD-95. Journal of Comparative Neurology *410*, 599-611.

Walters, B. B., and Matus, A. I. (1975). Proteins of the synaptic junction. Biochemical Society Transactions *3*, 109-112.

Webb, Y., Hermida-Matsumoto, L., and Resh, M. D. (2000). Inhibition of protein palmitoylation, raft localization, and T cell signaling by 2-bromopalmitate and polyunsaturated fatty acids. Journal of Biological Chemistry *275*, 261-270.

Wedegaertner, P. B., and Bourne, H. R. (1994). Activation and depalmitoylation of Gs alpha. Cell *77*, 1063-1070.

Woods, D. F., and Bryant, P. J. (1989). Molecular cloning of the lethal(1)discs large-1 oncogene of Drosophila. Developmental Biology *134*, 222-235.

Woods, D. F., and Bryant, P. J. (1991). The discs-large tumor suppressor gene of Drosophila encodes a guanylate kinase homolog localized at septate junctions. Cell *66*, 451-464.

Xia, J., Chung, H. J., Wihler, C., Huganir, R. L., and Linden, D. J. (2000). Cerebellar long-term depression requires PKC-regulated interactions between GluR2/3 and PDZ domain-containing proteins. Neuron *28*, 499-510.

Xia, J., Zhang, X., Staudinger, J., and Huganir, R. L. (1999). Clustering of AMPA receptors by the synaptic PDZ domain-containing protein PICK1. Neuron *22*, 179-187.

Yamazaki, M., Fukaya, M., Abe, M., Ikeno, K., Kakizaki, T., Watanabe, M., and Sakimura, K. (2001). Differential palmitoylation of two mouse glutamate receptor interaction protein isoforms with different N-terminal sequences. Neuroscience Letters *304*, 81-84.

Zamanillo, D., Sprengel, R., Hvalby, O., Jensen, V., Burnashev, N., Rozov, A., Kaiser, K. M., Koster, H. J., Borchardt, T., Worley, P., *et al.* (1999). Importance of AMPA receptors for hippocampal synaptic plasticity but not for spatial learning. Science *284*, 1805-1811.

Zhou, Q., Xiao, M., and Nicoll, R. A. (2001). Contribution of cytoskeleton to the internalization of AMPA receptors. Proceedings of the National Academy of Sciences of the United States of America *98*, 1261-1266.

Ziff, E. B. (1997). Enlightening the postsynaptic density. Neuron *19*, 1163-1174.

Ziff, E. B. (1999). Recent excitement in the ionotropic glutamate receptor field. Annual Reviews of the New York Academy of Sciences *868*, 465-473.

Zito, K., Fetter, R. D., Goodman, C. S., and Isacoff, E. Y. (1997). Synaptic clustering of Fascilin II and Shaker: essential targeting sequences and role of Dlg. Neuron *19*, 1007-1016.